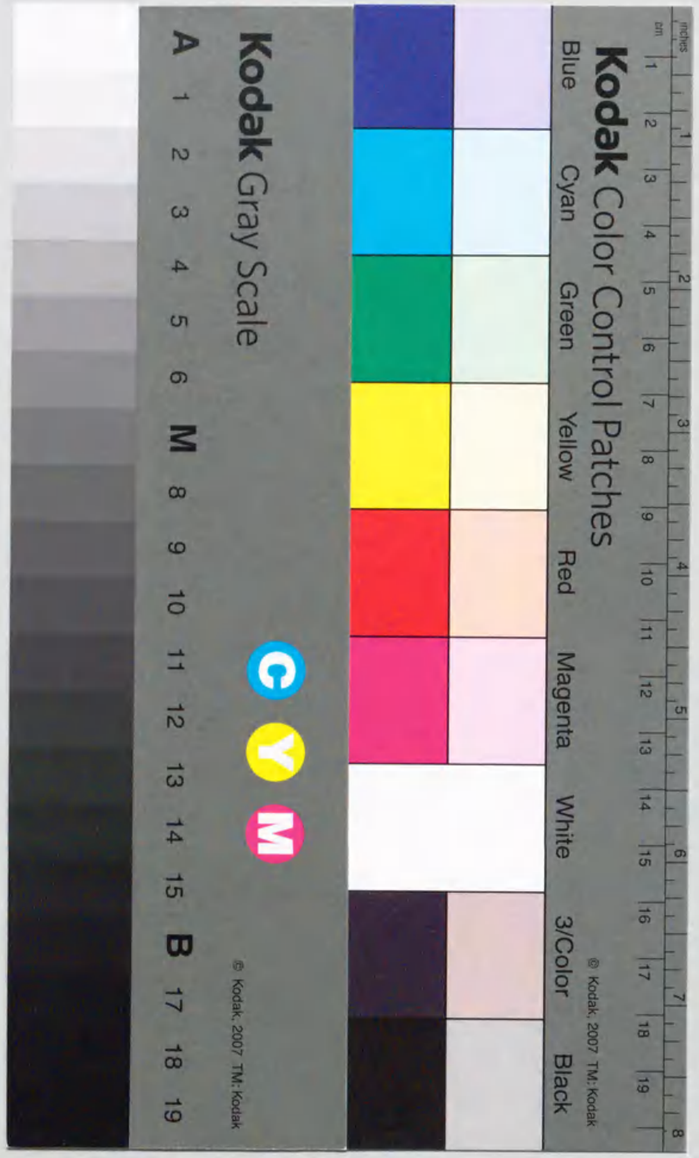

STUDIES ON THE COOPERATIVE BEHAVIOR BETWEEN LIPID MOLECULES AT AN AIR/WATER AND A WATER/OIL INTERFACE

（気／水および水／油界面上の脂質分子間の
協同特性に関する研究）

Masakazu Makino
牧野　正和

STUDIES ON THE COOPERATIVE BEHAVIOR BETWEEN LIPID MOLECULES AT AN AIR/WATER AND A WATER/OIL INTERFACE

（気／水および水／油界面上の脂質分子間の
協同特性に関する研究）

Masakazu Makino
牧野　正和

Nagoya University
名古屋大学

1997

CONTENTS

1. GENERAL INTRODUCTION

Recently, there has been increasing interest in self-oscillatory phenomena and also in the formation of spatio-temporal structure, accompanied by the rapid development of theories concerning the dynamics of such systems under nonlinear, nonequilibrium conditions. The discovery of model chemical reactions which produce self-oscillations and spatio-temporal structures has accelerated the study of nonlinear dynamics in chemistry. The Belousov-Zhabotinskii (B-Z) reaction is the most famous among such oscillatory chemical reactions, and has been studied most frequently over the past couple of decades.[1,2] The B-Z reaction has attracted considerable interest from scientists in various disciplines, since in this reaction the rhythmic change between oxidation and reduction states can be easily observed in a test tube. Since the amplitude, period and other experimental parameters are highly reproducible under a given condition, the mechanism of the B-Z reaction has been almost completely explained. The most important step in the induction of oscillations is the existence of autocatalytic and cooperative processes in the reaction network. Thus, a rapid change in the concentration of the intermediate species plays the most significant role in the self-oscillatory phenomenon.

Although the mechanism of the B-Z reaction has been clarified in detail, it may be unrealistic to suggest that the autocatalytic reaction of intermediate radicals is directly involved in various self-oscillatory phenomena in living organisms, including the beating of the heart, nervous excitations, circadian rhythm, and rhythm in cell division. About a decade ago, Yoshikawa proposed a working hypothesis that most of the rhythmic phenomena and the formation of spatio-temporal structure in biology could be related to nonlinear kinetic processes *via* biomembranes.[3,4] He and his co-workers have found that various

kinds of artificial membranes, such as a water/oil system, a porous membrane doped with lipid, and a bilayer lipid membrane, show self-oscillatory phenomena.[3-10] The oscillatory phenomena in these artificial membranes exhibit the highly nonlinear characteristics of a lipid membrane. Through these experiments, they have found that some nonlinear characteristics are based on cooperative processes, such as the rapid aggregation of lipid molecules adsorbed on an interface, and the rapid desorption of lipid aggregates from the interface. In addition, cooperative processes have been observed after the interface tension or concentration reaches a critical value under conditions that are far from equilibrium.

In this thesis, I would like to discuss the dynamic aspects of thin lipid films adsorbed on an interface, with special attention to their nonlinear properties, and give a general interpretation based on the cooperative behavior between lipid molecules on an interface.

In section 2,[11] the characteristic changes in the surface pressure (π) - surface area (A) curves of $C_6H_5(CH_2)_2C{\equiv}CC{\equiv}C(CH_2)_8COOH$ are described. Generally, the slope of a π-A curve, which is observed in a quasi-equilibrium compression process, is a non-negative value. However, with compression, an abrupt change in the surface pressure, such as a decrease to about 0 mN/m was observed in the π-A curve using the above chemical compound. By observing some π-A curves with various speeds of compression, it was found that the abrupt decrease was observed directly after a critical surface pressure (about 20 mN/m), and the degree of the decrease depended on the compression speed. With the help of a computer simulation, the abrupt decrease was explained in terms of the cooperative aggregation between lipid molecules at the critical surface pressure, and the dependence on the compression speed was due to the inhomogeneity of the concentration of lipid molecules and lipid aggregates at the air/water interface.

In section 3,[12] a relationship between Coulombic interaction among amphiphilic molecules and nonlinear properties is introduced. There have been many reports on the equations of state of lipid thin films adsorbed on an interface. Although virial equations are some of the most well-known state-equations, this equation does not include Coulombic (ion-ion) interaction directly. Therefore, Yoshikawa and his co-workers derived an equation which included a nonlinear term ($\Gamma^{1/2}$) to account for the Coulombic interaction between lipid molecules at an interface. To determine the effectiveness of this equation, actual experimental results were fitted to each of the equations (a virial equation and Yoshikawa's equation) under the same number of adjustable parameters, and then correlation coefficients were calculated using a regression analysis. Based on the correlation coefficients, Yoshikawa's equation which included a nonlinear term provided a good approximation.

In section 4,[9] an electrical-oscillation phenomenon observed at a water/oil interface is described. This experimental system, which was identified by Yoshikawa, is one of the most useful experimental model-systems for studying biomimetic phenomena, such as the burst of a nerve cell. To elucidate the mechanism of this electrical oscillation, the difference in the electrical potential between the water-phase and the oil-phase and the tension at the water/oil interface were observed simultaneously. The oscillations of the electric potential and the interface tension were synchronized. Using these findings, the mechanism of the oscillation was explained in terms of the cooperative desorption of lipids aggregates from the interface to the oil-phase, and a set of nonlinear differential equations was derived. With the help of a computer simulation, the actual oscillation of the electrical potential could be reproduced.

In sections 5,[13-15] 6,[16] and 7,[17,18] dynamic surface characteristics, especially the viscoelastic properties of dioleoylphosphatidylcholine (DOPC) thin film

with a periodic change in the surface area, and the cooperative behavior of phospholipid aggregates at an air/water interface are described.

In section 5, the basic viscoelastic properties of a DOPC thin film with a sinusoidal change in the surface area are introduced. Several important findings should be noted: (i) The DOPC thin film at an air/water interface was essentially a nonlinear viscoelastic body. (ii) This nonlinearity depended on the frequency of the change in the surface area and the aqueous subphase temperature, since dispersion of the frequency and temperature were observed. (iii) The viscoelastic properties could be explained using a kinetic model based on cooperative aggregation and dissociation among DOPC lipids at a critical surface pressure. To determine the change in the viscoelastic properties quantitatively, a Fourier transformation technique was used. The Real and Imaginary parts in the Fourier spectrum, which was observed by transformation of the time trace of the surface pressure, reflect the elastic and viscous properties of the DOPC thin film, respectively. The fundamental component, which has the same frequency as the surface area change (ω_0), in the spectrum represents the linear viscoelastic property, and the higher harmonic components, such as $2\omega_0$, $3\omega_0$, reflect the nonlinear viscoelastic properties. From these peak intensities, we can analyze the viscoelastic properties of DOPC thin film quantitatively. On the other hand, visualization of the DOPC thin film at the air/water interface was achieved using a Brewster angle microscope (BAM). Since DOPC aggregates were found, it seemed that the experimental findings, such as the actual dynamic π-A curves, could be explained by the kinetic model.

In section 6, the characteristic effect of sodium ion in the aqueous subphase on the viscoelastic properties of the DOPC thin film is examined. Using the same experimental apparatus, dynamic π-A curves were observed in the presence of inorganic compounds such as LiCl, NaCl, KCl, NH_4Cl, $MgCl_2$, and

$CaCl_2$. All of these inorganic compounds increased both the elasticity and the viscosity of the DOPC thin film. In particular, the sodium cation in the aqueous subphase markedly increased the viscosity. These experimental findings could also be explained using the cooperative aggregation model by considering an increase in the critical surface pressure compounds.

In section 7, experimental findings opposite those in the above section are described. In the presence of local anesthetics such as tetracaine, prilocaine, bupivacaine, lidocaine, and procaine, the area enclosed by the dynamic π-A curve decreased. In general, it is well-known that anesthetic compounds increase the fluidity of biomembranes. Therefore, the experimental results are consistent with the general opinion. However, local anesthetics markedly decreased the Imaginary 3rd component based on a comparison with the experimental findings in the presence of an alkaloid such as quinine. Therefore, it was concluded that local anesthetics not only increase the fluidity of the DOPC thin film, but also modify the DOPC thin film into a characterless linear viscoelastic body. These findings can also be explained using the cooperative aggregation model by considering a decrease in the critical surface pressure.

References

1) R. J. Field and M. Burger (eds.), Oscillations and Traveling Waves in Chemical Systems, John Wiley and Sons, New York, 1985.
2) G. Nicolis and I. Prigogine, Self-organization in Nonequilibrium Systems, John Wiley and Sons, New York, 1977.
3) K. Yoshikawa and Y. Matsubara, J. Am. Chem. Soc., **105** (1983) 5767.
4) K. Yoshikawa and Y. Matsubara, J. Am. Chem. Soc., **106** (1984) 4423.
5) K. Yoshikawa, T. Omochi, and Y. Matsubara, Biophys. Chem., **23** (1986) 211.
6) K. Yoshikawa, T. Fujimoto, T. Shimooka, H. Terada, N. Kumazawa, and T. Ishii, Biophys. Chem., **29** (1988) 293.
7) K. Yoshikawa, S. Nakata, T. Omochi, and G. Colaccico, Langmuir, **2** (1986) 715.
8) K. Yoshikawa, M. Shoji, S. Nakata, S. Maeda, and H. Kawakami, Langmuir, **4** (1988) 759.
9) K. Yoshikawa and M. Makino, Chem. Phys. Lett., **160** (1989) 623.
10) K. Yoshikawa, Excitable Liquid Membranes, T. Araki and H. Tsukube (eds.), CRC press, 1990.
11) M. Makino, M. Kamiya, T. Ishii, and K. Yoshikawa, Langmuir, **10** (1994) 1287.
12) K. Yoshikawa, M. Makino, S. Nakata, and T. Ishii, Thin Solid Films, **180** (1989) 117.
13) M. Makino, M. Kamiya, and K. Yoshikawa, Langmuir, submitted.
14) K. Yoshikawa and M. Makino, OME, **54** (1989) 31.
15) M. Makino and K. Yoshikawa, Nippon Kagaku Kai-shi, **10** (1990) 1143.
16) M. Makino, M. Kamiya, T. Ishii, and K. Yoshikawa, Bull. Chem. Soc. Jpn., in press.
17) M. Makino, M. Kamiya, N. Nakajo, and K. Yoshikawa, Langmuir, **12** (1996) 4211.
18) M. Makino, M. Kamiya, Nakajo, and K. Yoshikawa, Progress in Anesthetic Mechanism, **3** (1995) 247.

2. AUTOCATALYTIC AGGREGATION OF FATTY ACID WITH PHENYL AND DIACETYLENE MOIETIES AT AN AIR/WATER INTERFACE

At the first step in this study I would like to introduce characteristic phenomena concerning unique responses in a surface pressure (π) - surface area (A) curve. As for the mechanical response of thin lipid films, the π-A characteristics of lipid monolayer at an air/water interface have been well studied under quasi-static conditions. It has been established that different phases are observed for the ensemble of lipid molecules in a two-dimensional arrangement, similarly to the gas, the liquid, the solid phases, and some other intermediate phases as in three-dimensional molecular assemblies.

In the experiments on the π-A characteristics, it has been usually assumed that thermal equilibrium will be attained easily if the experiment is performed using a slow speed of compression of thin film at the interface. Measurements under thermal equilibrium are, of course, the necessary condition to obtain the physico-chemical properties of the individual "phase" of the lipid ensemble.

Contrary to the accumulated knowledge on the static or quasi-static characteristics of thin lipid films at the air/water interface, less attention has been paid to the dynamic or nonequilibrium behavior of the film. Studies on the dynamical characteristics of thin lipid films may be quite important, because the life phenomena are maintained under nonequilibrium conditions. According to the modern biochemistry, thin lipid membrane in living cells is not a rigid wall but a thermally fluctuating barrier with high fluidity. In the section 2, It will be showed that a thin lipid film exhibits the various interesting dynamic π-A characteristics, such as the "*overshoot hump*", the "*zero surface pressure*", and the "*flat plateau*".

2-1. Introduction

When an amphiphilic material is placed at an air/water interface, it may spread out to a thin film and, in most cases, form monolayers spontaneously. Thus, the Langmuir-Blodgett (LB) technique is a useful method to construct organic molecular assemblies with high order orientation and with accurate control of film thickness.[1,2] In recent years, the LB films have attracted much attention for their ability of producing new optical and/or electronic devices.[3-5] To realize the unique properties of the thin film obtained with the LB technique, it is essential to obtain stable and homogeneous films at the air/water interface. Toward this aim, a study of the physicochemical properties of monolayers at an air/water interface is expected to contribute the development of "ideal" films.

In recent studies, π-A isotherms have been measured for the monolayer of many amphiphilic molecules, containing conjugated diacetylene group[6-9] or containing both phenyl and diacetylene groups[10] which are expected to increase the conductivity of the LB films. Among these studies, the occurrence of an overshoot hump has been noticed in the π-A isotherms, at the onset of LC/LE coexistence phase, during compression of the monolayer. The overshoot hump has also been found in the π-A isotherms for other kinds of amphiphilic molecules, such as bipolar compounds.[11] The origin of the hump has been discussed in relation to the molecular structure of lipids,[8,9] the phase transition of the monolayer,[8] the ionic compounds in the subphase,[9,12] and the compression speed.[9,13] In spite of these extensive studies, a definitive mechanism for overshoot hump generation in the π-A isotherm has not yet been formulated. The origin of the overshoot hump has been ascribed to various factors such as (i) polymerization of amphiphilic lipids,[14] (ii) change in steric configurations,[9] (iii) lack of nucleation for the growth of domains

through "nonequilibrium" compression process,[13] or (iv) a kind of collapse of the monolayer.[10,15]

I am especially interested in the overshoot hump observed in the π-A isotherms of a lipid containing both phenyl and diacetylene groups.[10] The purpose of the present section is to investigate the characteristic features of the π-A curves and to clarify the origin of the overshoot hump appearance, considering cooperative process for the aggregation kinetics of amphiphilic-molecules at the air/water interface. Detailed measurements of the π-A curves were made while both the subphase component and temperature and the compression speed were changed. In present study, I focused my attention on the π-A curve during the first compression after formation of an amphiphilic layer on the subphase.

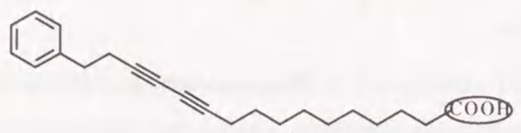

Figure 2-1.

Chemical structure of PhDA2-8.

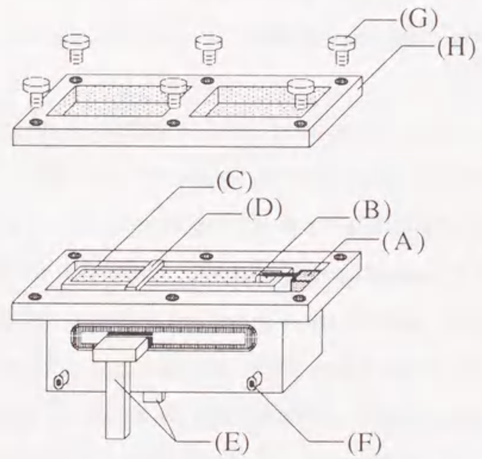

Figure 2-2.

Schematic representation of the experimental arrangement used for measuring the π-A curves of a thin film of PhDA2-8 molecules at the air/water interface.
(A) piezoelectric device; (B) filter paper (Wilhelmy plate);
(C) trough; (D) blade; (E) arms; (F) water circulating outlet;
(G) screws to fix the cover; (H) cover.

2-2. Materials and Method

The fatty acid (14-phenyl-9,11-tetradecadidynoic acid, PhDA2-8; $C_6H_5(CH_2)_2C{\equiv}CC{\equiv}C(CH_2)_8COOH$) was a gift from Dr. Yoshioka[10] (Kanegafuchi Chemical Industry Co., Ltd.). Figure 2-1 shows the chemical structure of the fatty acid examined in the present study. Analytical grade chemicals were purchased from Wako Pure Chemical Industries, Ltd. Water was freshly distilled for each experimental run over potassium permanganate and sodium hydroxide, and then purified through a Millipore Milli-Q filtering system maintained at a resistivity above 18.0MΩ·cm. The fatty acid is readily polymerized exhibiting a remarkable color change. In order to avoid the effect of polymerization, the π-A curves of the fatty acid were measured within 24 hr. after preparation of the developing solution. The developing solution of PhDA2-8 was diluted to 1.6mM concentration with chloroform, which had been purified by three consecutive distillations.

The π-A curves were measured with a trough, equipped with a moving blade and a piezoelectric device made by Kyowa Interface Sciences Co., Ltd. (Fig. 2-2). Both the trough (286mm long and 70mm wide) and blade were coated with Teflon. The subphase temperature was kept within ±0.1°C by using of a jacket connected to a thermostated water circulation system, and the environmental air temperature was kept at 18°C. The surface tension was measured with a Wilhelmy plate made of filter paper (Toyo Roshi Ltd., 25 x 25 x 0.25mm) using a piezoelectric device. The accuracy of the measurement was ±0.2mN/m. The surface pressure (π) is defined as;

$$\pi = \gamma_0 - \gamma \qquad (2\text{-}1)$$

where γ_0 is the surface tension of the subphase with absolutely pure water and γ is the surface tension of the lipid thin film covering the subphase.[13]

The whole experimental devise was sealed from the outer environment as shown in Fig. 2-2, in order to avoid contaminants such as air dust and oil materials. In the measurement of π-A curves, the blade was driven at a constant speed using a pair of mechanical side arms equipped with magnets.

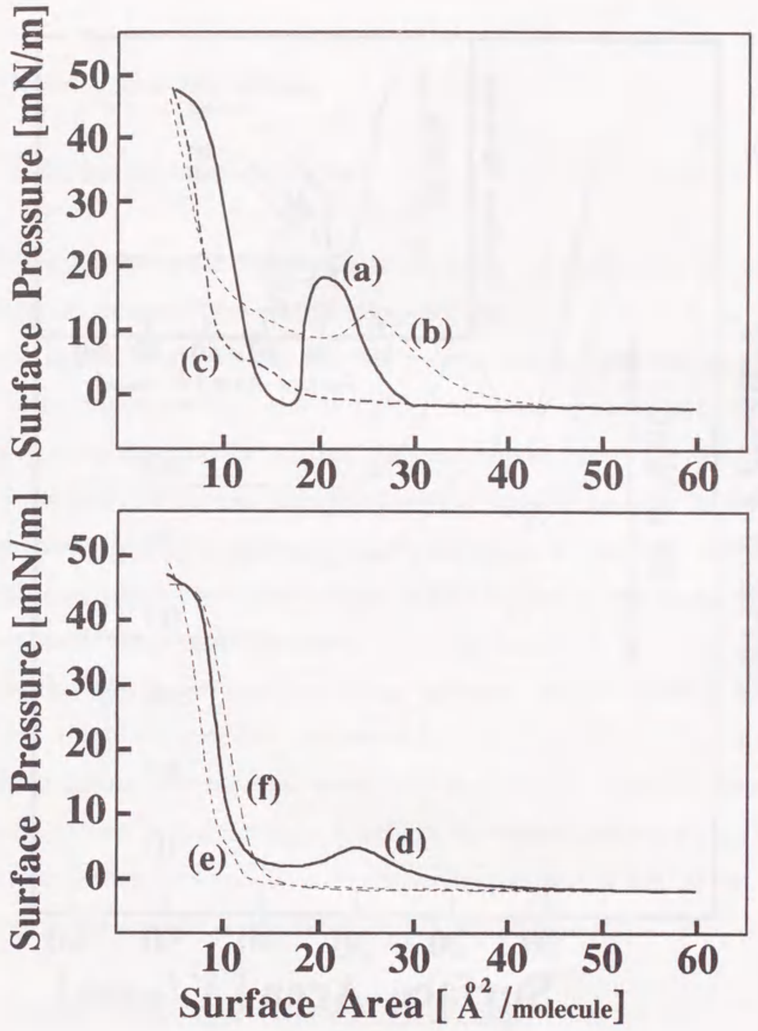

Figure 2-3.

Subphase effects on the PhDA2-8 π-A curves. The subphase temperature was 5.0°C and the compression speed was 7.5(Å²/molecule)/min. The subphase component was changed as follows:

(a) potassium bicarbonate (5×10^{-5} M) and cadmium chloride (3×10^{-4} M);
(b) potassium bicarbonate (5×10^{-5} M) and magnesium sulfate (3×10^{-4} M);
(c) potassium bicarbonate (5×10^{-5} M) and sodium chloride (3×10^{-4} M);
(d) cadmium chloride (3×10^{-4} M);
(e) potassium bicarbonate (5×10^{-5} M);
(f) pure water which was first distilled and then purified with a Millipore Milli-Q filtering system.

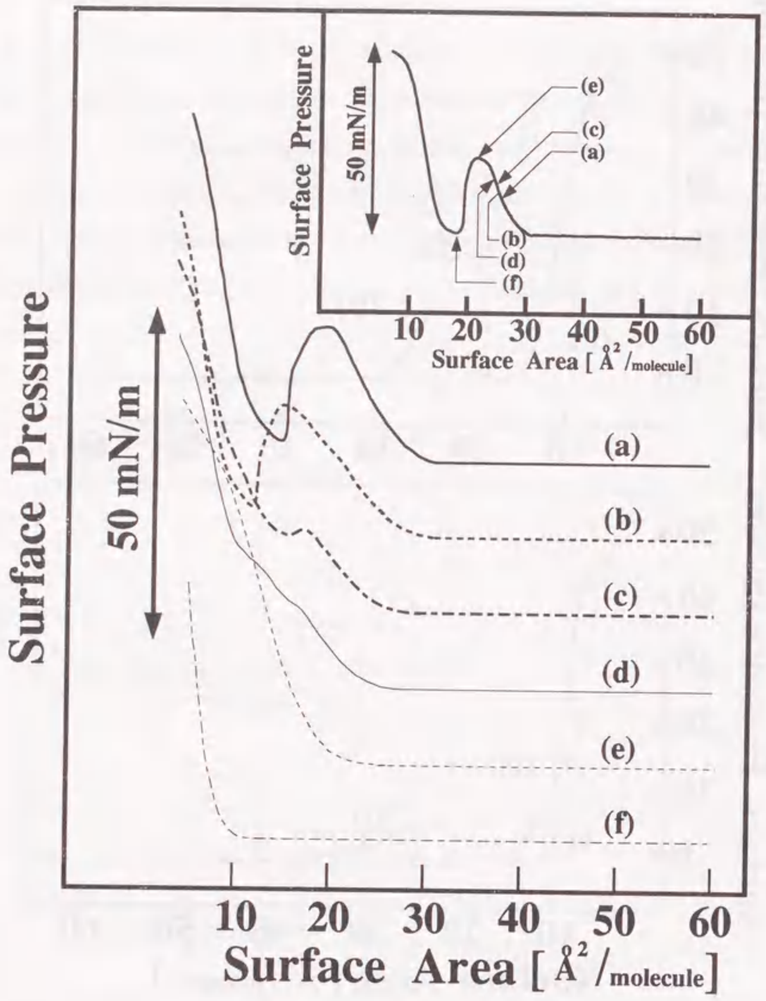

Figure 2-4.

Recompression effects on PhDA2-8 π-A curves over a subphase containing both $CdCl_2$ and $KHCO_3$. The subphase temperature was 5.0°C and the compression speed was 7.5(Å^2/molecule)/min. For recompression the blade was stopped at each of the following the surface pressures:
(a) 15 mN/m; (b) 16 mN/m; (c) 16.5 mN/m; (d) 17 mN/m; (e) 20 mN/m; (f) 0 mN/m.

2-3. Results and Discussion

Subphase Effects on the Hump

Figure 2-3 shows the π-A curves of the PhDA2-8 thin film at the air/water interface. A remarkable overshoot hump was observed in the π-A curves ((a), (b) and (d)). It is noteworthy that the overshoot hump was clearly observed with the subphase containing both $CdCl_2$ and $KHCO_3$ (curve (a)). Curve (a) shows a steep rise of the surface pressure up to 20mN/m. Beyond the maximum surface pressure, the curve shows a rapid decrease to 0mN/m (zero surface pressure). The pressure again begins to increase at around A = 15Å^2/molecule, which corresponds about half of the area at the starting point of the increase of the pressure before the overshoot hump.

Neither this large overshoot hump nor zero surface pressure could be observed unless the subphase contained both $CdCl_2$ and $KHCO_3$. It thus be suggested that, as for the thin films with amphiphilic molecules containing carbonyl moiety at the air/water interface, the well-established stabilization effect of cadmium ions may be enhanced in the presence of $KHCO_3$ as a result of its buffering capacity on the subphase pH around neutrality.

Recompression Effects on the overshoot hump

Figure 2-4 shows the recompression curves of a PhDA2-8 thin film. These curves were measured under the following conditions. In the course of the first-time compression process, the blade was stopped, and then the surface area of the initial area was expanded before continuing the compression. After 15min, recompression of the PhDA2-8 thin film was started at the same speed as in the first-time compression. The recompression curves (a)-(f) were

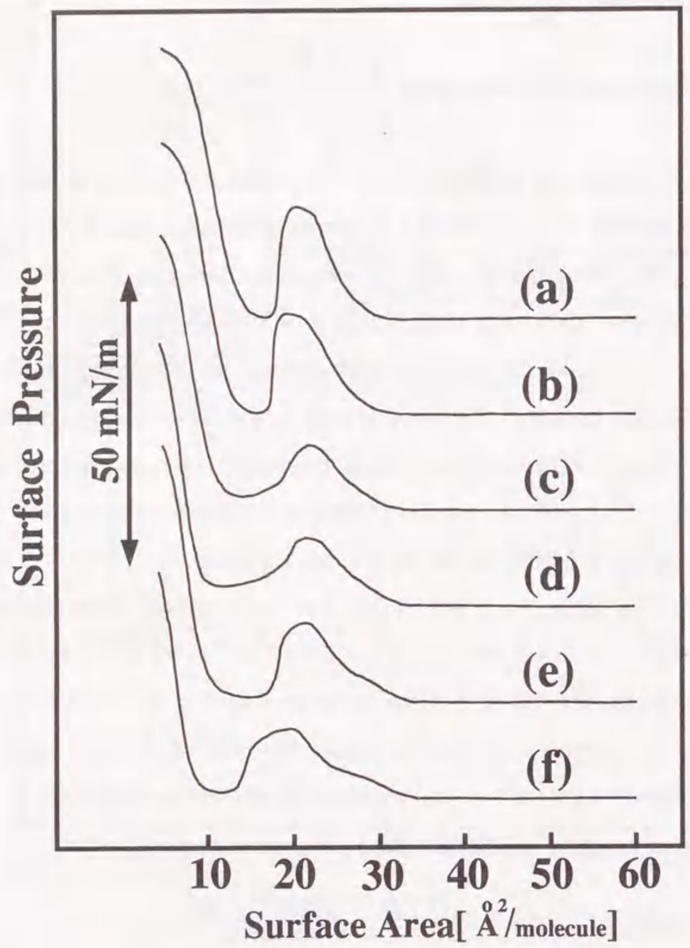

Figure 2-5.

Subphase-temperature effects on the PhDA2-8 π-A curves over a subphase containing both $CdCl_2$ and $KHCO_3$. The compression speed was 7.5(Å²/molecule)/min. The subphase temperature was;
(a) 5.0 °C, (b) 10.0 °C, (c) 15.0 °C, (d) 20.0 °C, (e) 25.0 °C, (f) 30.0 °C.

obtained with temporal stoppage of the blade at points (a)-(f), respectively (upper right of Fig. 2-4), during the first-time compression. As the stop points were shifted from (a) to (f), the recompression π-A curve migrated to the left as a whole, and the overshoot hump tended to disappear. In a recent work,[10] it has been suggested that the initially formed monolayer of PhDA2-8 molecules collapses to a multilayer when the surface pressure passes through the maximum point of the overshoot hump. This explanation is consistent with our observation, indicating that the PhDA2-8 molecules suffer some loss, possibly due to formation of the multilayers during the overshoot hump formation. In addition, it is assumed that the multilayers are formed, by an irreversible process, through an unstable state of the monolayer which existed during the overshoot hump. This idea is supported by the fact that the zero surface pressure was maintained as long as the blade was stopped at position (f) in the Fig. 2-4. The overshoot hump can be regarded as a phenomenon similar to "*supercooling*" or "*supersaturation*".[13]

Effect of subphase temperature on the overshoot hump

As shown by Fig. 2-5, the interesting characteristics, such as "the overshoot hump" and "the zero surface pressure" in the π-A curve of the PhDA2-8 molecules on the subphase containing both $CdCl_2$ and $KHCO_3$, exhibit marked temperature dependence. As the temperature decreased from 30.0°C (f) to 5°C (a), the overshoot hump became more marked.

For curve (a) at 5.0°C, the surface pressure reached zero exactly after overshoot hump formation, while, with the higher temperature, the pressure fell to a minimum pressure of several dynes. As the temperature decreased from 30.0 to 5.0°C, the surface pressure at the surface area of 20Å²/molecule increased by a factor of 1.48, but the limiting area was insensitive to change in the subphase temperature.

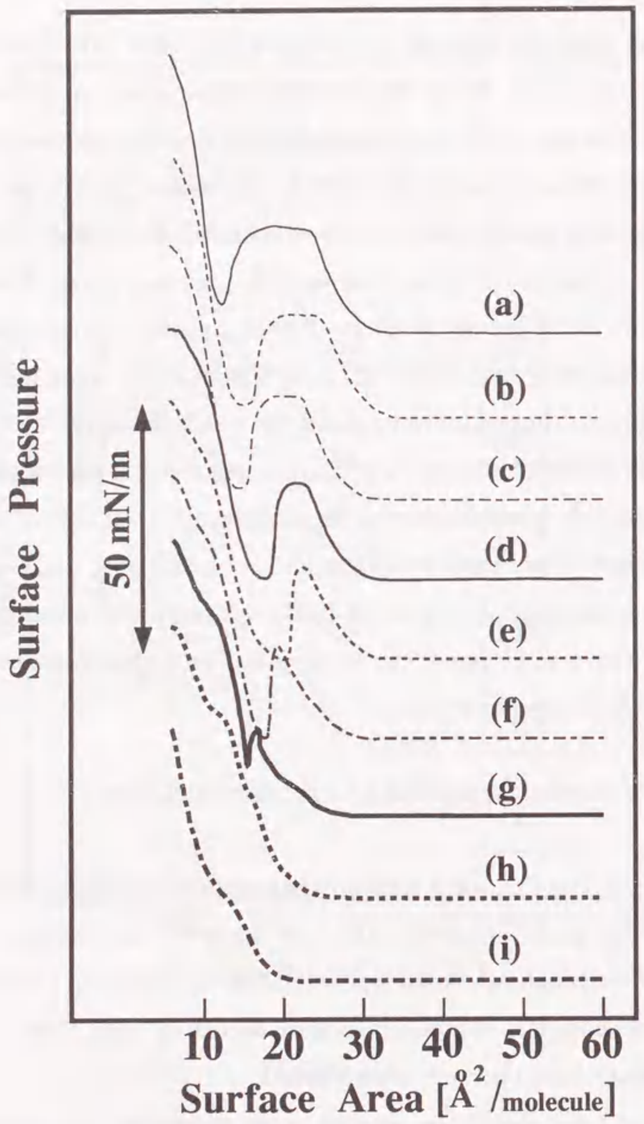

Figure 2-6.

Compression speed dependence of the PhDA2-8 π-A curves over a subphase containing both $CdCl_2$ and $KHCO_3$. The subphase temperature was 5.0°C. The compression speed was;
(a) 18.0, (b) 15.0, (c) 12.0, (d) 7.5, (e) 4.5, (f) 3.0, (g) 2.25, (h) 1.5, and (i) 0.15(Å²/molecule)/min.

Effect of compression speed on the overshoot hump

As has been indicated recently,[16] the relaxation process for compressing the monolayers of saturated fatty acids is slow and incomplete. In the present case, the π-A curves obtained under continuous compression may reflect nonequilibrium effects. Figure 2-6 shows the effects of the speed of compression on the π-A curve for the PhDA2-8 thin film at an air/water interface. An increase in the compression speed induces widening of a flat plateau in the maximum surface pressure region and a slight shifting to the right of the limiting area. It is interesting that the zero surface pressure phenomenon was observable only with an appropriate compression speed, as in (d), (e), and (f).

Theoretical interpretation of the characteristic features in the π-A curve

As has been mentioned above, the π-A curves of the PhDA2-8 thin film shows the existence of the zero pressure region after the formation of the overshoot hump. It is noteworthy that the remarkable overshoot hump and the subsequent zero surface pressure are observable only in a particular range of compression speeds, suggesting that the inclusion of the effect of nonequilibrium kinetics is essential. Since the characteristic change of the π-A curves depends on the compression speed, it may be expected the following kinetic effects to be important: (I) irreversible formation of a specific aggregated state of the surfactant molecules and (II) relaxation kinetics of spatial inhomogeneity of the surface concentration. The discussion that follows is based on this promise, because the characteristic features such as "overshoot hump", "zero surface pressure" and "flat plateau" seem to be generated as a result of competition between these different kinetic processes.

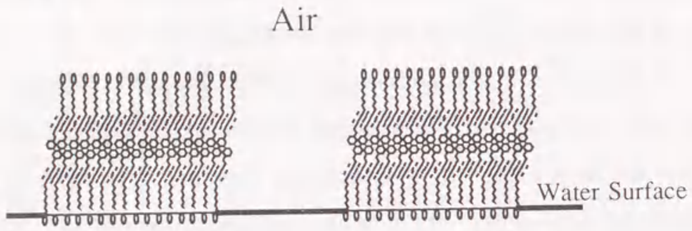

Figure 2-7.

A plausible structure of the bilayer formed at the zero surface pressure point (f) in Figure 2-4.

Recently,[17] it has been found that stable planar bilayer of fatty acid containing diacetylene groups is formed spontaneously at an air/water interface when the surface pressure is maintained at 35mN/m. It has also been observed[18,19] that, for a mixed monolayer composed of surface-active dye and fatty acid, the dye is squeezed out from the monolayer above a critical surface pressure and the bilayer is then formed under continuous compression process. These studies indicate that the lipid bilayer is formed only above a critical surface pressure. By analogy, my experiment suggests that the aggregation process of PhDA2-8 molecules also has a critical surface pressure of 20mN/m, above which the bilayer is formed. The expected structure of the bilayer is given in Fig. 2-7. Formation of the bilayer is supported by the fact that the surface area observed at the zero surface pressure is about one half of the surface area at the starting point of the increase of the pressure (limiting area) before the overshoot hump (see Fig. 2-4). The aggregation process corresponding to the kinetic effect-(I) may include autocatalytic and cooperative effects. The decrease of surface pressure down to zero is extraordinarily rapid compared with the increase of surface pressure up to the critical pressure value, which may be rate determined by the kinetic effect-(II).

Next, I will discuss the origin of the characteristic features observed in the π-A curve. When the PhDA2-8 thin film is compressed with relatively high speed, there will be a non-negligible effect of the special inhomogeneity over the lipid film, i.e., the surface pressure in the region near the blade becomes larger than that in the other region. By contrast, if the speed of compression is sufficiently smaller than the rate of relaxation of the spatial inhomogeneity, there should be no effective surface pressure gradient at the surface, i.e., a spatially uniform thin film of the PhDA2-8 will be formed. Thus, with relatively large compression speed, the surface pressure around the blade reaches the critical surface pressure (20mN/m) in preference to the other part

of the thin film and, as a result, the PhDA2-8 molecules near the blade begin to form the bilayer.

If the compression speed is lower than the rate of formation of a specific aggregated state, the autocatalytic and cooperative aggregation may be steeply spread over the whole of the thin film at the air/water interface so that a rapid decrease of surface pressure is observed. In practice, zero surface pressure is attained by special compression speed such as 7.5, 4.5, and 3.0($Å^2$/molecule)/min. With higher compression speeds, the aggregation process cannot proceed simultaneously whole over the surface. In this case, only a part of the PhDA2-8 molecules on the surface exhibits cooperative aggregation and this induces a small drop in the surface pressure. With continuous compression, the surface pressure again increases. This cycle repeats again and again, leading to an oscillation of the surface pressure. However, in my measurements such an oscillatory phenomenon was not observed, possibly due to damping effects transmitted from the part of the thin film next to the blade to the other parts around the Wilhelmy plate. In my case, the widening of the crest of the hump (flat plateau) was observed. I believe, however, that the above mechanism provides an explanation for the essential aspect of the observations of the "overshoot hump", "zero surface pressure" and "flat plateau" present in the π-A curves measured in this work.

On the basis of the above qualitative discussion of the characteristics of the π-A curves, I now provide a useful kinetic model for the molecular aggregation. Let [S] and [D] be the concentration of PhDA2-8 molecules in the "regular" and "aggregated" states, respectively. The "regular" state corresponds to the usual conformation of a surfactant molecule at the interface, i.e., the hydrophilic head faces the hydrophilic environment and the hydrophobic tail is expelled from the interface towards the hydrophobic environment. Then the aggregation can be described as

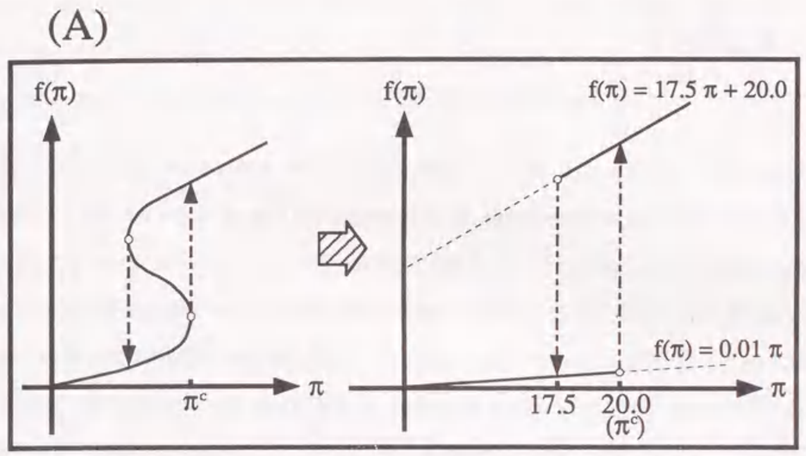

Figure 2-8.

(A) Schematic representation of the shape of function f(π). The arrows represents the first-order like phase transition effect. The two straight lines are f(π) = 17.5π + 20.0 and f(π) = 0.01π, respectively. $π^c$ indicates the critical surface pressure(ca. 20mN/m).
(B) Schematic representation of the relationship between the surface pressure (π) and the effective concentration of surfactant at the air/water interface ($Γ_{eff}$). The solid and dashed lines represent the expected and ideal relationships, respectively.

$$S + S \underset{k_{-1}}{\overset{k_1}{\rightleftharpoons}} D \qquad (2\text{-i}).$$

This step corresponds to the formation of bi-molecular aggregates of the PhDA2-8 molecules which leads to the construction of the bilayers. Because the above step takes place in the high surface pressure region corresponding to the condensed layer, it may be considered that the subsequent association process of each bi-molecular aggregate is much faster. Therefore, this step is rate determining for the overall kinetics at the air/water interface. Based on this kinetic model, the time-dependence of [D] is given by the differential equation (2-2).

$$\frac{d[D]}{dt} = k_1[S]^2 f(\pi) - k_{-1}[D] + \frac{N_D v}{A^2} \qquad (2\text{-}2),$$

where A is the surface area at time t, v is the compression speed, k_1 is the aggregation rate constant, k_{-1} is the dissociation rate constant, N_D is the number of bi-molecular aggregates of PhDA2-8 molecules at the air/water interface and $f(\pi)$ is a discontinuous function of surface pressure (π). This function has been introduced to account for the first order like phase transition,[20] which may play an important role in the autocatalytic and cooperative aggregation of PhDA2-8 molecules, which form the monolayer, to the stable bilayers which proceeds beyond the critical surface pressure. The function $f(\pi)$ can be given in a concrete expression as "S"-shape nonlinear function, schematically shown on the left in Fig. 2-8A. For the convenience of analysis, I take the approximation to express the "S"-shape characteristics with the combination of two straight lines as shown on the right in Fig. 2-8A. The third term of eq. (2-2) means the increment of [D] with compression at the air/water interface. To

simplify the analysis, it will be further assumed $k_1 >> k_{-1}$. This assumption is consistent with the observed stability of the bilayers formed at the zero surface pressure point. The kinetics of [D] can be then expressed as

$$\frac{d[D]}{dt} = k_1[S]^2 f(\pi) + \frac{N_D v}{A^2} \qquad (2\text{-}3),$$

and the kinetics of N_D can be obtained finally from

$$\frac{dN_D}{dt} = k_1 \frac{N_S^2}{A} f(\pi) \qquad (2\text{-}4),$$

where N_S is the number of PhDA2-8 molecules at the air/water interface.

Now I consider the relationship between the effective concentration (Γ_{eff}) and the surface pressure (π) at the air/water interface. Ideally, the surface pressure is directly proportional to the concentration of surfactants. However, as the actual π-A isotherms show several specific effects, such as limiting area and points of inflection, I shall assume the following relationships:

$$\Gamma_{eff} = [S] + \mathbf{a}\,[D] \qquad (2\text{-}5),$$

$$\Gamma_{eff} \le \Gamma_{eff,L} \Rightarrow \pi = 0 \qquad (2\text{-ii}),$$

$$\Gamma_{eff} > \Gamma_{eff,L} \Rightarrow \pi \propto (\Gamma_{eff} - \Gamma_{eff,L})^m \qquad (2\text{-iii}),$$

where Γ is the surface concentration of lipid molecules and it is inversely proportional to A, and **a** in eq. (2-5) is the correction factor representing the contribution of [D] (related to [S]) to the effective concentration, respectively. The effective concentration at the limiting area is expressed as $\Gamma_{eff,L}$. Judging from the actual π-A isotherms, the relationship between π and Γ_{eff} can be

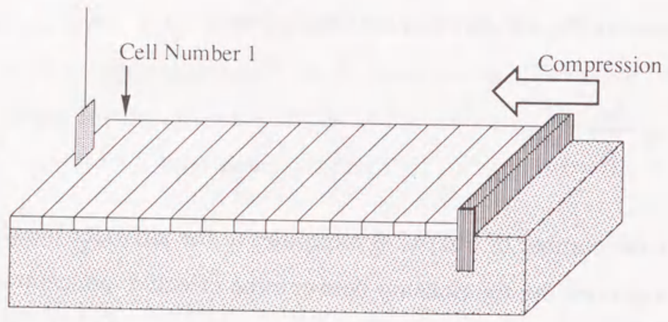

Figure 2-9.

Schematic representation of the model with rectangular cell.

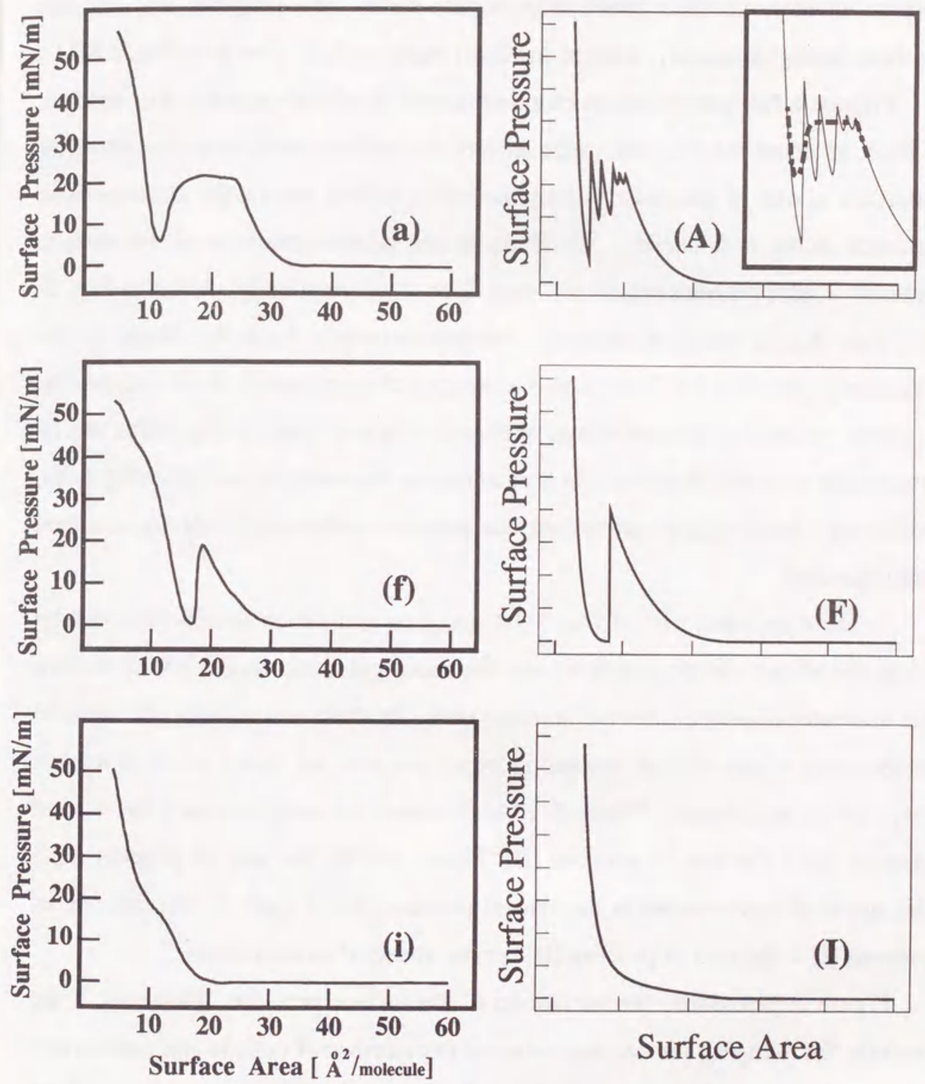

Figure 2-10.

Comparison between the results obtained by computer simulation and the experimentally observed π-A curves. The left-hand part of Figure 2-10(a), (f) and (i) is the same as in Figure 2-6. Parameters used in the simulation are;
a = 0.60, $\mathbf{k}_1$ = 0.75, (A) **v** = 1, (F) **v** = 0.5, (I) **v** = 0.01.

expressed in terms of a function of higher order. To simplify the analysis without losing generality, I put m in (2-iii) equal to 2, as shown in Fig. 2-8B.

To give a full interpretation of experimental results obtained in this section, it must be noted that the inhomogeneity of the surface pressure at the air/water interface is one of the most important factors giving rise to the characteristic features in the π-A curves. To illustrate the inhomogeneities of the surface pressure I adopt a rectangular cell model, as is schematically shown in Fig. 2-9. This model assumes that the air/water interface from the blade to the Wilhelmy plate can be divided into a number of equal small rectangular cells. I apply a simple argument that the rate of mass transfer by diffusion is proportional to the difference in concentration between the neighboring cells, while the concentration and the surface pressure within each cell are assumed homogeneous.

In the right-hand part of Fig. 2-10 is shown simulation results obtained by using the above kinetic equations and the rectangular cell model which divides the air/water interface into one hundred cells. In these simulations, the relative magnitudes of the rate of relaxation processes and the speed of compression were set up as follows. Figure 2-10A: the speed of compression > the rate of process (I) > the rate of process (II), Figure 2-10F: the rate of process (I) > the speed of compression > the rate of process (II), Figure 2-10I: the rate of process (I) > the rate of process (II) >> the speed of compression.

Figure 2-10A shows the oscillation of the surface pressure. However, if we include the damping factors and increase the number of cells in the simulation, the oscillation would be smoothed to a flat plateau such as it is represented by the dotted line.

It is evident that the above simulation results can reproduce essentially all characteristic features such as "flat plateau", "zero surface pressure", and "overshoot hump" observed in the actual π-A curves. These properties are

characteristic examples of nonlinearity in the nonequilibrium state of a thin film.

2-4. Conclusion

The π-A curves of a fatty acid containing both phenyl and diacetylene groups at the air/water interface were found to show such characteristics as "overshoot hump", "zero surface pressure", and "flat plateau". All of these non-equilibrium characteristics have been explained successfully by means of a kinetic simulation based on an autocatalytic and cooperative aggregation model of PhDA2-8 molecules and a rectangular cell model of surface area.

In the future, it will be necessary to obtain direct spectroscopic information on the stable aggregates (possibly bilayers) of PhDA2-8 fatty acids. Utilization of spectroscopic methods, such as epifluorescence microscopy,[13,21-24] may give us direct information on the unique nature in the transition of the thin film.

References

1) I. Langmuir, Trans. Far. Soc., **15** (1920) 62.
2) K. B. Blodgett, J. Am. Chem. Soc., **57** (1935) 1007.
3) Polydiacetylenes, Advances in Polymer Science; Cantow, H. -J., Ed.; New York, 1984; Vol.63.
4) G. Wegner, Recent Progress in the Chemistry and Physics of Poly(diacetylenes), in W. E. Hatfield(ed.), Molecular Metals, Plenum, New York, 1979, p209.
5) M. Brenton, J. Macromol. Sci. Chem., **21** (1981) 61.
6) A. Laschewsky, H. Ringsdorf, G. Schmidt and J. Schneider, J. Am. Chem. Soc., **109** (1987) 788.
7) B. Ostermayer, O. Albrecht and W. Vogt, Chem. Phys. Lipids, **41** (1986) 265.
8) B. Hupfe and H. Ringsdorf, Chem. Phys. Lipids, **33** (1983) 263.
9) D. J. Scoberg, D. N. Furlong, C. J. Drummond, F. Grieser, J. Davy and R. H. Prager, Colloids and Surfaces, **58** (1991) 409.
10) Y. Yoshioka, N. Nakahara and K. Fukuda, Thin Solid Films, **133** (1985) 11.
11) H. Matsuo, D. K. Rice, D. M. Balthasar and D. A. Cadenhead, Chem. Phys. Lipids, **30** (1982) 367.
12) B. Tieke and G. Lieser, J. Colloid Interface Sci., **88** (1982) 471.
13) S. W. Hui and H. Yu, Langmuir, **8** (1992) 2724.
14) D. Day and H. Ringsdorf, Journal of Polymer Science: Polymer Letters Edition, **16** (1978) 205.
15) C. McFate, D. Ward and J. Olmsted IIIrd., Langmuir, **9** (1993) 1036.
16) T. Kato, Y. Hirobe and M. Kato, Langmuir, **7** (1991) 2208.
17) J. C. Hatfield, J. W. Tayer and D. R. Bassett, Langmuir, **8** (1992) 2976.
18) Y. Kawabata, T. Sekiguchi, M. Tanaka, T. Nakamura, H. Komizu, K. Honda and E. Manda, J. Am. Chem. Soc., **107** (1985) 5270.
19) T. Kurata, A. Tsumura, H. Fuchigami and H. Koezuka, J. Phys. Chem., **95** (1991) 8831.
20) R. Tom, Stabilité Structurelle et Morphogénèse; Benjamin, New York, 1972.
21) A. Miller and H. Möhwald, J. Chem. Phys., **86** (1987) 4258.

22) H. M. McConnell, D. Keller and H. Gaub, J. Phys. Chem., **90** (1986) 1717.
23) N. Kimizuka and T. Kunitake, J. Am. Chem. Soc., **111** (1989) 3758.
24) M. Shimomura, K. Fujii, T. Shimamura, M. Oguchi, M. Shinohara, Y. Nagata, M. Matsubara and K. Koshiishi, Thin Solid Films, **210/211** (1992) 98.

3. EFFECTS OF COULOMBIC INTERACTIONS ON THE FEATURE OF THE ISOTHERM OF THE PHOSPHOLIPID THIN FILM

In the preceding section, the characteristic features in the π-A curve were shown, for example "overshoot hump" and "zero surface pressure" of a PhDA2-8 thin film, and these characteristics were explained in terms of the cooperative behavior between the PhDA2-8 molecules at an air/water interface. From the experimental findings, it was elucidated that neither overshoot hump nor zero surface pressure could be observed unless the subphase contained both $CdCl_2$ and $KHCO_3$ (see Fig. 2-3 (a)). Therefore, it was suggested that, as for the thin films with PhDA2-8 molecules containing carbonyl moiety, the well-established stabilization effect of cadmium ions might be enhanced in the presence of $KHCO_3$ as a result of its buffering capacity on the subphase pH around neutrality. In other words, the interaction between charged head groups (such as carbonyl moiety) may play an important role in the feature of the π-A isotherms.

In section 3, I would like to discuss the thermodynamic aspects of a phospholipid monolayer with special emphasis on the effects of the Coulombic interaction between the charged head-groups of the phospholipid molecules. Inclusion of the Coulombic interaction enables to obtain a new insight into the origin of the cooperative behavior between phospholipid molecules at the air/water interface.

3-1. Introduction

The ensemble of lipid molecules situated at the air/water interface can be regarded as composed of interacting "aggregates" in two-dimensional space. Different types of physico-chemical interactions have been found among the "aggregates", such as hydrophobic interaction, hydrogen bonding, van der Waals interaction, etc. Therefore, it can be expected that the essential feature of the thermodynamic state of the ensemble of the two-dimensional "aggregates" can be interpreted similarly as in the model of two-dimensional non-ideal gas. In other words, the surface pressure (π) - surface area (A) isotherm of the lipid film at the interface may be expressed by means of the virial expansion in a two-dimensional space.

Recently, Mingins and his co-workers observed the π-A isotherms of various phospholipids at an oil/water interface.[1] A marked first-order phase transition of the phospholipid monolayer was obtained with increasing the surface concentration of the phospholipid. However, they did not perform a detail analysis on the feature of the π-A isotherms. Therefore, in the following, I would like to discuss the actual isotherm of phospholipid film, by comparing the standard virial expansion with a different type of expansion implying the specific aspect of electrostatic interactions.[2]

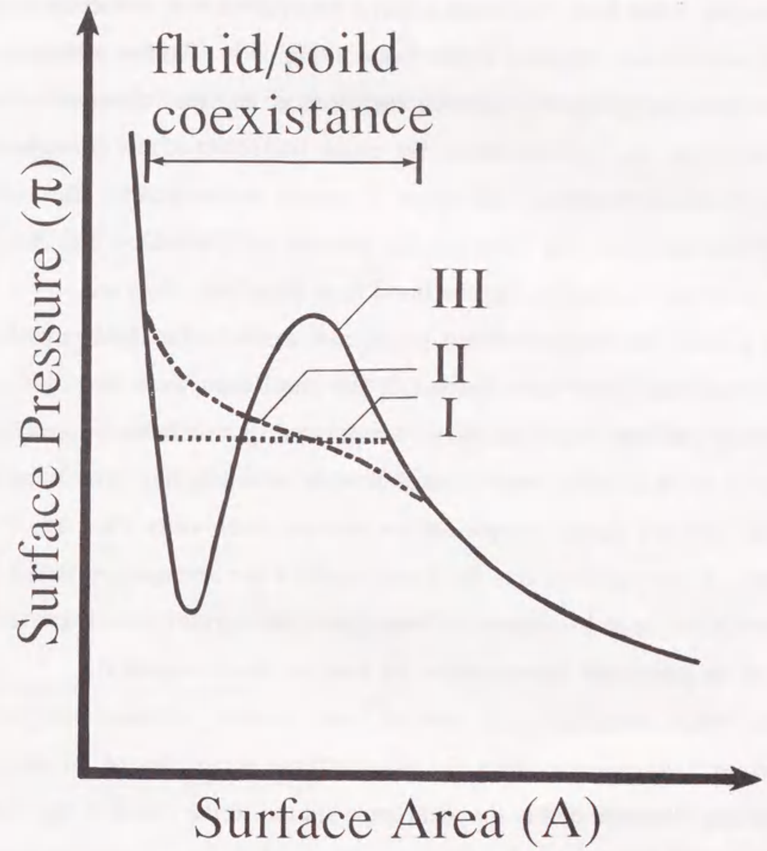

Figure 3-1.

Schematic representation of the π-A relationship of a lipid monolayer.

3-2. Theoretical Background[2]

In general, it has been well-known that a set of ideal π-A isotherms of lipid thin film will show as depicted by the line-I in Fig. 3-1. The flat plateau in the line-I indicates a region of fluid/solid coexistence, and the inflection point at the onset of the flat plateau shows the phase transition of the phospholipid monolayer at an interface. However, in actual measurement, the surface pressure does not generally show the flat plateau, as in line-II in Fig. 3-1, and the π-A isotherms as depicted by the line-I have been little observed.

To explain the feature of the actual π-A curves of a lipid monolayer, various equations have been derived.[3] As line-III shows in Fig. 3-1, two-dimensional van der Waals equation in representing π-A behavior, excepting the region of fluid/solid coexistence, is very much better than would be expected for any purely empirical expression with only two adjustable constants. Virial equation has the form expected for an equation based on a methodological, sound treatment of molecular interactions which are closely related to the parameter considered in the van der Waals' equation.

In 1982, Mingins et al. carried out a careful measurement of the equilibrium π-A characteristics for phospholipid molecules at an oil/water interface and observed nearly the ideal trace similar to the line-I in Fig. 3-1.[1]

On the other hand, it has been proposed that a theoretical model to interpret the π-A, or π-Γ, relationship by Yoshikawa et al.[2] When they took into account the effects of interaction between the polar head groups using similar degree of the approximation as in the Debye-Hückel theory, the following relationship results:

$$\pi = RT\Gamma\,(1 - \xi\Gamma^{1/2} + \alpha\Gamma) \qquad (3\text{-}1),$$

where α is the second virial coefficient in the usual two-dimensional van der Waals equation, and ξ is the parameter proportional to the Debye-Hückel length around the charged group.

Let us compare the theoretical isotherm of eq. (3-1) with the π-Γ relationship represented as the standard expansion with the second α and third β virial coefficients as in

$$\pi = RT\Gamma\,(1 + \alpha\Gamma + \beta\Gamma^2) \qquad (3\text{-}2).$$

Both eqs. (3-1) and (3-2) contain two "adjustable" parameters. Thus, the comparison of these equations with the results of actual measurements will allow us to the determine the validity of the unique expansion in eq. (3-1). Equation (3-2), standard virial expansion, can be re-arranged into

$$f(\Gamma) = \frac{\pi}{RT\Gamma^2} - \frac{1}{\Gamma} = \alpha + \beta\Gamma \qquad (3\text{-}3).$$

Similarly, eq. (3-1) gives

$$f(\Gamma) = \frac{\pi}{RT\Gamma^2} - \frac{1}{\Gamma} = \alpha - \xi\Gamma^{-1/2} \qquad (3\text{-}4).$$

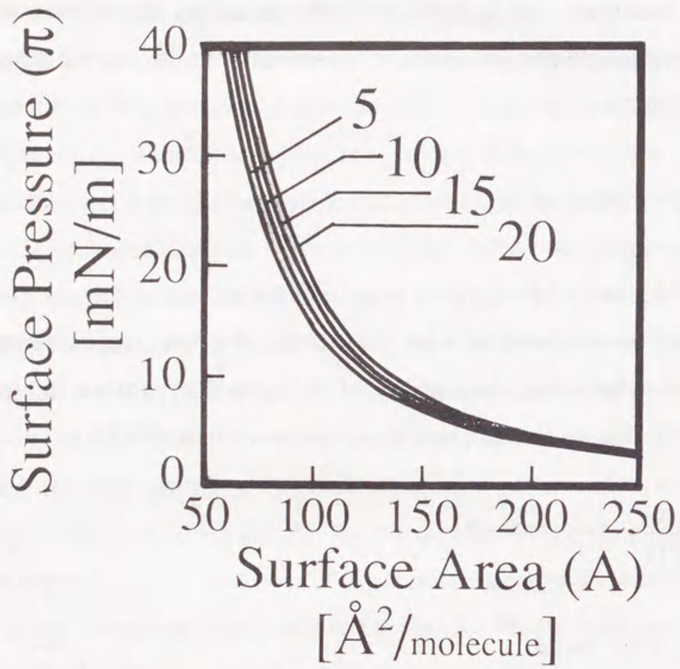

Figure 3-2.

π-A isotherm for 1,2-dimyristoyl lecithin at an n-heptane-aqueous NaCl solution interface. The numerals on the curves are the temperatures given in Celsius.

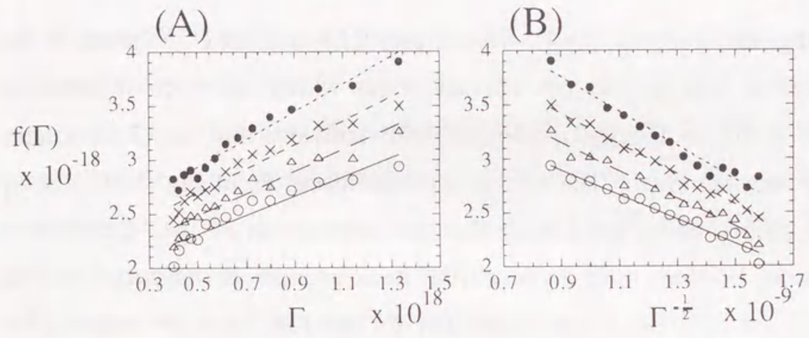

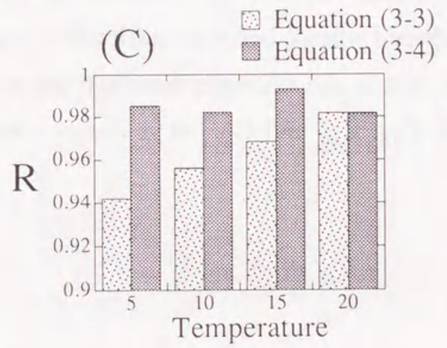

Figure 3-3.

(A) The plot of f(Γ) *vs.* Γ based on the data of Figure 3-2.
(B) The plot of f(Γ) *vs.* $\Gamma^{-1/2}$ for the following temperatures:
○, 5 °C; △, 10 °C; ×, 15 °C; ●, 20 °C.
(C) The comparison of the correlation coefficients, R, between the two different analysis.

3-3. Results and Discussion

Using eqs. (3-3) and (3-4), we can plot f(Γ) *vs.* Γ or $\Gamma^{-1/2}$ based on the experimental data on the π-A characteristics which had been reported by Mingins et al.(see Fig. 3-2).[4] Figure 3-3B indicates that eq. (3-4) is more realistic than eq. (3-3). The correlation coefficient, R, in Fig. 3-3C, for eq. (3-4) is nearly unity, suggesting that the assumption of the "Coulombic" interaction between the hydrophilic head-groups is essential in the interpretation of the isotherm, especially for the low Γ (or the large A, $\Gamma = nA^{-1}$, n stands for molar quantity) region.

Equation (3-1) implies that the π-Γ relationship becomes nonlinearity represented as "N"-shaped when ξ becomes sufficiently large. Indeed, Mingins et al. have reported that at the oil/water interface the π-A isotherms of the phospholipids with C_{18}, C_{20} and C_{22} alkyl chains show clear first-order transitions.[1]

3-4. Conclusion

It was elucidated that a Coulombic interaction between head-groups of amphiphilic compounds, which were adsorbed onto the oil/water interface, was important at the phase transition toward a condensed phase. If one takes the interaction between aggregates of amphiphilic molecules at the interface into consideration, it should be noted that the physico-chemical terms, such as surface pressure, was expressed by using unique terms included in eq. (3-4). Furthermore, it is an important point that the unique term ($-\xi\Gamma^{1/2}$) can be derived as a nonlinear function.

References

1) J. Mingins, J. A. G. Taylor, B. A. Pethica, C. N. Jackson, and B. Y. T. Yue, J. Chem. Soc., Faraday Trans. I, **78** (1982) 323.
2) K. Yoshikawa, S. Maeda, and H. Kawakami, Ferroelectrics, **86** (1988) 281.
3) A. W. Adamson, in "Physical Chemistry of Surfaces," 5th ed, John Wiley & Sons, Inc., New York (1990).
4) K. Yoshikawa, M. Makino, S. Nakata, and T. Ishii, Thin Solid Films, 180 (1989) 117.

4. SELF-PULSING AT A WATER/OIL INTERFACE IN THE PRESENCE OF PHOSPHOLIPIDS

In previous section, it was described that an importance of Coulombic interaction between amphiphilic head-groups at an oil/water interface. It should be noted that the interaction plays an important role in nonlinear behavior of the phospholipid thin film. In this section, I would like to introduce that the nonlinear interaction between lipid molecules at a water/oil interface generates the rhythmic oscillatory phenomena such as an electrical oscillation and a periodical interfacial change. Analysis on the oscillation performed by using a set of differential equations including the cooperative factors, which has been introduced in the previous section as an "N"-shaped nonlinear function, and the critical values of lipid concentration at the interface.

4-1. Introduction

Self-oscillation is one of the most fascinating phenomena in living organisms. There have been many studies on electrical phenomena associated with excitation or oscillation of biological membranes, such as those in nervous membranes and in beating heart cells. Despite extensive efforts, the physicochemical mechanism of bio-oscillation or bio-rhythm remains unknown. Biochemical approaches to this problem have encountered sever difficulties, i.e. the excitability and/or the ability for self-oscillation is destroyed during biochemical analysis. A study on artificial excitable membranes is therefore important. There have been many studies of oscillatory phenomena in artificial membranes, but the reproducibility of the oscillations has often rather poor.

Recently, Yoshikawa and his co-workers have found that sustained electrical oscillations are generated in a liquid membrane consisting of water/oil phase, where the aqueous phase contains surfactant and alcohol.[1-4] As the reproducibility of the oscillation in that system was quite good, the effect of various chemical species on the oscillation was studied qualitatively. It has been found that the frequency, amplitude and shape of the electrical oscillation change markedly on the various chemicals to the aqueous phase. Such a phenomenon has been interpreted in term of a nonlinear oscillation far from equilibrium.

In section 4, I would like to report on an oscillatory phenomenon at a water/oil interface in the presence of phospholipid by using the water/oil system. This finding is a quite important because phospholipid molecules are the main constituent of biomembranes. It was found that electrical oscillations were generated synchronously with rhythmic changes in the interface tension, suggesting a mechanism involving the periodic formation and destruction of

the phospholipid monolayer at the interface. The oscillation was explained as the cooperative character between lipid molecules on the interface with the aid of computer simulation.

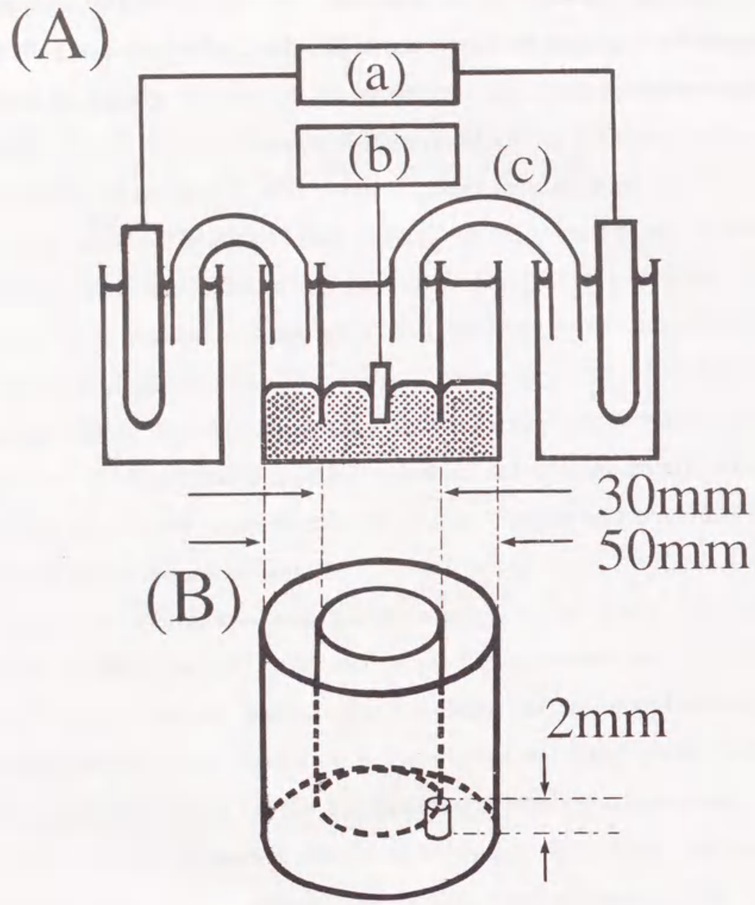

Figure 4-1.

(A) Side view of the experimental apparatus for the simultaneous measurements of electrical potential and interfacial tension.
(a) High impedance voltmeter, (b) electronic balance, (c) salt bridge.
(B) Bird-eye view of the apparatus.

4-2. Materials and Method

Experiments for the measurement of oscillations were performed using a cell in the form of a concentric hollow cylinder shown schematically in Fig. 4-1. A nitrobenzene solution (13ml) of 0.5mM tetraethylammonium bromide (TEAB) was placed at the base of the cell. TEAB was used to decrease the electrical resistance of the bulk organic-phase. An aqueous solution (8ml) containing both surfactant, sodium oleate or 1,2-dipalmitoyl-3-*sn*-phosphatidylethanolamine (DPPE), and alcohol, butanol, was carefully introduced into the inner cylinder and, simultaneously, 0.5M NaCl aqueous solution (14ml) was introduced into the outer cylinder. All measurements were carried out at 20±1°C.

The voltage across the aqueous/organic/aqueous phase, or the thin lipid film, was measured with a high-impedance voltmeter connected by two salt bridges to two Ag/AgCl electrodes. Interfacial tension was monitored by the Wilhelmy method using a hydrophilic glass plate (10 x 15 x 1mm). Analytical grade reagents were used. Nitrobenzene was distilled before the experiment. DPPE was available from Serdary Research Lab., Inc., Canada.

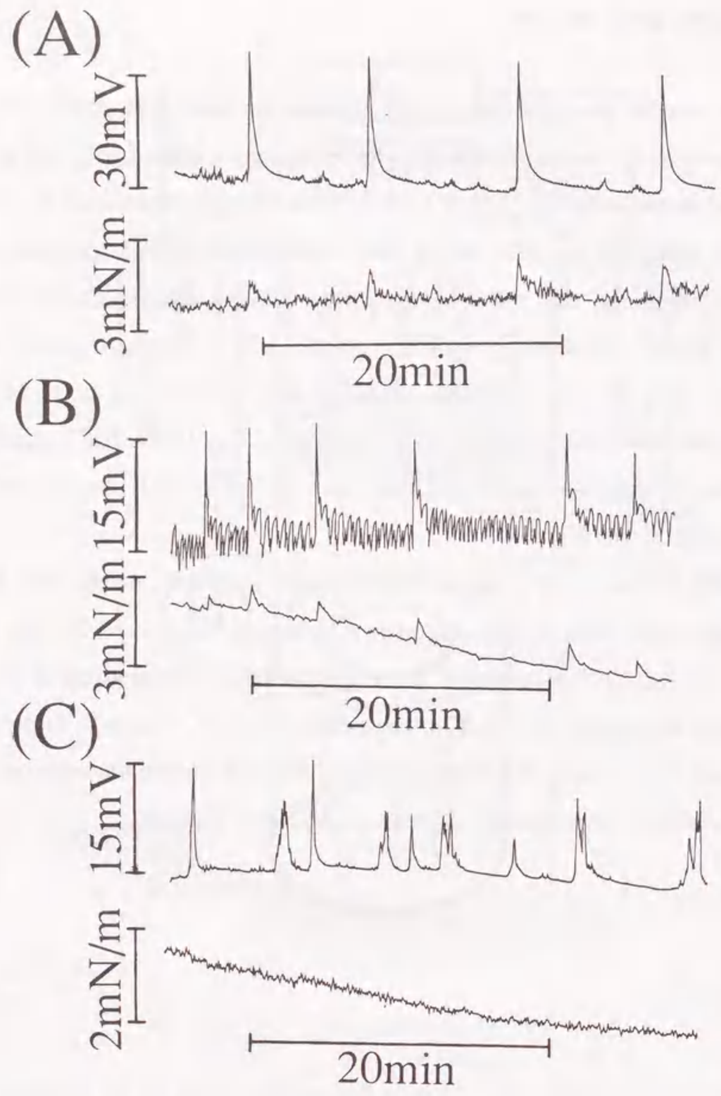

Figure 4-2.

Variations of the electrical potential and the interfacial tension. The aqueous phase in the inner cylinder are;
(A) 0.1 mM sodium oleate plus 5 vol% butanol.
(B) 0.07 mM DPPE plus 5 vol% butanol and
(C) 5 vol% butanol without surfactant.

4-3. Results and Discussion

An electrical oscillation and periodical changes of the surface tension at a water/oil interface

Figure 4-2 shows the results of the simultaneous measurement of electrical potential and interfacial tension for the liquid membrane with an aqueous phase of (A) 0.1mM sodium oleate plus 5vol% butanol, (B) 0.07mM DPPE plus 5vol% butanol and (C) 5vol% butanol. Rhythmic changes of the electrical potential (Figs. 4-2A and 4-2B) continued for 1-2 hr. The amplitude, the frequency, and the wave-form of the oscillations were found to be essentially the same for each experiment performed under fixed conditions. On the other hand, in the absence of the surfactant irregular pulses were observed (Fig. 4-2C). Such an irregular change in the electrical potential in Fig. 4-2C is attributable to the so-called Marangoni effect,[5] i.e. spontaneous interfacial turbulence accompanied by mass transfer across the interface. Let us note that the electrical potential and the interfacial tension change in a synchronized manner as it is shown in Figs. 4-2A and 4-2B, whereas no apparent change in the interfacial tension can be observed in Fig. 4-2C. When experiments were performed with DPPE and without butanol, only a few pulses were observed and sustained oscillations were not generated. Thus, the main driving force for the oscillations appears to be the diffusion of alcohol from the bulk aqueous phase to the organic phase through the interface, and the surfactant molecules induce a simultaneous or cooperative change over the entire interface.

As the interfacial tension is directly related to the concentration of surfactant molecules at the interface,[5] the rhythmic changes in the interfacial tension suggest that the concentration of surfactant, sodium oleate in Fig. 4-2A and DPPE in Fig. 4-2B, at the water/oil interface changes repeatedly between

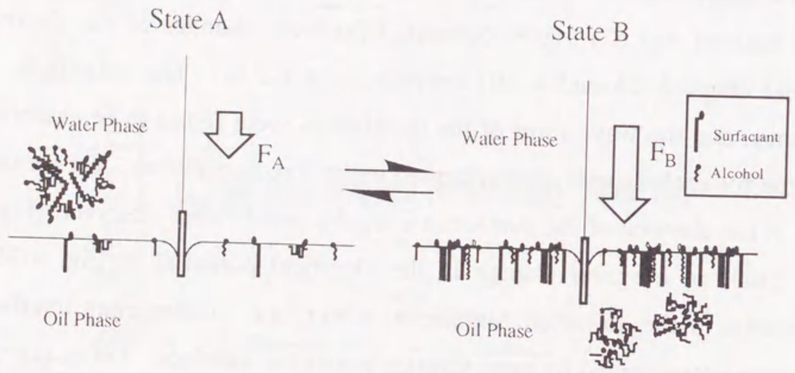

Figure 4-3.

Schematic representation of the repetitive formation and reconstruction of the lipid thin film.

Table 4-I
Repeated change of the interfacial state.

		State	
		A ⇌	B
Electrical potential	ΔE	low	high
Force change on the glass plate	ΔF	low	high
Surface tension	$\Delta\gamma$	high	low
Concentration of the surfactant	$\Delta\Gamma$	low	high

high and low values. The increase in the concentration of the surfactant molecules at the interface corresponds to the growth of the aggregates (monolayer) on the water/oil interface, which increases the electrical potential of the electronic bilayer. The synchronized change is shown schematically in Fig. 4-3 together with Table 4-I.

Theoretical explanation of the oscillations

Based on the above results and discussion, the mechanism for the rhythmic oscillations at the water/oil interface with surfactant and alcohol molecules may be explained in the following way[3,4,6] with Table 4-I. As the first step, surfactant and alcohol molecules diffuse from the bulk aqueous phase to the interface. The surfactant and alcohol molecules near the interface tend to form a monolayer. When the concentration of the surfactant together with the alcohol reaches an upper critical value, the surfactant molecules are abruptly transferred to the organic phase with the formation of inverted micelles or inverted microemulsions. This step should be associated with the transfer of alcohol from the interface to the organic phase. Thus, when the concentration of the surfactant at the interface decreases below the lower critical value, accumulation of the surfactant begins and the cycle is repeated. Rhythmic changes in the electrical potential and the interface tension are thus generated.

The foregoing interpretation of the mechanism, although necessarily somewhat speculative, provides a useful kinetic model.[7,8] Let X, Y, and Z be the concentrations of the key chemicals; X_i, the concentration of surfactant at and/or near the interface; Y_i, the concentration of alcohol near the interface; Z_i the concentration of the aggregate or complex of surfactant and alcohol at and/or near the interface.

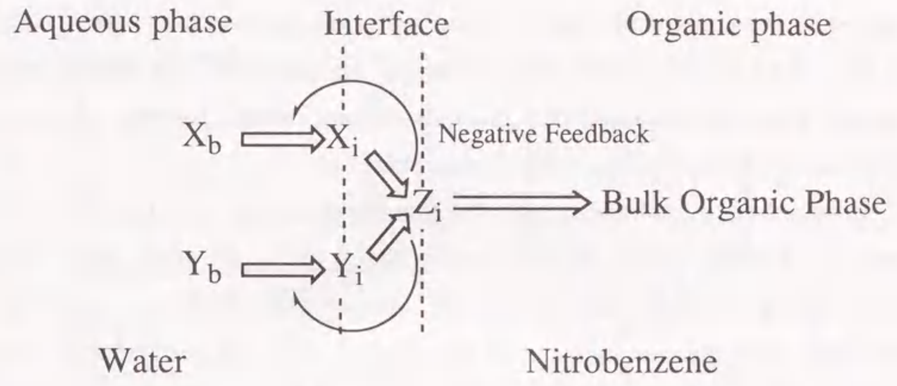

Scheme 4-1.
The process of transfer of surfactant and alcohol from the aqueous phase to the organic phase through the interface.

Scheme 4-1 can be considered as a possible explanation for the mechanism of oscillation in a liquid membrane. X_b and Y_b are the concentration of the surfactant and alcohol, respectively, in the bulk aqueous phase.

Scheme 4-1 is composed of the following steps (4-i)-(4-iv).

$$X_b \xrightarrow{D_X} X_i \qquad \text{(4-i)}$$

$$Y_b \xrightarrow{D_Y} Y_i \qquad \text{(4-ii)}$$

$$X_i + Y_i \xrightarrow{k_3} Z_i \qquad \text{(4-iii)}$$

$$Z_i \xrightarrow{k_4} \text{bulk organic phase} \qquad \text{(4-iv)}$$

Steps (4-i) and (4-ii) correspond to the migration of surfactant and alcohol from the bulk aqueous phase toward the water/oil interface. Step (4-iii) is the formation of aggregates of surfactant and alcohol at the interface, and is

related to the construction of the monolayer associated with surfactant and alcohol. Step (4-iv) indicates the migration of the aggregates of surfactant and alcohol from the interface into the bulk organic phase, forming inverted micelles or microemulsions in the organic phase.

It may be expected that the rates of transfer of surfactant and alcohol, D_X and D_Y, are affected by the negative feedback of Z_i. In other words, the diffusion rate, D_X, of surfactant from the aqueous phase to the interface may decrease with the net increase in the concentration of surfactant at the interface, X_i plus Z_i. A similar situation may hold for the diffusion rate, D_Y, of alcohol from the aqueous phase to the interface. Hence, the system kinetics may be considered under the following assumptions: (a) the concentration of surfactant and alcohol in the bulk aqueous phase, X_b and Y_b, remain constant; (b) the rates of diffusion of surfactant and alcohol from the bulk aqueous phase to the interface are expressed as $D_X(X_b - X_i)$ and $D_Y(Y_b - Y_i)$, respectively; (c) the negative feedback of Z_i on the diffusion of X and Y are given $Y_b - k_1Z_i$ and $- k_2Z_i$, respectively; (d) the rate of step (4-iv) is expressed as a function, $F(X_i,Y_i)$,with the rate constant k_3; and (e) the rate of step (4-iv) is expressed as a function, $G(Z_i)$, with the rate constant k_4.

Under these assumptions, the kinetics of the migration of surfactant and alcohol are described by the differential eqs.:

$$\frac{dX_i}{dt} = D_X (X_b - X_i) - k_1 Z_i \qquad (4\text{-}1),$$

$$\frac{dY_i}{dt} = D_Y (Y_b - Y_i) - k_2 Z_i \qquad (4\text{-}2),$$

$$\frac{dZ_i}{dt} = k_3 F(X_i,Y_i) - k_4 G(Z_i) \qquad (4\text{-}3),$$

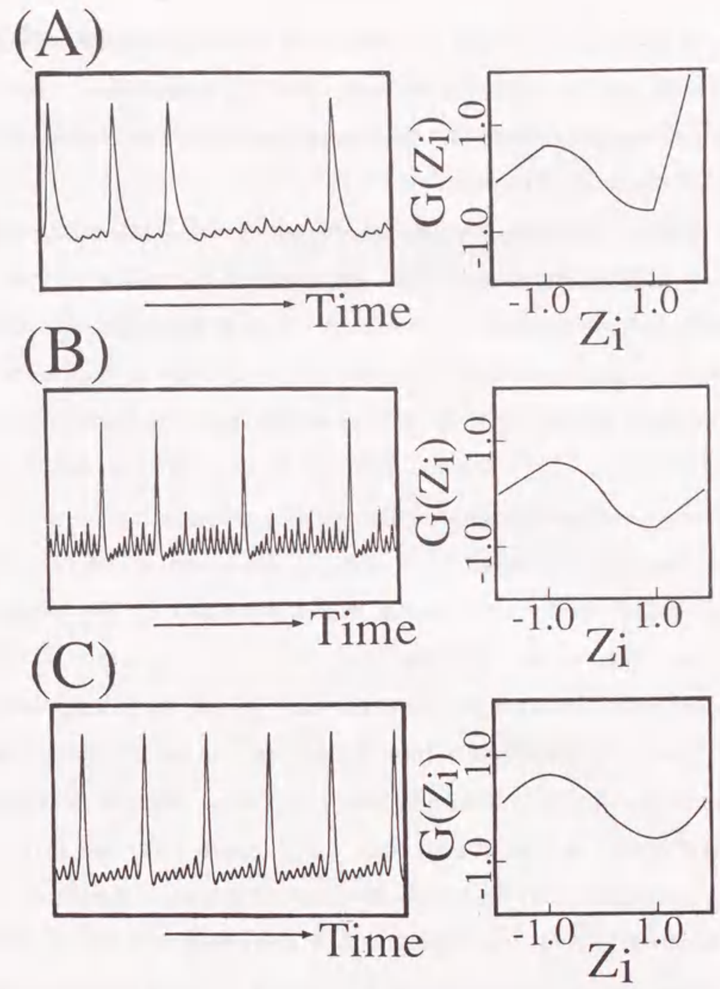

Figure 4-4.

Computer simulation of the oscillation of with variation of the nonlinear function $G(Z_i)$. Parameters are ;

(A) $D_X = 0.1$, $D_Y = 0.025$, $X_b = 0.4$, $Y_b = 2.56$, $k_1 = 0.2$, $k_2 = 0.05$, $k_3 = 2.5$, $k_4 = 2.5$.

(B) $D_X = 0.2$, $D_Y = 0.05$, $X_b = 0.4$, $Y_b = 2.5804$, $k_1 = 0.4$, $k_2 = 0.1$, $k_3 = 5.0$, $k_4 = 5.0$.

(C) $D_X = 0.1$, $D_Y = 0.025$, $X_b = 0.4$, $Y_b = 2.8$, $k_1 = 0.2$, $k_2 = 0.05$, $k_3 = 2.5$, $k_4 = 2.5$.

The shapes of $G(Z_i)$ are shown on the right side of Figure 4-4.

$F(X_i,Y_i)$ may be given by $(X_i + Y_i)$, a simple form for the synergetic effect of X_i and Y_i, which has the physical meaning that the monolayer is formed together with surfactant and alcohol. Self-oscillatory states can be obtained if $G(Z_i)$ has an "N"-shape nonlinearity.

Figure 4-4 shows numerical results for the set of eqs. (4-1), (4-2), (4-3). Comparison with the experiments, Figs. 4-4A and 4-4B indicates that the oscillation patterns have been well reproduced. Thus it becomes evident that repetitive formation and destruction of the monolayer are the key steps for the rhythmic pulsing. In the right of Fig. 4-4, the shape of the "N"-type nonlinearity, $G(Z_i)$ versus Z_i, is shown. When $G(Z_i)$ is a smooth function as in Fig. 4-4C, growing oscillations with regular bursting pulses are generated. On the other hand, the period between the bursting pulses becomes irregular when the derivative of $G(Z_i)$ is discontinuous as in Fig. 4-4A and B. The steepness on the right-hand side of the "N"-shape function is the important factor to induce the small pulses between the great bursting pulses, suggesting that the migration of phospholipid molecules from the interface to the organic phase is more significant that the migration of oleate molecules. Similar differences between phospholipid and oleic acid have been reported for the pressure-concentration relationships of their monolayers at an air/water interface. The shape of the function $G(Z_i)$ is thus expected to be correlated with the "N"-shape nonlinearity of the pressure-concentration relationship for lipid molecules at an interface.

4-4. Conclusion

In present section, rhythmic phenomena were analyzed by using a set of differential equations which were including the nonlinear factors($G(Z_i)$). The nonlinearity can be regarded as one of the expression of the cooperative interaction between lipid molecules adsorbed on a water/oil interface. If we understand the origin of the spatio-temporal phenomena such as the electrical oscillation, it should be noted that nonlinear characteristics, an "N"-shape relationship between the surface pressure *vs*. the surface concentration plays an important role.

References

1) K. Yoshikawa and Y. Matsubara, J. Am. Chem. Soc., **105** (1983) 5967.
2) K. Yoshikawa, S. Nakata, T. Omochi, and G. Collacicco, Langmuir, **2** (1986) 715.
3) K. Yoshikawa, M. Shoji, S. Nakata, S. Maeda, and H. Kawakami, Langmuir, **4** (1988) 759.
4) K. Yoshikawa and M. Makino, Chem. Phys. Lett., **160** (1989) 623.
5) A. W. Adamson, Physical Chemistry of Surface, 5th ed., John Wiley & Sons Inc., New York, 1990.
6) M. G. Velarde(ed.), Physicochemical Hydrodynamics Interfacial Phenomena, Plenum Press, New York, 1988.
7) K. Yoshikawa, S. Maeda, and H. Kawakami, Ferroelectrics, **86** (1988) 281.
8) K. Yoshikawa, M. Makino, S. Nakata, and T. Ishii, Thin Solid Films, **180** (1989)117.

5. DYNAMIC PROPERTIES OF A PHOSPHOLIPID THIN FILM AT AN AIR/WATER INTERFACE WITH A PERIODIC CHANGE IN SURFACE AREA

In the preceding section, the self-pulsing oscillation was observed at a water/oil interface which the fatty acid or phospholipids were adsorbed at, and the origin of the oscillation was explained as the periodical formation and deformation of the lipid thin film. In a thermodynamic point of view, the water/oil interface can be regarded as a non-equilibrium system. Therefore, we notice that an important relationship between these self-oscillatory phenomena and non-equilibrium system. In other wards, it should be pointed out an importance of the dynamic behavior of lipid thin films at an interface to understand the oscillatory phenomena deeply. In this section, I would like to introduce the dynamic behavior of phospholipid.

Dynamic surface pressure (π) - surface area (A) characteristics were measured using periodic changes in the surface area of an unsaturated phospholipid (1,2-dioleoyl-3-*sn*-phosphatidylcholine; DOPC) thin film formed at an air/water interface. It was found that the dynamic π-A curve traced a single closed hysteresis loop after several cycles of compression and expansion, and that the loop shape was markedly dependent on the frequency of surface area change, the subphase temperature and the chemical species dissolved in an aqueous subphase. In order to evaluate the loop shape in a quantitative manner, we carried out Fourier-transformation of the time-dependent change in surface pressure. As the higher harmonic components were obtained in the Fourier spectra, it has become clear that the DOPC thin film during compression and expansion behaves as a nonlinear viscoelastic body. We established a useful kinetic model taking into account of cooperative aggregation/dissociation of DOPC domains at the air/water interface with the

periodic surface area change. The hysteresis loops were examined with the aid of a computer simulation with the inclusion of the cooperative factor.

5-1. Introduction

Phospholipid monolayers at an air/water interface have been regarded as a good model of biomembrane, because several physicochemical properties such as surface pressure can be monitored directly.[1,2] Actually, there have been many studies on the surface pressure (π) - surface area (A) curves obtained under a quasi-static compression. The π-A curve affords the quantitative measure of elastic modulus of the monolayer in convenient manner.[3,4] However, it is clear that the variety of dynamic aspects in biomembrane, such as self-oscillatory phenomena (bursting of nerve cell, active transport and energy transition) are generated from nonequilibrium conditions. Therefore, in order to understand the essential parts in the functions of the biomembrane, it is necessary to elucidate the physicochemical properties of membranes under nonequilibrium or dynamic experimental conditions.

The past experimental studies on the dynamic behavior of lipid thin film spread over an air/water interface are roughly categorized into two different methods.[1,5] First method is the measurement under very small micro-deformation of the surface area, such as thermal fluctuation,[6] capillary wave,[7] etc.[8] Second method is the measurement under large-deformation of surface area by using mechanical movement of a pair of blades or Teflon ribbons.[9-12] In a rheological point of view, the former method concerns with the dynamic behavior of lipid thin film between 10^{-6} and 1sec.[13-15] The observed surface pressure change has been analyzed within linear stress-relaxation framework because the most lipid thin films have been regarded as linear viscoelastic bodies in this time scale. On the other hand, the viscoelastic properties of the lipid thin film in the order of $1 \sim 10^3$sec is elucidated from the latter method.[16] Although numerous studies have claimed that the lipid thin films behave as

nonlinear viscoelastic bodies during the large-deformation such as the periodical compression and expansion,[1,17-20] there has been not established method of analysis on the nonlinear characteristics.

Recently, the structure of the phospholipid monolayer mixed with fluorescence compounds at an air/water interface has been successfully visualized by using a fluorescent microscopy.[21,22] It was found that the phospholipid molecules form domain structure at the phase transition region accompanied with compression, and that the shape of the domains markedly depends on the experimental conditions such as compression rate, subphase temperature and kinds of the phospholipids. As the formation of the domains appears around the inflexion point in the π-A curve, it is expected that the nonlinear viscoelastic properties with large-deformation are closely related to the inhomogeneity of the lipid thin film. In other words, the shape of the dynamic π-A curves reflects not only the elastic modulus of the lipid thin film but also the characteristics on the interaction between domains and/or aggregates.

Recently, we have established the experimental condition to observe a single closed hysteresis loop with periodical change of the surface area.[23] As an analysis method of the dynamic π-A curve, we adopted Fourier-transformation technique to evaluate the viscoelastic properties of lipid thin film. This method has the merits such as (i) the linear and nonlinear properties in the thin film are distinguishable, and (ii) the elastic and viscous characteristics are also distinguishable as the components in the Fourier real and imaginary parts, respectively.[23-25] In the present study, dioleoylphosphatidylcholine (DOPC) was chosen as the chemical material to constitute a monolayer. It is noted that unsaturated phospholipids are the main components of biomembranes. To clarify the viscoelastic behavior of the membrane, we measured the dependence of the dynamic surface pressure of

the DOPC monolayer on frequency change of the surface area, subphase temperature and inorganic species. In addition to this, by using a Brewster angle microscopy (BAM), the structure of DOPC thin film at the air/water interface was observed directly.[26-28] We propose a useful kinetic model which includes the cooperative aggregation/dissociation between the DOPC two-dimensional domains during the periodical compression and expansion process. The experimental trends of the characteristic feature in the dynamic π-A curves, especially nonlinear viscoelastic properties of the DOPC thin films, are reproduced with the aid of the computer simulation based on the kinetics.

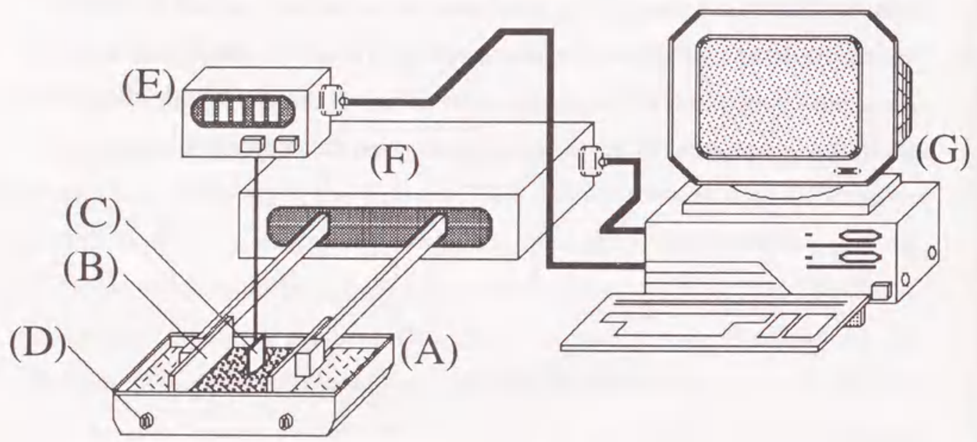

Figure 5-1.

Schematic representation of the experimental arrangement used for the measurement of the dynamic π-A curves of a DOPC thin film at the air/water interface;
(A) trough, (B) blade, (C) platinum plate(Wilhelmy plate),
(D) connector for water circulation, (E) electronic balance,
(F) controller of the blades, (G) micro-computer.

5-2. Materials and Method

DOPC, a synthetic phospholipid, was obtained from Avanti Polar Lipid Inc. Other reagents were analytical grade chemicals and were purchased from Wako Pure Chemical Industries, Ltd. Before each experiment, water was distilled with an all-glass apparatus (SA-2000E, Tokyo Rika Kikai Co. Ltd., Japan), and purified further with a Millipore Milli-Q filtering system maintained at a resistivity above 18.0MΩcm. Chloroform was purified by three consecutive distillations. DOPC (0.133mM) dissolved in chloroform was used as the spreading solution.

Dynamic surface pressure measurement

Dynamic π-A curves were obtained using a trough equipped with a pair of moving blades, as shown in Fig. 5-1. This experimental apparatus was designed by us and manufactured by Kyowa Interface Science Co., Ltd.[25] The trough (200mm long, 50mm wide and 10mm deep) was coated with Teflon. The subphase temperature was controlled within ±0.1°C using a water-jacket connected to a thermostated circulation system, and environmental air temperature was kept at 19°C. The surface tension at the air/water interface was measured using a Wilhelmy plate of platinum (24.5 x 10.0 x 0.15mm), polished with 250-mesh emery. The accuracy of the measurement was estimated to be ±0.2mN/m. The surface pressure (π) has been defined as the eq. (2-1) in section 2. The observed surface pressure was successively stored in a personal computer (PC-9801, NEC, Japan), and then Fourier-transformed to a frequency domain. The blade motion was regulated with a pulse-step motor.

The chloroform solution of DOPC was spread over the air/water interface using a microsyringe. After waiting for 30min to attain thermal equilibrium, the surface area was changed repeatedly. The dynamic surface pressure was observed after four compression and expansion cycles, because it was confirmed that the π-A curve became to trace a single-closed loop at most four cycles of the compression and expansion.

Brewster angle microscopic observation of monolayers

Visualization of the DOPC monolayer at the air/water interface was carried out by Brewster angle microscope,[29] BAM, (Nippon Laser & Electronics Labs., model NL-EMM633). The microscope system was mounted on a moving-wall type film balance (Nippon Laser & Electronics Labs., model NL-LB150-MW). An incident laser light with *p* -polarization was used under the Brewster angle (ca. 62°) against the surface of aqueous subphase. The wave length was 632.8nm, and the extinction ratio was $1/10^{-5}$. The resulting picture of the reflected beam was stored with a video recorder. In the present study, the BAM micrograph was obtained at a constant surface pressure after gradual compression of the spread monolayer of DOPC.

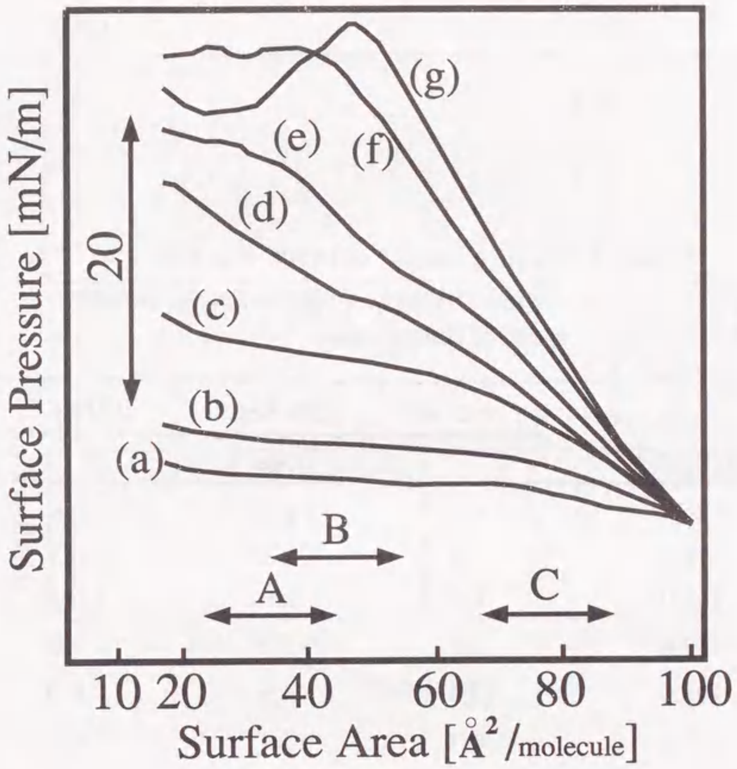

Figure 5-2.

π-A curves of a DOPC thin film at the air/water interface with a constant speed of compression. The compression speed was;
(a) 39.5mm²/sec, (b) 78.8mm²/sec, (c) 118mm²/sec, (d) 157mm²/sec,
(e) 196mm²/sec, (f) 275mm²/sec, and (g) 390mm²/sec, respectively.
The subphase temperature was 20°C. A, B, and C in Fig. 5-2 indicate the region in which measurements were performed with periodic compression and expansion (cf. Figs. 5-3, 5-4, 5-5, 5-6, 5-8).
A; from 22 to 42Å²/molecule, B; from 34 to 54Å²/molecule and
C; from 68 to 88Å²/molecule.

Table 5-I. Elastic modulus* of DOPC thin film around 55Å^2/molecule obtained under constant speed of compression.

Compression speed [mm^2/sec]	control**	0.5M NaCl	0.5M KCl
	[N/m^3]		
39.5	0.1	0.2	0.6
78.8	0.4	1.2	0.5
118.0	1.4	2.6	1.9
157.0	2.8	3.1	2.8
196.0	3.4	4.6	**6.2**
275.0	**6.6**	5.4	6.6
390.0	8.3	7.9	8.4

* Estimated experimental error is ±0.2N/m^3

** The subphase is dissolved water without any salts.

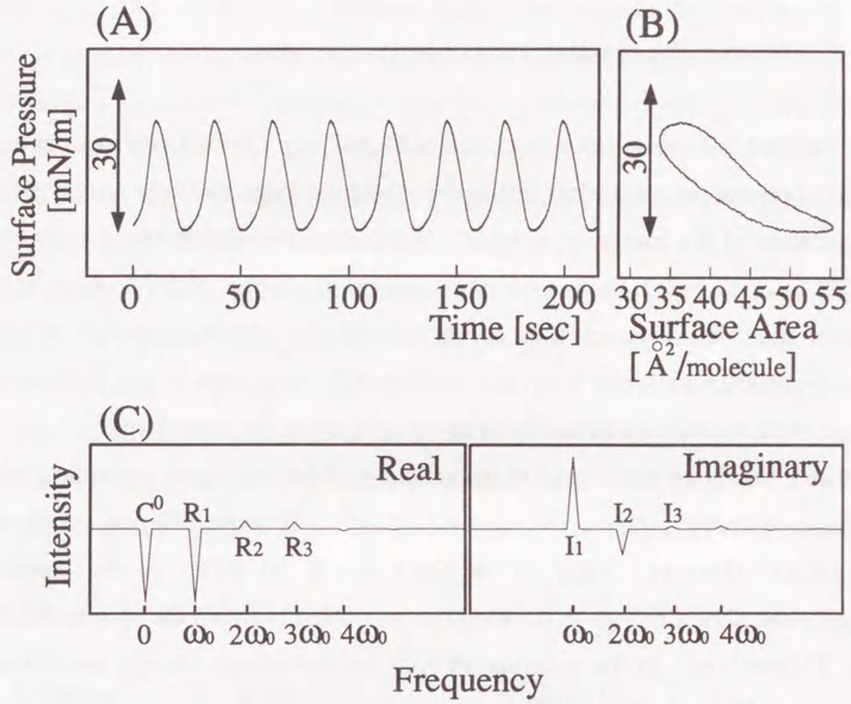

Figure 5-3.

Dynamic surface pressure of a DOPC thin film with a sinusoidal change in surface area. The frequency was 31.8mHz. The surface area changed from 34 to 54Å^2/molecule (see B in Fig. 5-2).
(A) Time trace of the dynamic surface pressure,
(B) Hysteresis loop, dynamic π-A curve, after four cycles of compression and expansion.
(C) Complex Fourier-transformation of (A).

5-3. Results and Discussion

π-A curve with constant speed of the compression

Figure 5-2 shows the π-A curves of DOPC thin film with constant speed of the compression. It is clear that as the whole the slope becomes steeper with the increase of the compression speed. When the compression speed was very high(e.g., Fig. 5-2g), inflection point appeared around 50Å^2/molecule. It is known that the slope of π-A curve reflects the elastic modulus of the monolayer at an air/water interface, and the inflection point in the π-A curve suggests the occurrence of the domains or collapse of the monolayer.[1,3]

Table 5-I shows the change of the elastic modulus calculated from the slope of the π-A curve around 55Å^2/molecule (see Fig. 5-2) with different subphase conditions; dissolved water, 0.5M NaCl and 0.5M KCl. In the control experiment, abrupt change in the modulus was noted between the speeds of 196 and 275mm^2/sec. In the presence of KCl, similar abrupt change was found between 157 and 196mm^2/sec. On the contrary, no abrupt change was observed in the presence of NaCl.

Nonlinear viscoelasticity of DOPC thin film with periodical change of the surface area

Figure 5-3A shows the time-dependent change in the surface pressure induced by a sinusoidal change in the surface area for DOPC thin film on the subphase of distilled water. Figure 5-3B shows the π-A curves in the steady closed loop, which was obtained after four cycles of compression and expansion. If the thin film is an ideal viscoelastic body, the dynamic π-A curve must trace a genuine elliptical loop. As the π-A curves traced a warped

elliptic feature as in Fig. 5-3B, the actual DOPC thin film should be interpreted as a nonlinear viscoelastic body. To evaluate the nonlinearity of the viscoelastic characteristics in a quantitative manner, the time dependence of the surface pressure in the steady cycles of compression and expansion was Fourier-transformed for the time trace. Figure 5-3C shows the Fourier spectra with the frequency domain. The real, R, and imaginary, I, parts correspond to the elastic and viscous components of the DOPC thin film, respectively. The constant peak intensity (C^0) in the real part has the physical meaning as the time average of the surface pressure change.

It is well established that, on the case of an ideal viscoelastic body, sinusoidal stress with frequency ω_0 induces sinusoidal strain with the same frequency ω_0. On the other hand, higher harmonics (R_2, I_2 ...) in the frequency spectra represent the nonlinear viscoelastic characteristics (see Fig. 5-3C).

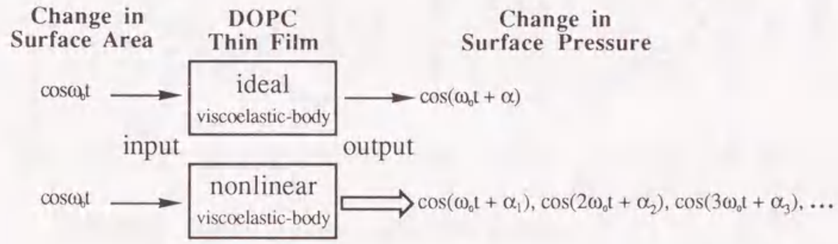

Scheme 5-1

The difference in the responses of ideal (linear) and nonlinear viscoelastic bodies to the sinusoidal stress is illustrated in the above scheme. In a nonlinear viscoelastic body, the frequency of the output strain can be expressed with the expansion of the higher harmonics.

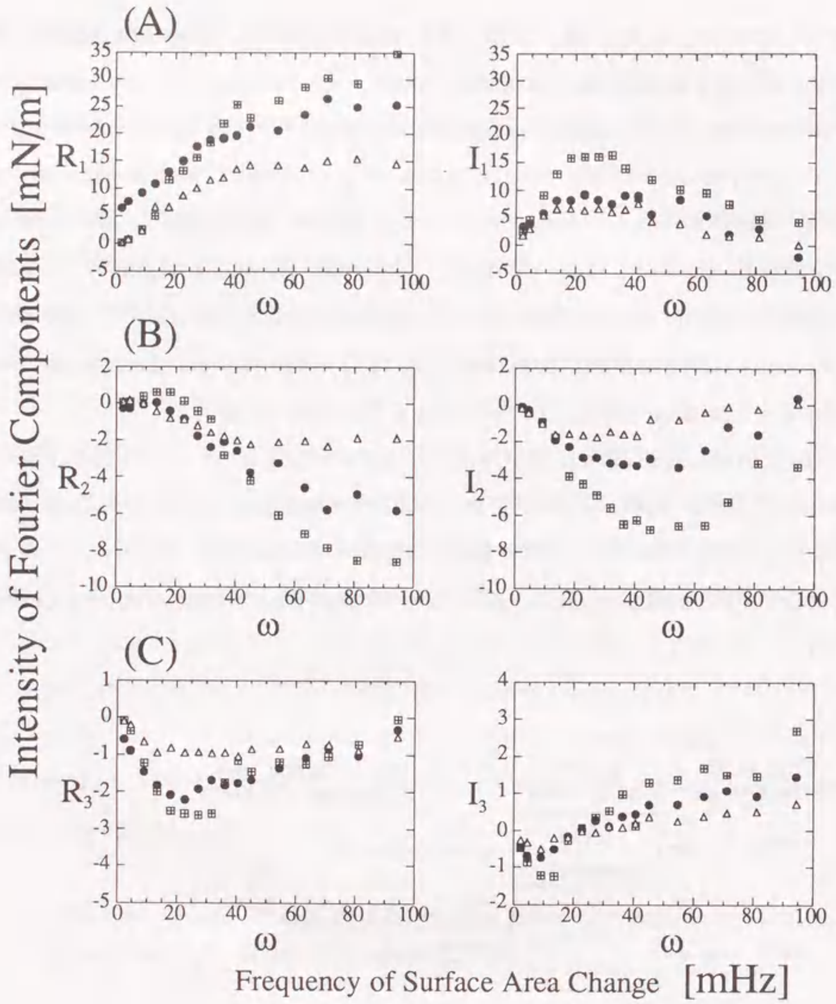

Figure 5-4.

Frequency dependence of the intensities of Fourier components. The left side of this figure indicates the Fourier real spectra, and the right side indicates the imaginary spectra. The frequency was changed from 2.3 to 94.3mHz.
(A) fundamental harmonic components, (B) second harmonic components,
(C) third harmonic components.
The change in the surface area and the compression ratio were,
⊞; from 22 to 42Å^2/molecule, 0.476, ● ; from 34 to 54Å^2/molecule, 0.370 and
△ ; from 68 to 88Å^2/molecule, 0.227.

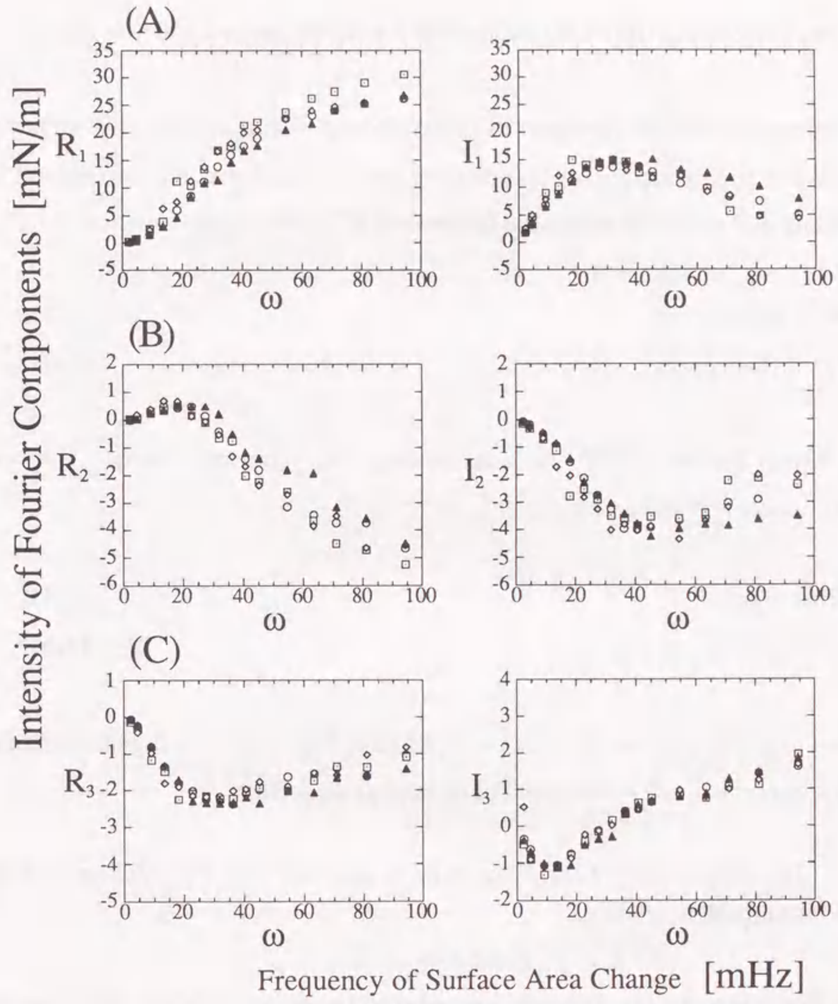

Figure 5-5.

Effect of metal mono-valent cations on the frequency dispersion of DOPC thin film. The surface area changed from 34 to 54Å^2/molecule. The left side of the Figure indicates the Fourier real spectra, and the right side indicates the imaginary spectra.
(A) fundamental harmonic components, (B) second harmonic components,
(C) third harmonic components.
○ ; 0.5M LiCl, ⊡ ; 0.5M NaCl, ◇ ; 0.5M KCl, ▲ ; 0.5M NH_4Cl.

$$\pi = \pi_0 + \pi_1\cos(\omega_0 t+\alpha_1) + \pi_2\cos(2\omega_0 t+\alpha_2) + \pi_3\cos(3\omega_0 t+\alpha_3) + \cdots \quad (5\text{-}1).$$

When $\cos(\omega_0 t+\alpha_1)$ is rewritten as $(\cos\alpha_1\cos\omega_0 t - \sin\alpha_1\sin\omega_0 t)$, it is apparent that the real and imaginary components in the first harmonic correspond to elasticity and viscosity within the framework of "*linear approximation*",

$$R_1 = \pi_1\cos\alpha_1 \quad (5\text{-}2),$$
$$I_1 = \pi_1\sin\alpha_1 \quad (5\text{-}3).$$

The higher harmonic terms such as $\cos(n\omega_0 t+\alpha_n)$ represents as eqs. (5-4) and (5-5), where n is integer.

$$R_n = \pi_n\cos\alpha_n \quad (5\text{-}4),$$
$$I_n = \pi_n\sin\alpha_n \quad (5\text{-}5).$$

In our experimental results as is exemplified in Fig. 5-3C, the higher harmonic components with $n \geq 4$ are found to be negligible small.

The dependence of the Fourier peak intensities on the frequency of the surface area change

We measured the dynamic viscoelastic behavior of DOPC thin film by changing the frequency in the cycle of compression and expansion, and analyzed the nonlinear components using of the Fourier transformation (see Fig. 5-4). As the compression ration was increased from 0.227 to 0.476, the maximum of I_1 migrated to the right. This experimental tendency was marked for the I_2 as shown in the right-side of Fig. 5-4B.

Figure 5-5 shows the frequency dispersion of the intensities in the Fourier spectra in the presence of inorganic salts. At low frequencies, the frequency

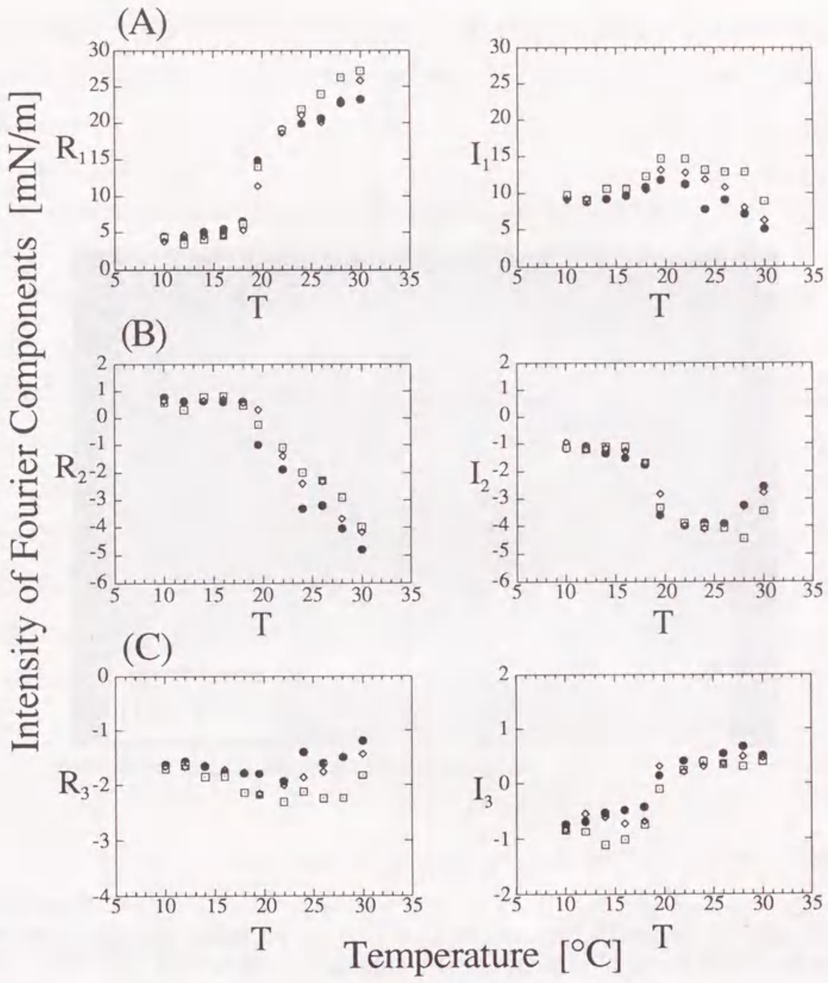

Figure 5-6.

Effect of subphase temperature on the Fourier peak intensities. The surface area was changed from 34 to 54Å^2/molecule. The frequency of this change in surface area was 31.8mHz. The left side of the Figure indicates the Fourier real spectra, and the right side indicates the imaginary spectra.
(A) fundamental harmonic components, (B) second harmonic components,
(C) third harmonic components.
●; control experiment, ⊡; 0.5 M NaCl, ◇; 0.5 M KCl.

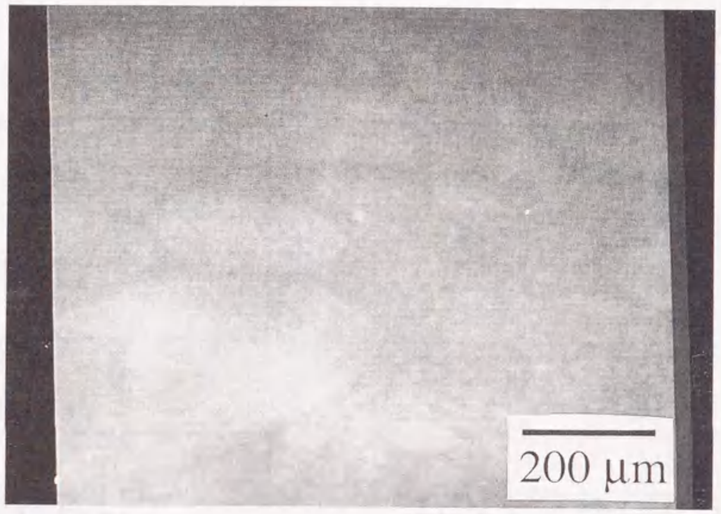

Figure 5-7.

"Oil droplet" or "island structure" of DOPC at an air/water interface observed with a Brewster angle microscope. The subphase temperature was 20°C. The surface area was 600Å^2/molecule.

dependence in the presence of 1:1 salts was almost the same as in the absence of them. At high frequencies, there existed clear difference between different salts.

Temperature dependence of the Fourier peak intensities

Temperature dependence of the nonlinear viscoelasticity, or the Fourier intensity, was measured for the range between 10 and 30°C. As shown in Fig. 5-6, it is noted that the viscoelasticity of DOPC thin film exhibits abrupt transition around 20°C. It is known that DOPC shows gel/liquid-crystal transition at -22°C.[30] However, there has been no report on the transition of DOPC near room temperature. Thus, the transition around 20°C is attributable to some kind of "*kinetic*" process of DOPC film under dynamic change of the surface area. In the Discussion, we interpreted such a transition in relation to the effects of domain formation in the DOPC thin film.

Domain formation at the air/water interface

Figure 5-7 shows the results of BAM observation on the structure of DOPC domains at 600Å^2/molecule. The dark area in the figure indicates the region of free water surface. The bright part is attributed to the presence of DOPC monolayer, where incident light is reflected owing to the presence of the lipid film.

This result clearly indicates that the DOPC molecules form domains at the interface. Many isolated domains were explicitly observed even at 0mN/m, and the scale of the largest domain was ten times comparing with that of saturated phospholipids.[1] The manner in the change of the surface pressure accompanied with the compression is expected to be neatly concerned with the domain formation. If the DOPC thin film is compressed, it seems that the

isolated domains collide and gather with increasing the surface pressure. Therefore, it is considered that the collision and the gathering between DOPC domains are intrinsic processes which are associated with the dynamic surface pressure change.

Evaluation of the elastic modulus and relaxation time of DOPC thin film based on the nonlinear Maxwell model

In general, it has been considered that elastic modulus and relaxation time reflect the viscoelastic properties of a lipid thin film with time-dependent surface area change.[15,31] Maxwell model, which is illustrated schematically by a spring and a dashpot (see scheme 5-2), is a useful model to evaluate the dynamic behavior of lipid thin film with sinusoidal perturbation. However, from our experimental results, it has been clear that the DOPC film at the air/water interface should be regarded as a nonlinear viscoelastic body under the dynamic compression and expansion process. Therefore, it is necessary to improve the Maxwell model to analyze the nonlinear characteristics of DOPC film, because Maxwell model is only applicable to characterize linear viscoelastic behavior.

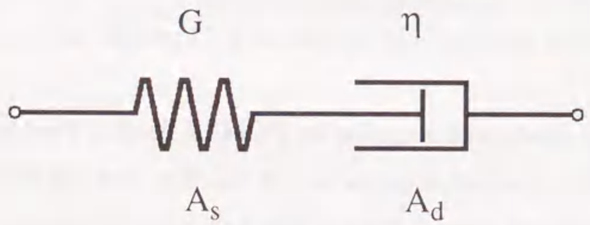

Scheme 5-2

In our experiments, the surface area was changed in a sinusoidal manner. Thus, the time dependent change of the surface area, ΔA, is given by,

$$\Delta A = A_0(1 - \cos\omega t) \qquad (5\text{-}6).$$

Here, we would like to assume that ΔA is divided two different contributions, A_s and A_d, which are the surface area changes corresponding to the spring and the dashpot, respectively.

$$\Delta A = A_s + A_d \qquad (5\text{-}7),$$

A_s and A_d will be expressed as follows:

$$A_s = A_{0s} - A_{1s}\cos\omega t \qquad (5\text{-}8),$$
$$A_d = A_{0d} - A_{1d}\cos\omega t \qquad (5\text{-}9),$$

In order to interpret the nonlinear viscoelastic properties in a quantitative manner, we adapt the polynomial expansion.

$$\pi = G_1A_s + G_2A_s^2 + O(A_s^3) + \eta_1\frac{d}{dt}A_d + \eta_2\left(\frac{d}{dt}A_d\right)^2 + O\left\{\left(\frac{d}{dt}A_d\right)^3\right\} \quad (5\text{-}10).$$

Where G_1 and η_1 indicate the linear elastic and viscous coefficients, respectively. G_2 and η_2 are the terms originated from the nonlinear elastic and viscous property. In order to simplify the discussion of the nonlinear viscoelastic properties of the DOPC thin film, here we will neglect the higher polynomial terms such as A_s^3, $(dA_d/dt)^3$, A_s^4, $(dA_d/dt)^4$, etc. In the actual experiments, it has been confirmed that the higher components have negligible contributions (see Fig. 5-3C).

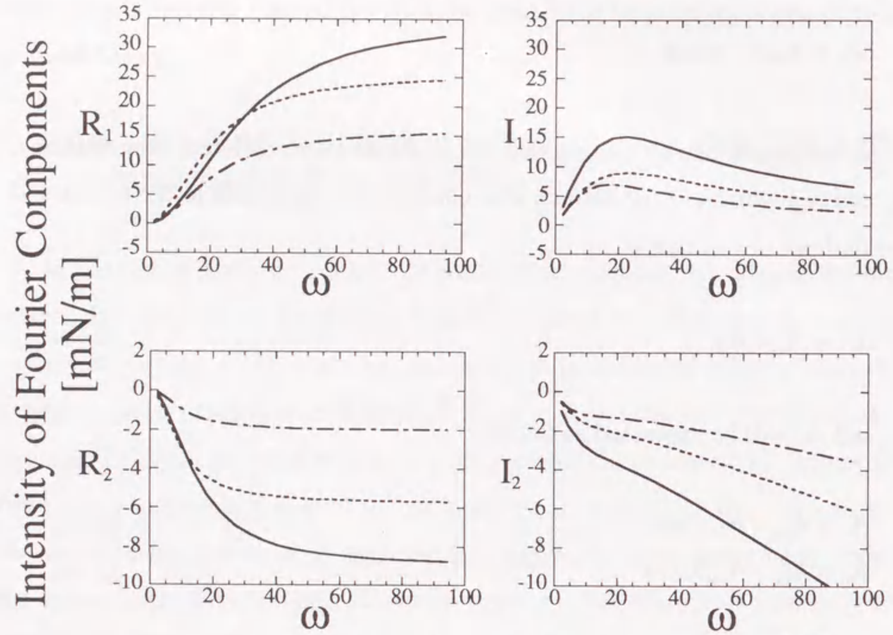

Figure 5-8.

Theoretical frequency dispersion based on the non-linear Maxwell model. All of the parameters were deduced by least-square fitting to the experimental results (Fig. 5-4A).
Top; fitting curves of fundamental harmonic components of Fourier spectra,
Bottom; simulated curves using parameters which were obtained by fitting.
———— ; from 22 to 42Å^2/molecule, correlation coefficient (r) = 0.99,
---------- ; from 34 to 54Å^2/molecule, r = 0.96, and
—·—·—·—·— ; from 68 to 88Å^2/molecule, r = 0.98.

Table 5-II. Elastic modulus and relaxation time of DOPC thin film in the presence of 0.5M inorganic salt.

category	Elastic modulus (G_1') [N/m^3]	Relaxation time (τ) [sec]
control (without salt)	(18[a]	34[a])
	13	52
	(8[b]	48[b])
LiCl	16	27
NaCl	17	29
KCl	14	35
NH_4Cl	15	27
$MgCl_2$	16	28
$CaCl_2$	17	28
$AlCl_3$	17	30

The elastic modulus and the relaxation time were evaluated based on nonlinear Maxwell model, for the surface area between 34 and 54Å^2/molecule, except for the control values given within the parentheses.

a) Data obtained for the region of surface area change between 22 and 42Å^2/molecule.

b) Data obtained for the region of surface area change between 68 and 88Å^2/molecule.

From eqs. (5-8), (5-9) and (5-10), we obtain eqs. from (5-11) to (5-14).

$$R_1 = \frac{G_1'}{1 + \tau^2\omega^2}\tau^2\omega^2 \qquad (5\text{-}11),$$

$$I_1 = \frac{G_1''}{1 + \tau^2\omega^2}\tau\omega \qquad (5\text{-}12),$$

where $\tau = G_1/\eta_1$, and $G'_1 = G''_1 = - G_1A_1 - 2G_2A_{0s}A_{1s}$.

$$R_2 = \frac{G_2'}{1 + 4\tau^2\omega^2}\tau^2\omega^2 \qquad (5\text{-}13),$$

$$I_2 = \frac{G_2''}{1 + 4\tau^2\omega^2}\tau\omega \qquad (5\text{-}14),$$

where $G'_2 = 2G_2A^2_{1s}\tau^2 - \eta_2A^2_{1d}/2$, and $G_2'' = - G_2A^2_{1s} - \eta_2A^2_{1d}\omega^2$. In order to obtain these rheological parameters (G'_1, G'_2, G''_2 and τ) from the experimental results (Fig. 5-4), we have used these relations with least-square fitting.

Figure 5-8 shows the change of the Fourier intensity spectra which was calculated based on the above mentioned nonlinear Maxwell model. The correlation coefficients are nearly unity, indicating that the proposed theoretical model is rather than satisfactory. On the other hand, the intensities (R_2 and I_2) of the second harmonic components were poorly reproduced with this nonlinear Maxwell model, suggesting the limitation of the analysis of experimental trend based on the nonlinear Maxwell model.

Table 5-II shows the dynamic elastic modulus (G'_1) and the relaxation time (τ) obtained in the presence and the absence of inorganic cations. It is found that the elastic moduli in the presence of poly-valent cations are generally

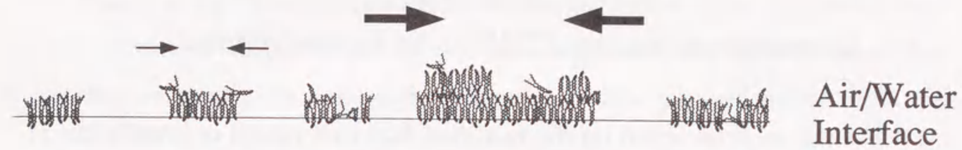

Figure 5-9.

Schematic representation of the plausible structure of DOPC domains and oil-droplets at the air/water interface.

larger than those in the presence of mono-valent cations, except for the case with Na^+. Such a trend is attributable to the stabilizing effect with poly-valent cations, compared to mono-valent cations.[32] The relatively large effect of sodium cation seems to be interesting, in compression with the some unique character of Na^+ in biochemical system.[33-37]

Cooperative aggregation of DOPC at the air/water interface

As the analysis based on the modified Maxwell model is insufficient to describe the nonlinear viscoelastic properties of DOPC thin film, we would like to try to propose a novel model to explain the observed dynamic π-A curve of DOPC film. In our experiment with BAM microscopy, it has become clear that the DOPC molecules form domains or islands at the air/water interface (see Fig. 5-7). Such a fact indicates that the kinetic process on the growth and/or dissolution of the DOPC domains may play an important role on the observed dynamic viscoelastic behavior. The following kinetic effects are expected to be important: (kinetic effect-I) the formation and growth of the domains of DOPC molecules and (kinetic effect-II) the collapse of the DOPC thin film with compression and the formation of large aggregated structure such as oil-droplets. Figure 5-9 shows the plausible structure change of the DOPC domains under compression.

Here, let us try to explain the change of the slope of the π-A curves in the Fig. 5-2. When the DOPC thin film is compressed with relatively high speed, there will be no enough time for the domains to grow sufficiently. Consequently, the surface pressure increases in a transient manner, and the slope of the π-A curves becomes steep. The domains at the air/water interface begin to collide with compression, and then form large aggregates such as oil-droplet. This induces an inflection point in the π-A curves (kinetic effect-II).[38] The kinetic effect-II, thus, implies the cooperative effects in the process of

domain growth. In present paper, the surface pressure at the inflection point is termed critical surface pressure. On the other hand, when the compression speed is low, the domains can grow in a sufficient manner, and the aggregates are gradually formed at the air/water interface. The surface pressure, therefore, gradually increases (kinetic effect-I).

Based on the above discussion of the characteristics in the π-A curves, we now provide a kinetic model to interpret the growth and dissolution of the domain structures under sinusoidal compression and expansion processes.

$$S + S \underset{k_{-1}}{\overset{k_1}{\rightleftharpoons}} D \qquad (5\text{-i}),$$

$$S + D \underset{k_{-2}}{\overset{k_2}{\rightleftharpoons}} D_L \qquad (5\text{-ii}),$$

Where S indicates the regular states, D is the small domain, D_L is the large domain such as oil-droplet, k_1, k_{-1}, k_2 and k_{-2} are the rate coefficients, respectively. The first step (5-i) corresponds to the formation of DOPC small domains, which leads to the inhomogeneous structure of thin film at the air/water interface. The second step (5-ii) corresponds to the collision between domains and the formation of DOPC large domains at the air/water interface.

The time-dependence of [S], [D], and [D_L] can be given by

$$\frac{d[S]}{dt} = -k_1[S]^2 + k_{-1}[D] - k'_2 f(\pi)[S][D] + k_{-2}[D_L]^{1/2} + Ns\frac{d}{dt}\left(\frac{1}{A}\right) \quad (5\text{-}15),$$

$$\frac{d[D]}{dt} = k_1[S]^2 - k_{-1}[D] - k'_2 f(\pi)[S][D] + k_{-2}[D_L]^{1/2} + N_D\frac{d}{dt}\left(\frac{1}{A}\right) \quad (5\text{-}16),$$

$$\frac{d[D_L]}{dt} = k'_2 f(\pi)[S][D] - k_{-2}[D_L]^{1/2} + N_L\frac{d}{dt}\left(\frac{1}{A}\right) \quad (5\text{-}17),$$

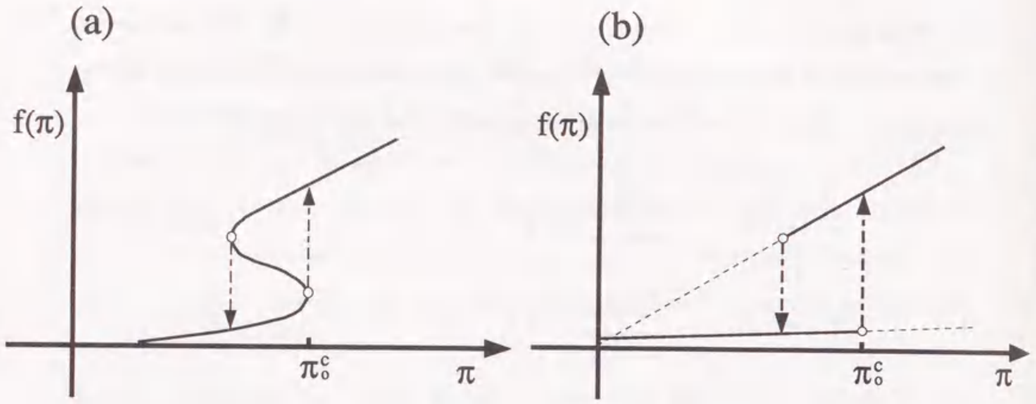

Figure 5-10.

(a) Schematic representation of an "S"-type nonlinearity, $f(\pi)$ *vs.* π.
(b) Schematic representation of the relation between $f(\pi)$ and π.
The nonlinearity was simplified by using two functions, $f(\pi) = 0.002\pi + 15$, and $f(\pi) = 2\pi$. The arrows indicate the cooperative effect similar to a first-order phase transition. π^c_o represents the critical surface pressure.

where k_2 is equal to $k'_2 f(\pi)$, A the surface area at time t, Ns the number of DOPC molecules in the regular state, N_D the number of domains, and N_L the number of large domains at the air/water interface. The effect due to the finite thickness of the oil-droplet will be neglected because the value is much smaller than the size of particle (oil-droplet) diameter. Furthermore, as the size of the large domain must be much larger than that of the regular and small domains, we estimate that the aggregation and/or the dissociation rate is proportional to the length of the its surroundings rather than the concentration. Therefore, we assume that the reversal kinetics in step (5-ii) can be represented as the 1/2 power of $[D_L]$. Because the rate of two-dimensional aggregation/dissociation should be proportional to the length of its surrounding, rather than the concentration, based on the model that the growth of DOPC domains at the air/water interface is considered as an edge-growth. Here, it should be pointed out that the viscoelastic properties in this work are attributable to the kinetic process of growth and a dissociation of the lipid domain rather than a process involving a change in a homogeneous monolayer at an air/water interface.[39]

We assume that $f(\pi)$ is a discontinuous function of surface pressure (π). This function is in a simple form similar to a first-order phase transition, which may play an important role in the cooperative aggregation at the air/water interface during dynamic experimental conditions.[40-42] It is expected that $f(\pi)$ can be expressed as an "S"-shaped curve, as shown by the left-hand side of Fig. 5-10A.[22,43] For the sake of numerical analysis, we approximate the "S"-shaped characteristics with the combination of two straight lines, as shown by the right-hand side of Fig. 5-10. $f(\pi)$ may increase drastically in a discontinuous manner over the critical surface pressure, π^c, as follows,

$$\pi \leq \pi^c \implies f(\pi) \approx 1 \qquad (5\text{-}18),$$

$$\pi > \pi^c \Longrightarrow f(\pi) \gg 1 \qquad (5\text{-}19).$$

We assume that the dynamic surface pressure is proportional to both S and D, similar to the relationship in an ideal gas:

$$\pi \propto \mathbf{a}\,[S] + \mathbf{b}\,[D] \qquad (5\text{-}20),$$

where **a** and **b** are a function of temperature, and are the correction factors for the contributions of [S] and [D], respectively.

To fully interpret the experimental results obtained in this work, we must consider that the inhomogeneity of the surface pressure at the air/water interface is one of the most important factors giving rise to the characteristic features of the hysteresis loops. We have previously adopted the inhomogeneities of surface pressure in a numerical simulation using a rectangular cell model, as shown in Fig. 2-9.[43] This model assumes that the air/water interface from the blade to the Wilhelmy plate can be divided into a number of equally small cells. We apply a simple argument that the rate of mass transfer by diffusion is proportional to the difference in concentration among neighboring cells, while the concentration and the surface pressure within each cell is homogeneous.

Computer simulations using a cooperative interaction among domains

In the right-hand part of Fig. 5-11 is shown the simulation results obtained by using the above kinetic equations and rectangular cell model which divides the air/water interface into twenty cells. In this simulation, the relative magnitudes of the compression speed were set up in terms of period parameter (f_p). The simulated results show the small oscillation in the late stage of the compression process. If we include a damping factors and increase the number

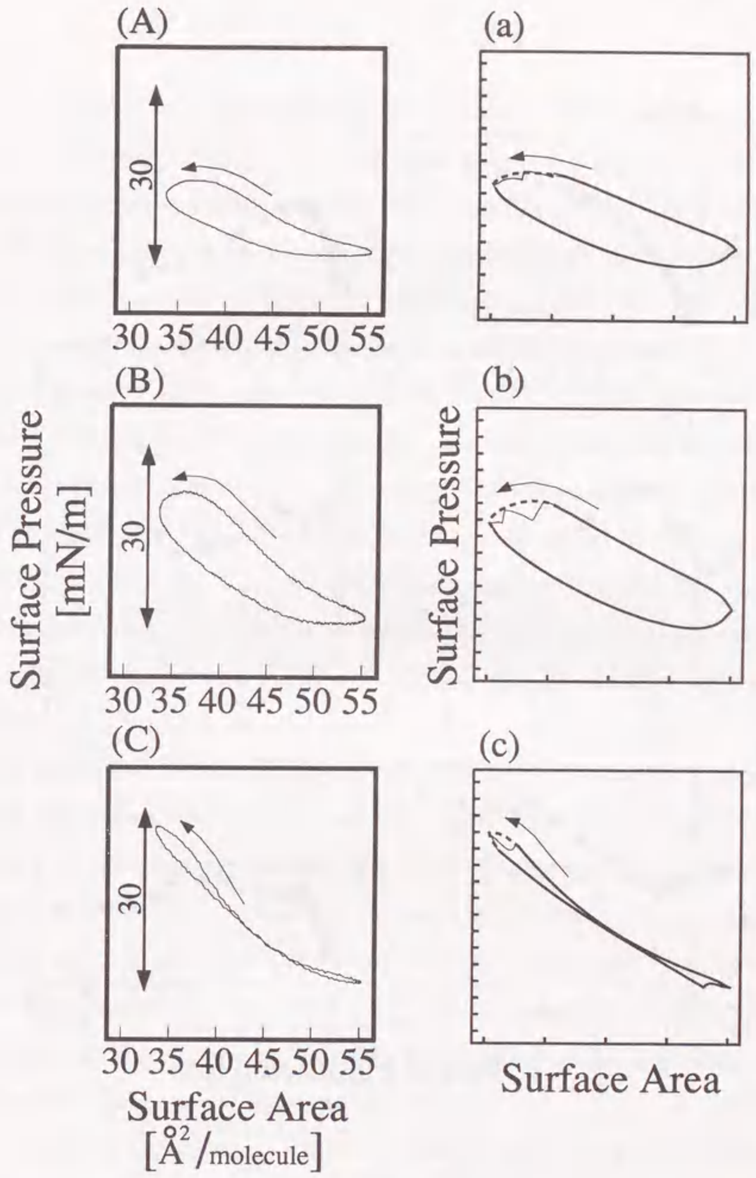

Figure 5-11.

Comparison of the results obtained by computer simulation and the observed π-A curves. The frequency of the change in surface area was;
(A) 2.3mHz, (B) 31.8mHz and (C) 94.3mHz.
Parameters used in the simulation were; $k_1 = 17.5$, $k_{-1} = 0.1$, $k_2 = 0.01$, $k_{-2} = 1.0 \times 10^{-5}$, $\pi^c_o = 20.0$, **a** = 0.5, **b** = 0.25. The period parameter, f_p, was;
(a) 1.54×10^{-3}, (b) 2.86×10^{-3} and (c) 14.3×10^{-3}.

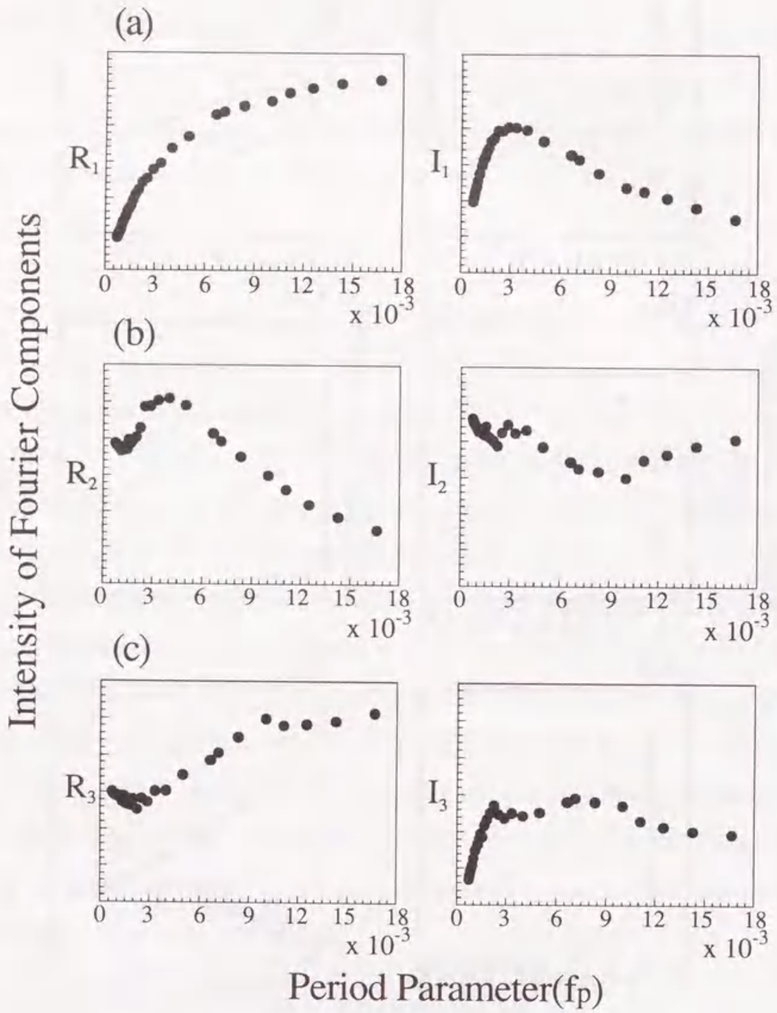

Figure 5-12.

The dependence of Fourier peak intensities on the period parameter based on the cooperative aggregation/dissociation model. The left side of the Figure indicates Fourier real spectra, and the right side indicates the imaginary spectra. The period parameter was changed from 0.67 x 10^{-3} to 16.7 x 10^{-3}. (a) fundamental harmonic components, (b) second harmonic components, (c) third harmonic components.

of cells in the simulation, the oscillation would be smooth, as is represented by the dotted line. Figure 5-12 indicates that the change of Fourier peak intensities with the change of the period parameter. It is clear that the change of calculated peak intensity is corresponding with the experimental trend (see Fig. 5-4). It is noted that the above simulation can reproduce essential Fourier peak intensity change including the higher harmonic components.

In a recent work,[44] it was found that two DOPC droplets begin to aggregate around 20°C.[45,46] This study indicates that the aggregation occurs above a critical subphase temperature. By analogy, our experiment suggests that the abrupt change of Fourier peak intensities is observed at the characteristic temperature (c.a. 20°C). As the kinetic model includes the cooperative aggregation/dissociation process between the DOPC two-dimensional domains, we apply the kinetics to the analysis on the dynamic π-A curve observed above 20°C. Figure 5-13A shows the dynamic π-A curves observed at 30°C, and Fig. 5-13a shows the simulation results. $f(\pi)$ is illustrated in the right upper of Fig. 5-13a. By comparing the shape of $f(\pi)$, represented in the Fig. 5-10 and Fig. 5-13a, it is clear that the discontinuity becomes to be small with increase of the subphase temperature. Therefore, it seems to be that the formation of large domain (D_L) is inhibited with increasing the temperature. In other words, increasing the temperature may be corresponding to the inhibition of the cooperative aggregation among DOPC domains at the air/water interface during periodical compression and expansion.

Finally, I should discuss the effect of the inorganic salts dissolved in the aqueous subphase on the dynamic viscoelastic properties of DOPC thin film. Summarizing the results, it is highly probable that the area of the hysteresis loop was increased and the dynamic surface pressure at the range from 34 to 37 $Å^2$/molecule markedly decreased with compression. Generally, it is well known that the metal cations dissolved in the subphase combine with the

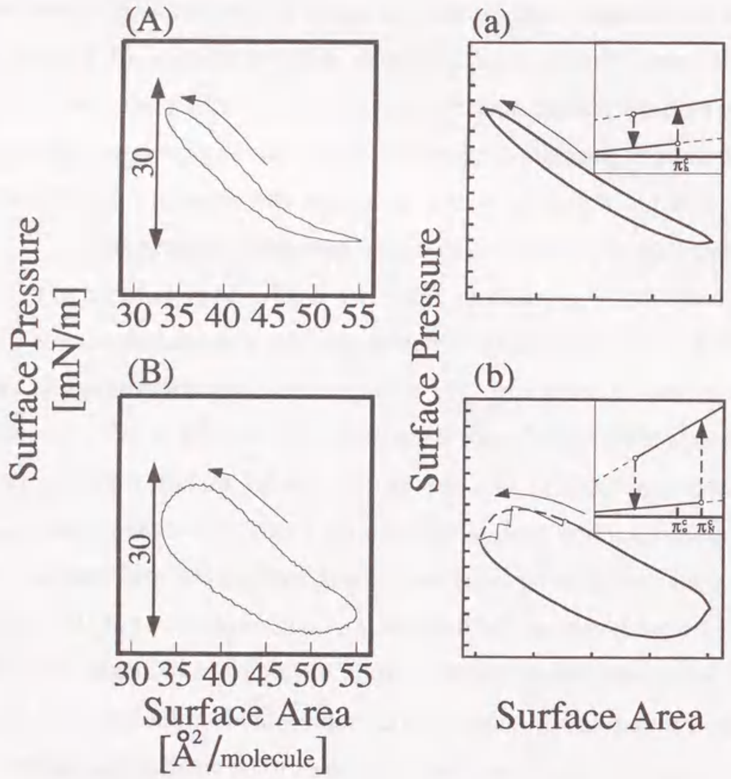

Figure 5-13.

Comparison of the results obtained by computer simulation and the observed π-A curves. (A) The subphase temperature was 30.0°C. (B) The aqueous subphase included 0.5M NaCl and the subphase temperature was 20°C.
Parameters used in the simulation were; $f_p = 2.86 \times 10^{-3}$;
(a) $k_1 = 17.5$, $k_{-1} = 0.1$, $k_2 = 0.01$, $k_{-2} = 0.00001$, $\pi^c_h = 20.00$,
a = 0.5, **b** = 0.25, and
(b) $k_1 = 17.5$, $k_{-1} = 0.1$, $k_2 = 0.001$, $k_{-2} = 0.00003$, $\pi^c_N = 30.00$,
a = 0.5, **b** = 0.25.
The nonlinear characteristics of $f(\pi)$ were represented by the combination of the following two linear relationships;
(a) $f(\pi) = 0.002\pi + 15$ and $f(\pi) = 2\pi$,
(b) $f(\pi) = 0.002\pi + 15$ and $f(\pi) = 0.1\pi + 20$.

hydrophilic moieties in amphiphilic compounds and enhance the stability of the monolayer formed at an air/water interface.

In present work, Na^+ ion indicated marked stability and flexibility of DOPC thin film at the air/water interface. Based on the above discussion, the simulated dynamic surface pressure and the relation between $f(\pi)$ and π are shown in Fig. 5-13b. It should be noted that the increase of the critical surface pressure from π^c_o to π^c_N is representing the increase of the discontinuity and enhances the cooperative interaction among DOPC domains. However, if we explain the effect of sodium cation on the dynamic behavior of DOPC thin film, we should observe the viscoelastic properties of the films in the presence of the other mono- and poly-valent metal cations such as Li^+, NH_4^+, Ca^{2+}, and Mg^{2+}. For the experimental findings which were observed by using those metal cations, next section shows in detail.

In present section, our simulations considering the cooperative factors essentially reproduce the characteristics observed in the actual experiments. Therefore, this kinetic model can be applied to explain the dynamic viscoelastic behavior of DOPC thin film at an air/water interface with periodic compression and expansion.

5-4. Conclusion

The dynamic π-A curves of an unsaturated phospholipid, DOPC, thin films at the air/water interface were found to show dependence on frequency of the surface area change, subphase temperature. All of these nonequilibrium characteristics have been explained successfully by means of a kinetic simulation based on the cooperative aggregation/dissociation model of DOPC domains and a rectangular cell model of surface area. Utilization of this experimental technique and analysis method may give us further detail information regarding significant changes in the lipid film under dynamic experimental conditions.

References

1) A. W. Adamson, Physical Chemistry of Surface, 5th ed.; John Wiley & Sons, Inc.: New York, 1990.
2) F. Mac Ritche, Chemistry at Interfaces; Academic Press: San Diego, 1990.
3) I. Langmuir, Trans. Far. Soc., **15** (1920) 62.
4) K. B. Blodgett, J. Am. Chem. Soc., **57** (1935) 1007.
5) F. Boury, Tz. Ivanova, I. Panaïotov and J. E. Proust, Langmuir **11** (1995) 599.
6) J. C. Earnshaw, In Polymer surface and interface II; W. J. Feast, H. S. Munro and R. W. Richards, Eds.; J. Wiley & Son: Chichester, New York, 1993, p101.
7) E. H. Lucassen-Reynders, In Anionic Surfactant; E. H. Lucassen-Reynders, Eds.; Marcel Dekker: New York and Basel, 1983, p173.
8) C. H. Sohl, K. Miyano and J. B. Ketterson, Rev. Sci. Instrum., **49** (1978) 1464.
9) R. M. Mendenhall, A. L. Mendenhall Jr., Rev. Sci. Instrum., **34** (1963) 1350.
10) F. Van Voorst Vader, J. F. Erkens and M. Van Tempel, Trans. Far. Soc., **60** (1964) 1170.
11) R. Bienkowski and M. Skolnick, J. Coll. Interface Sci., **39** (1972) 323.
12) S. A. Tabak and R. H. Notter, Rev. Sci. Instrum., **48** (1977) 1196.
13) E. H. Lucassen-Reynders and J. Lucassen, Adv. Colloid Interface Sci., **2** (1969) 347.
14) J. A. Mann, In Techniques of Surface Chemistry and Physics; R. J. Good, R. R. Stroberg and R. L. Patric, Eds.; Marcel Dekker: New York, 1972, Vol. 1, p77.
15) D. Edwards, H. Brenner and D. T. Wasan, In Interfacial transport processes and rheology; Butterworth-Heinemmann: Oxford, 1991.
16) D. S. Dimitrov and L. Ter-Minassian-Saraga, J. Coll. Interface Sci., **65** (1978) 483.
17) D. Lusted, J. Coll. Interface Sci., **44** (1973) 72.
18) A. F. M. Snik, A. H. M. Joos and A. J. Kruger, J. Coll. Interface Sci., **70** (1979) 147.
19) P. Joos, M. Van Uffelen and G. Serrien, J. Coll. Interface Sci., **152** (1992) 521.

20) K. Yoshikawa, M. Shoji and T. Ishii, Biochem. Biophys. Res. Commun., **160** (1989) 699.
21) H. M. McConnell, D. Keller and H. Gaub, J. Phys. Chem., **90** (1986) 1717.
22) A. Miller and H. Möhwald, J. Chem.Phys., **86** (1987) 4258.
23) M. Makino, M. Kamiya, N. Nakajo and K. Yoshikawa, Progress in Anesthetics Mechanism, **3** (1995) 247.
24) M. Makino, K. Yoshikawa and T. Ishii, Nippon Kagaku Kaishi, **10** (1990) 1143.
25) M. Makino and K. Yoshikawa, In New Developments in Construction and Functions of Organic Thin Films, T. Kajiyama and M. Aizawa, Eds.; Elsevier Science: Amsterdam, (1996) pp211.
26) D. Hönig and D. Möbius, J. Phys. Chem., **95** (1991) 4590.
27) S. Hénon and J. Meunier, Rev. Sci. Instrum., **62** (1991) 936.
28) D. Lefevre, F. Porteu, P. Balog, M. Roulliay, G. Zalczer and S. Palacin, Langmuir, **9** (1993) 50.
29) K. Hirano and H. Fukuda, Langmuir, **11** (1995) 4173.
30) D. Chapman, In Form and Function of Phospholipids, G. B. Ansell, C. Dawson and J. N. Hawthorne, Eds.; Elsevier Science: Amsterdam, 1973, p.117.
31) F. Boury, Tz. Ivanova, I. Panaïotov and J. E. Proust, Langmuir, **11** (1995) 2131.
32) D. J. Ahn and E. I. Franses, J. Chem. Phys., **95** (1991) 8486.
33) L. Loshchilova and B. Karvaly, Biochim. Biophys. Acta, **514** (1978) 274.
34) H. Uedaira and Y. Suzuki, Bull. Chem. Soc. Jpn., **52** (1979) 2787.
35) J. E. Desnoyer and C. Jolicoeur, In Modern Aspects of Electrochemistry, J.O'M. Bockris and B. E. Conway, Eds.; Plenum, New York, 1969.
36) R. Sundler, Biochim. Biophys. Acta, **771** (1984) 59.
37) H. Hauser and M. C. Philips, Prog. Surf. Membr. Sci., **13** (1979) 297.
38) R. H. Notter, S. Holcomb, R. D. Mavis, Chem. Phys. Lipids, **27** (1980) 305.
39) D. Vollhardt and U. Retter, J. Phys. Chem., **95** (1991) 3723.
40) L. W. Horn and N. L. Gershfeld, Biophys. J., **18** (1977) 301.
41) K. Tajima and N. L. Gershfeld, Biophys. J., **22** (1978) 489.
42) G. M. Bell, L. L. Combs and L. J. Dunne, Chem. Rev., **81** (1981) 15.
43) M. Makino, M. Kamiya, T. Ishii and K. Yoshikawa, Langmuir, **10** (1994) 1287.
44) W. Breisblatt and S. Ohki, J. Membr. Biol., **23** (1975) 385.

45) W. Breisblatt and S. Ohki, J. Membr. Biol., **29** (1976) 127.
46) M. K. Chaudhury and S. Ohki, Biochim. Biophys. Acta, **642** (1981) 365.

6. CHARACTERISTIC EFFECTS OF SODIUM CATIONS ON THE DYNAMIC BEHAVIOR OF PHOSPHOLIPID THIN FILM

In the preceding subsection, the dynamic viscoelastic properties of DOPC thin film was observed with periodical surface area change. It was found that the sodium cations in the aqueous subphase increased both the viscosity and elasticity of the thin film comparing with them in the presence of potassium cations. In section 3, it has been already pointed out that a Coulombic interaction between head-groups of lipid molecules adsorbed on the interface is important in order to understand the surface pressure - surface area (surface concentration) relationship.

In this section, I would like to represent the unique effect of the sodium cations on the dynamic viscoelastic properties by comparing the viscoelastic behavior which was observed with various inorganic cations, such as Li^+, NH_4^+, Ca^{2+}, Mg^{2+}.

6-1. Introduction

Although, in the past, there have been numerous studies on the dynamic π-A curve of lipid monolayers at an air/water interface,[1-5] the viscoelastic properties with a periodic change in the surface area have not yet been fully clarified. This may be due to a difficulty in obtaining reproducible characteristics. The poor reproducibility has been attributed to such factors as that along with a periodic change in the surface area some lipid molecules at the air/water interface leak to the subphase[6] and stick to a blade and/or a trough,[6] and that the contact angle against a Wilhelmy plate increases.[7] In fact, most previous reports concerning the dynamic π-A curves have shown a time-dependent shrinkage of the π-A curve. In other words, a spiral loop has been observed.[6,8]

Recently, it has been reported by Yoshikawa and his co-workers that dynamic π-A curves with compression and expansion in the presence of taste compounds, such as nicotine (bitter), sodium chloride (salty), sucrose (sweet), and citric acid (sour) were traced closed-hysteresis loops in the shape of a somewhat distorted ellipsoid.[9,10] The π-A curve changes in a characteristic manner depending on the taste category of the chemicals added. The shape of a hysteresis loop is expected to reflect the viscoelastic properties of a lipid thin film.[11] If the lipid thin film is a linear viscoelastic-body, the dynamic π-A curve traces a genuine elliptical loop. However, most curves are in the form of a distorted ellipsoid, due to the nonlinearity of a lipid thin film. This distortion, or nonlinearity, has been ignored in previous studies on the dynamic π-A characteristics.

To evaluate this nonlinearity in a quantitative manner, an analysis method to perform a Fourier transformation on a time-dependent change in

pressure was adapted. This method has been introduced and explained in the section 5.

In this section, I would like to report on the dynamic surface behavior of DOPC thin film at the air/water interface in the presence of metal cations with the help of the experimental apparatus which was the same equipment in section 5. We have found that Na^+ has a marked effect on the dynamic behavior of a phospholipid thin film. Therefore, we try to discuss our experimental findings on the basis of the cooperative aggregation and dissociation of phospholipid aggregates at the air/water interface.

6-2. Materials and Method

A synthetic phospholipid, 1,2-dioleoyl-3-*sn*-phosphatidylcholine (DOPC), was obtained from Avanti Polar Lipid Inc. All other reagents were analytical-grade chemicals, and were used without further purification (WAKO Pure Chemical Industries Ltd.). Before each experiment, water was purified using a Millipore-MilliQ Labo filtering system at a resistivity above 18MΩcm, and then distilled with an acid permanganate medium. Chloroform was purified by three consecutive distillations. DOPC (0.133mM) in chloroform was prepared as a spreading solution.

The experimental apparatus had been described in the section 5.[12] The surface area was changed repeatedly from 25 to 100Å^{2}molecule^{-1} in a sinusoidal cycle with a period of 60s.[13] The obtained dynamic surface-pressure data were successively stored in an NEC PC-9801 personal computer (NEC, Japan). We observed the dynamic surface pressure after four cycles of compression and expansion, as the π-A curves began to trace a single-closed loop within four cycles of compression and expansion. Thus, the surface pressure at the maximum surface area was taken as a reference, i.e., π=0 at the maximum of A (see e.g. Figs. 6-2 and 6-4). The time-course in the dynamic surface pressure was then Fourier-transformed to a frequency domain.

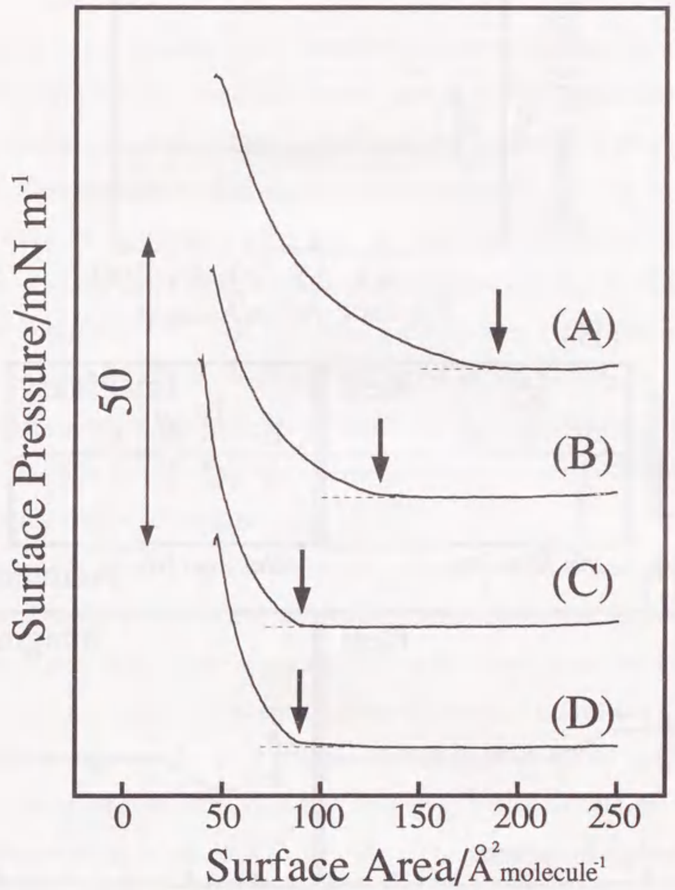

Figure 6-1.

Quasi-static π-A isotherms of a DOPC monolayer at an air/water interface. The arrows indicate the limiting area. The subphase temperature was 13°C.
The surface pressure at the starting point of the compression is 0mNm^{-1}.
(A) 1M NaCl, (B) 1M $MgCl_2$, (C) 1M KCl, (D) distilled water.

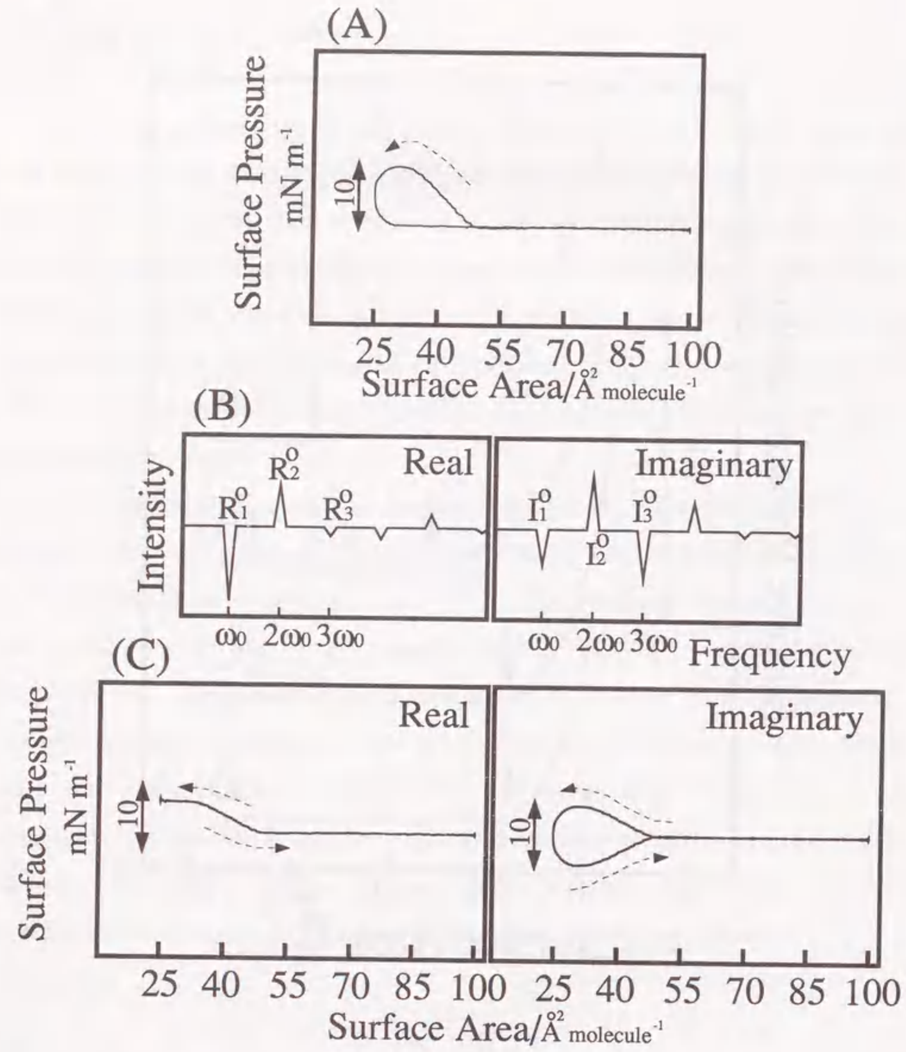

Figure 6-2.

Dynamic surface behavior of a DOPC thin film at an air/water interface, as the response to the sinusoidal change of A with a period of 60 s. (A) Dynamic π-A curve under steady state. (B) Fourier spectra. The real and imaginary parts indicate the functions of cosine and sine terms, respectively.
(C) Inverted Fourier spectra.

6-3. Results and Discussion

Figure 6-1 shows the π-A isotherm of DOPC monolayers, which were slowly compressed at a constant speed with 0.3125Å^{2}molecule^{-1}min^{-1}. In previous studies, the π-A isotherm of a lipid thin film at an air/water interface was very often measured under quasi-static compression. In this condition, the limiting area corresponds to the area of the cross-section of a surfactant molecule, and the slope reflects the elastic property of the monolayer at the air/water interface.[11,14] The observed limiting area increases in the order control < KCl < $MgCl_2$ < NaCl, and the slope in the vicinity of the limiting area becomes small in the presence of NaCl. We observed the dynamic surface behavior in order to elucidate the viscoelastic properties of a DOPC thin film as the surface area was changed sinusoidally.

Figures 6-2A and 6-2B show the dynamic π-A curve and Fourier-transformed spectra of the dynamic surface pressure for the time trace of the surface pressure (π(t)). For a viscoelastic-body, it has been well established that the cosine(real) and sine(imaginary) parts in the Fourier spectra correspond to the energy accumulated and dissipated terms, respectively.[15] Therefore, it is clear that the real and imaginary parts indicate the elastic and viscous components of the DOPC thin film. The presence of higher harmonics in the frequency spectra implies that these viscoelastic characteristics have non-negligible nonlinear components. Figure 6-2C shows the inverted Fourier transformation of the frequency spectra in Fig. 6-2B. With this data-processing method, the elastic and viscous terms can be evaluated separately.

We then examined the dynamic π-A curves by changing the metal cations. In this experiment, to clarify the effect of cations, we used only chloride salts, such as LiCl, KCl, and NaCl. It is noted that the anions in the subphase also contribute to the change in the area of the hysteresis loop.[16]

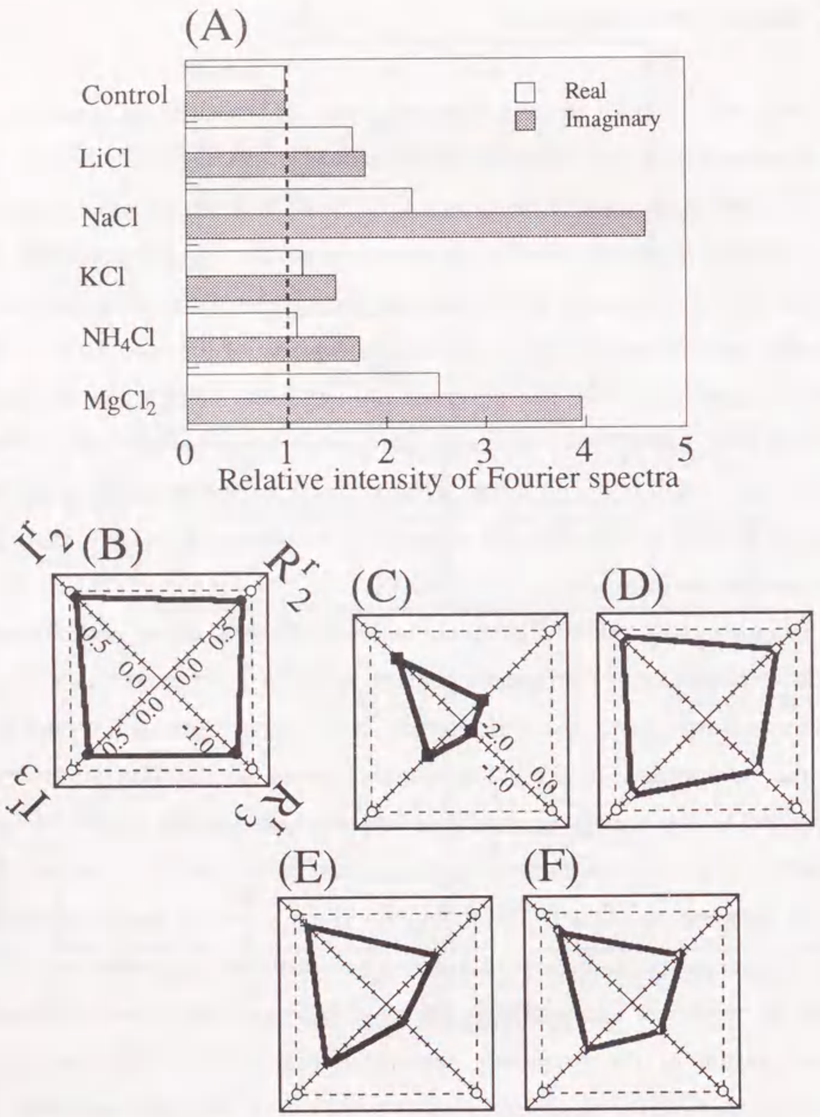

Figure 6-3.

(A) Change in the intensity of Fourier fundamental harmonic components relative to those in the control experiment. Changes in the relative intensity of higher-harmonic components: (B) 1M LiCl, (C) 1M NaCl, (D) 1M KCl, (E) 1M NH_4Cl, (F) 1M $MgCl_2$. Broken lines indicate the results of the control experiment.

Figure 6-3A shows the change in the relative intensity (R_1/R^o_1 and I_1/I^o_1) of the fundamental harmonic components of the Fourier-transformed spectra. The ideal (linear) elasticity increased in the order control < NH_4Cl, KCl < LiCl < NaCl < $MgCl_2$, while the viscosity increased in the order control < KCl < LiCl, NH_4Cl << $MgCl_2$ < NaCl. These results are roughly consistent with the previously established view that divalent metal cations tend to stabilize the lipid monolayer at the air/water interface rather than mono-valent metal cations.[11,17] However, Na^+ ion enormously increased the linear viscous property of the DOPC thin film. In order to elucidate the effect on the higher harmonic components in the Fourier spectra, the relative intensity ratios were derived as follows:

$$R^r_n = \frac{\frac{R_n}{R_1}}{\frac{R^o_n}{R^o_1}} \qquad (6\text{-}1),$$

$$I^r_n = \frac{\frac{I_n}{I_1}}{\frac{I^o_n}{I^o_1}} \qquad (6\text{-}2),$$

where R^o_n and I^o_n are the intensities of the Fourier n^{th}-harmonic components, obtained in a control experiment (see Fig. 6-2B). R_n and I_n are the intensities of the components in the presence of inorganic salts. As shown in Figs. 6-3B-3F, the intensity ratio markedly decreased in the presence of NaCl. In particular, R^r_3 became a negative value, while I^r_2 and I^r_3 showed little change compared to R^r_2 and R^r_3 with the addition of inorganic salts.

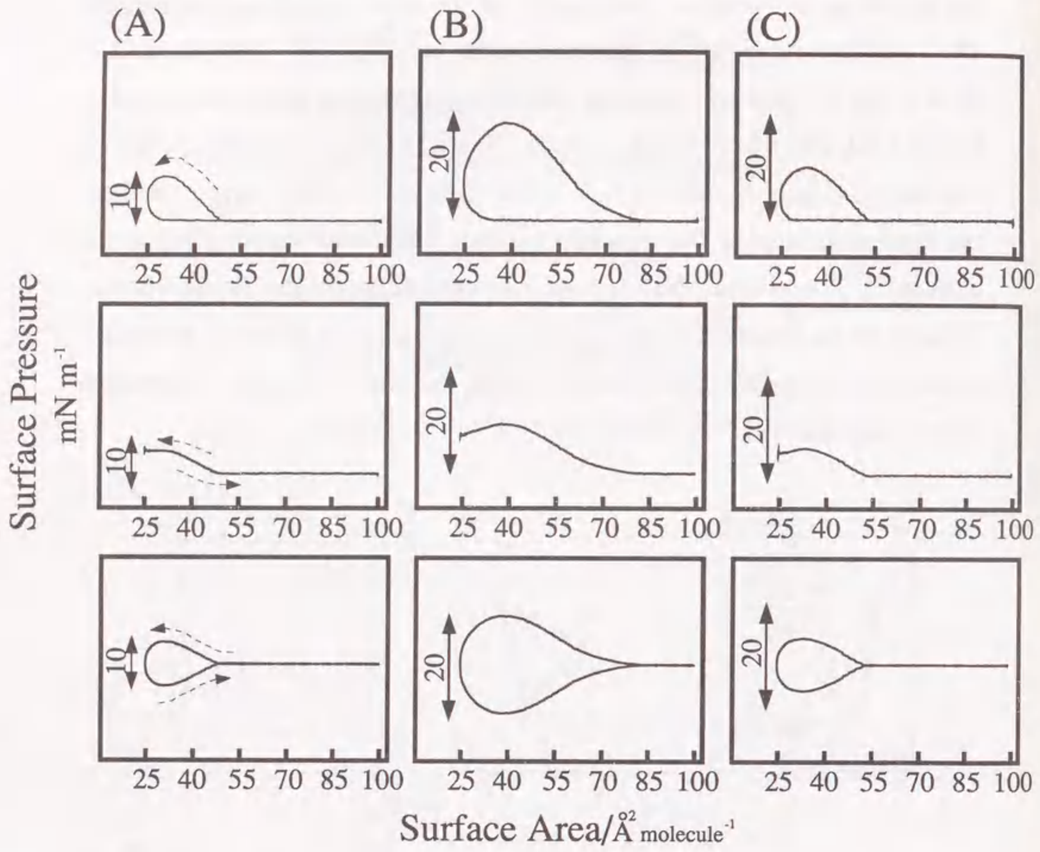

Figure 6-4.

Inverted Fourier spectra of the dynamic change in surface pressure.
(A) Control, (B) 1M NaCl, (C) 1M KCl.
Top; dynamic π-A curves, Middle; inverted real Fourier spectra,
Bottom; inverted imaginary Fourier spectra.

Figure 6-4 shows the dynamic π-A curves and inverted Fourier spectra. By adding NaCl to the aqueous subphase, the limiting area was shifted to the right and the slope of the surface pressure became small in the vicinity of the limiting area. Such a trend is consistent with that of the experimental results with a quasi-static π-A isotherm, as exemplified in Fig. 6-1. In contrast, in the control experiment and also with KCl, the slope of the π-A curve was steep and the area of the hysteresis loop was small. It is therefore clear that Na^+ makes the DOPC thin film more flexible than do other mono-valent cations.

Furthermore, the inverted Fourier real spectra for the control experiment traced a flat plateau from ca. 25 up to 40Å^{2}molecule^{-1}. On the other hand, for the same range of surface area, the spectra traced a decreasing curve with compression in the presence of inorganic salts. Generally, as indicated in Fig. 6-1, the surface pressure does not decrease with compression under quasi-equilibrium. Therefore, the decrease in the surface pressure can be interpreted as a relaxation phenomenon related to the collapse of the DOPC thin film at the air/water interface, judging from the collapse point in Fig. 6-1. It is clear that the dynamic surface pressure observed for the range between 25 and 40Å^{2}molecule^{-1} is markedly decreased in the presence of Na^+. These experimental results suggest that the interaction between Na^+ and phospholipid head groups should be unique compared to that with other ions.

Loshchilova and Karvaly studied the influence of mono-valent cations on phosphatidylcholine bilayers using laser Raman spectroscopy.[18] They found that Na^+ was the most effective in changing the order parameters of the head groups. Uedaira and Suzuki studied the ultrasonic velocity of aqueous solutions of alkali metal chlorides.[19] They reported that the maximum value of the ultrasonic velocity *vs.* temperature curve was shifted the most in the presence of Na^+.

As for these significant effects of Na^+, Desnoyers and Jolicoeur proposed a possible explanation:[20] these maxima may appear because "the strength of ion-solvent interactions decreases with increasing size of the ions, but the coordination number of the ion increases with increasing size." On the contrary, the coordination numbers of alkali metal ions were formed to be 4 for Li^+, Na^+, and K^+ ions, according to an X-ray analysis and a neutron-scattering experiment.[21] In order to obtain clear insight concerning the significant effect of Na^+, additional work is necessary, including a discussion on the state of the water molecules, especially the water structure in the vicinity of the phosphatidylcholine head groups under kinetically controlled conditions.[22,23]

Based on the above results, we tried to elucidate the origin of the hysteresis loop of the dynamic surface pressure and the effects of mono-valent cations, such as Na^+, on a DOPC thin film with the aid of a computer simulation. We previously explained the dynamic surface behavior using the kinetic model, which includes the cooperative aggregation of surfactant molecules onto the air/water interface(see previous section). Based on the (5-i), (5-ii), and the same differential equation in section 5, I analyzed the dynamic surface pressure change with periodic compression and expansion.

$f(\pi)$ is a discontinuous function including a critical value (π^c), which have been introduced in the section 5. We assume that the surface pressure (π) is given as the summation of two contributions due to S and D. To explain the above effects of Na^+, it is necessary to assume that the slope of $f(\pi)$ is small at a low surface pressure, and that the discontinuity in $f(\pi)$ and the critical surface pressure (π^c) are enhanced, considering the experimental results that the limiting area was shifted and the dynamic surface pressure decreased with compression in the range from 25 to 40$Å^2$molecule^{-1}.

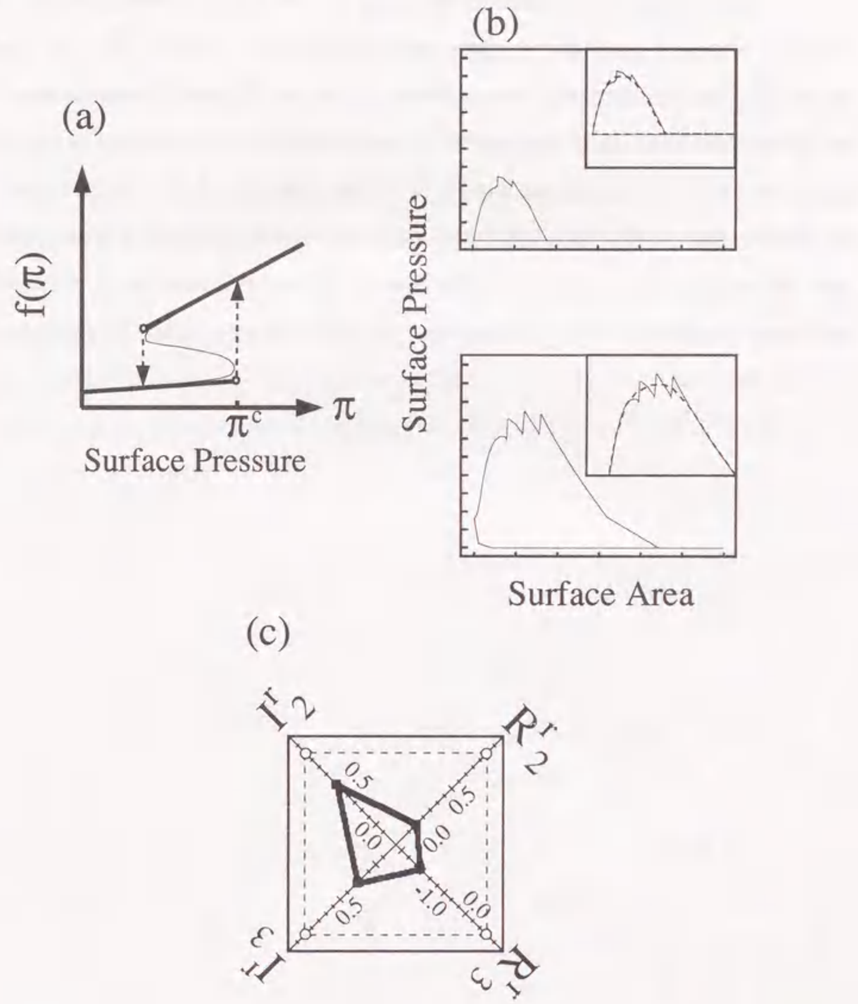

Figure 6-5.

Computer simulation based on the cooperative aggregation/dissociation model. (a) The feature of the discontinuous function, $f(\pi)$. $\pi < \pi^c$; $f(\pi) = 0.002\pi + 15$, $\pi \geq \pi^c$; $f(\pi) = \pi + 50$. (b) Computer simulation of the observed dynamic π-A curves. Top; $\pi^c = 2.5$, Bottom; $\pi^c = 5.5$. Parameters; k_1=17.5, k_{-1}=1.0 x 10^{-1}, k'_2=1.0 x 10^{-2}, k_{-2}=1.0 x 10^{-5}. (c) Simulated relative Fourier peak intensities which were calculated from (b) in Fig. 6-5.

Fig. 6-5 shows the relation between $f(\pi)$ and π, the simulated dynamic surface pressure, and the relative peak-intensities obtained as the Fourier transformation on the time-change of the simulated dynamic surface pressure. It is clear that the peak-intensities in the simulation correspond well to the experimental trend given in Fig. 6-3. Here, the calculated surface pressure oscillates near to π^c, since the damping factor of the dynamic surface pressure was not included in this study. By including the viscous factor, the surface pressure should follow the dotted line, which corresponds to the experimental trends.

6-4. Conclusion

We measured the time-dependent surface pressure of a dioleoylphosphatidylcholine film at an air/water interface. Our results indicate that: (i) the surface pressure of the thin film traces a closed hysteresis loop accompanied by repetitive cycles of compression and expansion, and (ii) the area of the hysteresis loop markedly increases in the presence of sodium ions. We proposed a kinetic model for this phenomenon which included cooperative aggregation/dissociation at the air/water interface. The experimental findings were successfully reproduced with the aid of a computer simulation based on this theoretical model.

References

1) R. M. Mendenhall and A. L. Mendenhall, Jr., Rev. Sci. Instrum., **34** (1963) 1350.
2) R. Bienkowski and M. Skolnick, J. Colloid Interface Sci., **39** (1972) 323.
3) M. L. Longo, A. M. Bisango, J. A. N. Zasadzinski, R. Bruni, and A. J. Waring, Science, **261** (1993) 453.
4) T. Kato, H. Akiyama, and T. Tanaka, Chem. Phys. Lett., **184** (1991) 455.
5) D. Lusted, J. Colloid Interface Sci., **44** (1973) 72.
6) R. H. Notter, S. A. Tabak, and R. D. Mavis, J. Lipid Res., **21** (1980) 10.
7) A. Mennella and N. R. Morrow, J. Colloid Interface Sci., **172** (1995) 48.
8) A. F. M. Snik, J. Kruger, and P. Joos, J. Colloid Interface Sci., **66** (1978) 435.
9) K. Yoshikawa, M. Shoji, and T. Ishii, Biochem. Biophys. Res. Commun., **160** (1989) 699.
10) M. Makino, K. Yoshikawa, and T. Ishii, Nippon Kagaku Kaishi, **10** (1990) 1143.
11) A. W. Adamson, in "Physical Chemistry of Surfaces," 5th ed, John Wiley & Sons, Inc., New York (1990).
12) M. Makino and K. Yoshikawa, in "New Developments in Construction and Functions of Organic Thin Films," ed by T. Kajiyama and M. Aizawa, Elsevier Science, Amsterdam, (1996) pp211-246.
13) J. Lucassen and D. Giles, J. Chem. Soc. Faraday Trans. 1, **71** (1975) 217.
14) I. Langmuir, J. Am. Chem. Soc., **39** (1917) 1848.
15) G. Loglio, U. Tesei, and R. Cini, J. Colloid Interface Sci., **71** (1979) 316.
16) G. L. Ganines, Jr., P. E. Behnken, and S. J. Valenty, J. Am. Chem. Soc., **100** (1978) 6549.
17) K. B. Blodgett and I. Langmuir, Phys. Rev., **51** (1937) 964.
18) E. Loshchilova and B. Karvaly, Biochim. Biophys. Acta, **514** (1978) 274.
19) H. Uedaira and Y. Suzuki, Bull. Chem. Soc. Jpn., **52** (1979) 2787.
20) J.E. Desnoyer and C. Jolicoeur, in "Modern Aspects of Electrochemistry," ed by J.O'M. Bockris and B.E. Conway, Plenum, New York(1969), Vol. 5.
21) H. Ohtani and M. Maeda, Kagaku Sosetsu, **11** (1976) 119.
22) R. Sundler, Biochim. Biophys. Acta, **771** (1984) 59.
23) H. Hauser and M. C. Philips, Prog. Surf. Membr. Sci., **13** (1979) 297.
24) M. Makino, M. Kamiya, T. Ishii, and K. Yoshikawa, Langmuir **10**, (1994) 1287.
25) D. Vollhardt and U. Retter, J. Phys. Chem., **95** (1991) 3723.
26) N. L. Gershfeld, Annu. Rev. Phys. Chem., **27** (1976) 349.
27) H. W. Horn and N. L. Gershfeld, Biophys. J., **18** (1977) 301.

7. EFFECTS OF LOCAL ANESTHETICS ON THE DYNAMIC BEHAVIOR OF PHOSPHOLIPID THIN FILM

Under appropriate conditions, it was found that the dynamic π-A curve traced a single closed hysteresis loop after several cycles of compression and expansion. Fourier transformation of the time-dependent change in the dynamic surface pressure is useful for analyzing the shape of the hysteresis loop, which reflects nonlinear viscoelastic properties, in a quantitative manner.

This observation of the dynamic surface behavior and the analysis method have been already introduced in the section 5 and 6. In last section in this study, I would like to reveal a characteristic effect of local anesthetics, such as tetracaine, prilocaine, bupivacaine, mepivacaine, lidocaine and procaine, on the shape of the loop-area, and introduce a relationship between a nonlinear viscoelastic behavior of the lipid thin film and an anesthetic potency, since anesthetic mechanism has not been entirely clear.

7-1. Introduction

In the past, dynamic π-A characteristics have been studied mainly in relation to the viscoelastic properties of pulmonary surfactants in alveoli.[1,2] Ever since the pioneering work of von Neergeerd in 1929,[3] dynamic π-A characteristics have also been studied by Pattle,[4] Clements[5] and many other researchers.[6-10] Recently, this dynamic behavior has been studied by Joos et al.,[11] Lucassen-Reynders,[12] and other research groups.[13-15] These studies have shown that most π-A curves trace spiral hysteresis loops with compression and expansion, i.e., the loop-area decreases monotonously with time. This decreasing-spiral shape has been attributed to (i) relaxation of the lipid thin film toward a steady state,[8,16] and (ii) unavoidable changes in the contact angle of the Wilhelmy plate with the air/water interface during the cycling experiment.[17]

We have found[18,19] that, under certain conditions, the π-A curve of phospholipid film shows a steady closed loop after several cycles of compression and expansion. The viscoelasticity of phospholipid thin film has been interpreted in an aquantitative manner, by separating the hysteresis loop into its elastic and viscous components.

Lung compliance *in vivo* is reduced by the administration of anesthetics.[1] This phenomenon has been ascribed to the decrease in free energy at the surface of alveoli. The purpose of the present paper is to quantitatively investigate the effects of local anesthetics on the dynamic properties of phospholipid thin film.

(A) 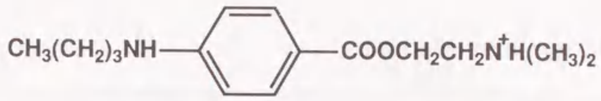

(B) 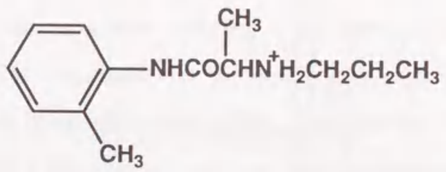

(C) 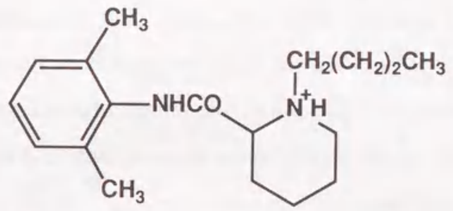

(D) 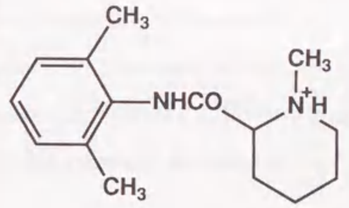

(E) 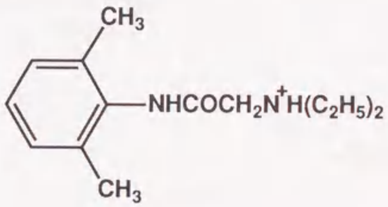

(F) 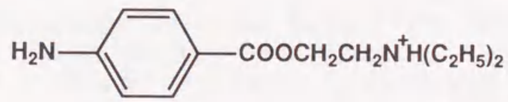

Figure 7-1.

Chemical structure of the local anesthetics.
(A) tetracaine, (B) prilocaine, (C) bupivacaine, (D) mepivacaine, (E) lidocaine, (F) procaine.

7-2. Materials and Method

Figure 7-1 shows the chemical formulas of the local anesthetics (tetracaine, prilocaine, bupivacaine, mepivacaine, lidocaine, and procaine) examined in the present study, which were obtained from SIGMA Chemical Company. Other reagents were analytical grade chemicals and were purchased from Wako Pure Chemical Industries, Ltd. The other materials and the water used in this study were treated the same procedure in the previous section.

With lidocaine and procaine, we made chloroform solutions and then added them directly to the DOPC monolayer which had been previously spread at the air/water interface using a microsyringe. In the experiments with the other local anesthetics, they were dissolved in the aqueous subphase, and DOPC solution was then applied to the entire air/water interface. After waiting for 30 min to attain thermal equilibrium, the surface area was changed repeatedly from 37.5Å^2/molecule to 62.5Å^2/molecule in a sinusoidal cycle with a period of 432sec.

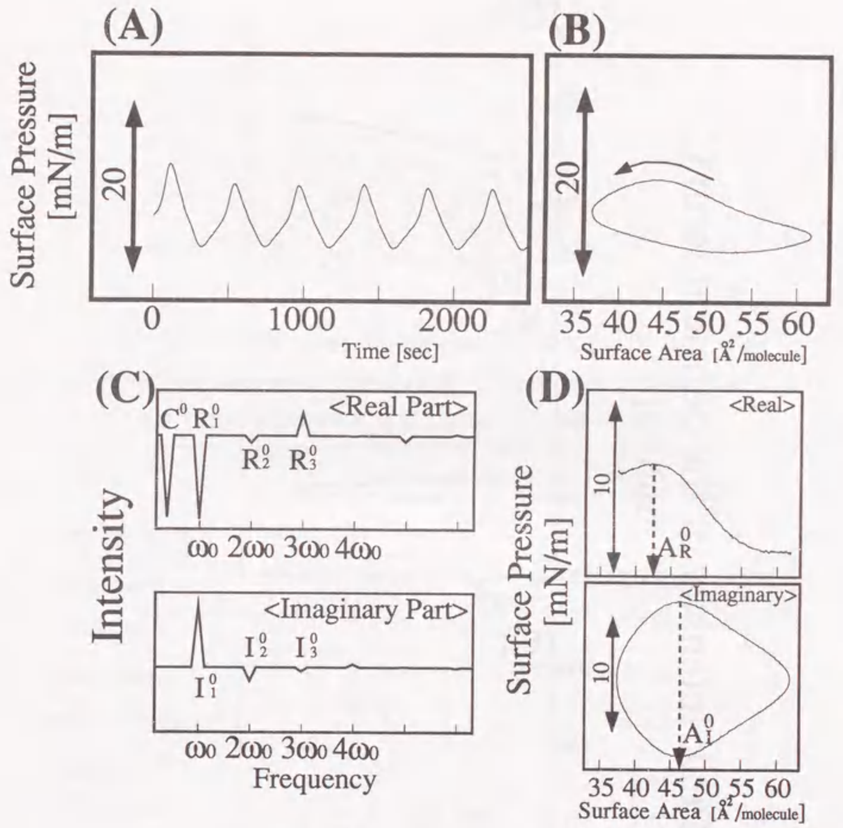

Figure 7-2.

(A) Dynamic surface pressure (π) change for the DOPC thin film with repeated compression and expansion with the cycle of 432sec.
(B) Dynamic π-A curve after three cycles, the curve begins to trace a single closed loop.
(C) Fourier transformed spectra of the time trace of surface pressure recorded after three cycles. **Top** ; Real part (elastic component),
Bottom ; Imaginary part (viscous component).
(D) Inverted Fourier spectra for the real and imaginary parts. A^0_R and A^0_I indicate the surface area, for the real and imaginary parts at which maximum surface pressure is observed, respectively.

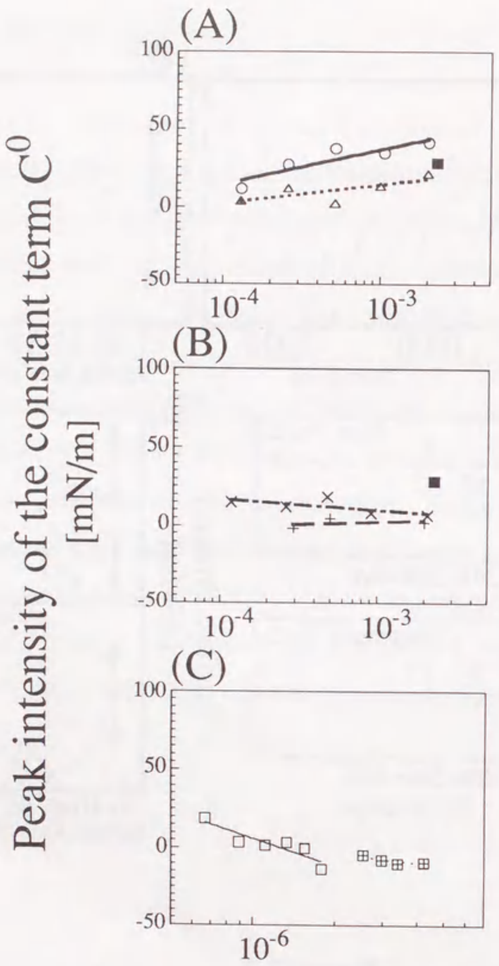

Figure 7-3.

Change of constant peak intensity(C^0) of Fourier real spectra. The large intensity indicates that the π-A curve is traced the closed-loop at high surface pressure region.
(A) ○ ; tetracaine, △ ; prilocaine, ■ ; quinine chloride.
(B) × ; bupivacaine, + ; mepivacaine, ■ ; quinine chloride.
(C) □ ; lidocaine, ⊞ ; procaine.

Table 7-I

The slope of straight line (Fig.7-3)
and the change of intensity of 0^{th} harmonic components
between absence and presence of local anesthetics

	Slope	ΔC^0
	[(mN/m)/mol]	
tetracaine	22 [a]	+ 16.3
prilocaine	12 [a]	− 9.6
bupivacaine	-7 [a]	− 20.8
mepivacaine	3 [a]	− 25.1
lidocaine	-58 [b]	—
procaine	-21 [b]	—

[a] Local anesthetics were added to the aqueous subphase.

[b] Local anesthetics were directly added onto the DOPC molayer.

7-3. Results and Discussion

Quantitative analysis of the dynamic π-A curve of phospholipid thin film

Figure 7-2A and B show the time-dependent change in the surface pressure π induced by a sinusoidal change in the surface area A, and the π-A curves in the steady loop after several cycles of compression and expansion, respectively. Figure 7-2D shows the inverted Fourier transformation of the frequency spectra in Figure 7-2C. With this method of data processing, the elastic and viscous terms can be evaluated separately. We regard these experimental findings as the control in this study under the experimental conditions which has been described in "Materials and Method".

Adsorption of local anesthetic molecules onto the lipid film

We measured the effect of local anesthetics on the dynamic π-A curve for DOPC film at an air/water interface by changing the concentration of the anesthetics from 1.0×10^{-4} to 5.0×10^{-2}M. Although tetracaine, prilocaine and bupivacaine induced marked changes in the π-A curves, mepivacaine, lidocaine and procaine showed only small changes. This finding may be attributed to the fact that the anesthetics in the latter group prefer the aqueous environment, and thus very little of these species were adsorbed into the phospholipid film. Thus, for the latter group, we applied solutions of the anesthetics directly onto the phospholipid film. With this procedure, notable changes in the dynamic π-A curve were observed. Figure 7-3 shows the change in the amplitude of the constant peak, C^0, or the 0^{th} harmonic, with the addition of local anesthetics. The value of C^0 changes almost linearly with the concentration of the anesthetic. Table 7-I summarizes the effects, by anesthetic, on the slope of this

linear relationship and the change in the intensity of the constant peak (C^0), and reveals that the effects of the local anesthetics on the lipid film follow the order tetracaine > prilocaine > bupivacaine >> mepivacaine > lidocaine > procaine. This ordering may reflect the strength of the equilibrium adsorption of the anesthetics to the lipid membrane.

In this regard, Matsuki and his co-workers recently studied the degree of adsorption of local anesthetics into phospholipid film at the air/water interface under thermo-equilibrium conditions.[21] They found that, by adding local anesthetics, the surface pressure of the phospholipid film increased in the order dibucaine > tetracaine > bupivacaine >> mepivacaine > lidocaine >> procaine. They claimed that this order coincides with the anesthetic potency of these anesthetics. It is interesting that this order is almost the same as that in our experiment. Thus, it is clear that the 0^{th} harmonic in the Fourier transformation of the dynamic change of the surface pressure can be regarded as an index of the degree of adsorption of the anesthetic to the phospholipid film.

To confirm this notion, we also measured the dynamic surface behavior in the presence of quinine chloride, which is adsorbed on the lipid film with high efficiency because of its strong hydrophobicity.[18] Indeed, the 0^{th} component, C^0, increased significantly with the addition of quinine chloride. According to the Meyer-Overton rule regarding the effects of anesthesia,[22] anesthetic potency is proportional to hydrophobicity. However, it should also be clear that hydrophobicity is not the only factor which determines anesthetic potency.[23-29] For example, quinine chloride, which has strong hydrophobicity, has essentially no anesthetic potency. Thus, we may have to search for determinants of anesthetic potency other than equilibrium parameters such as adsorbability. In the next section, we discuss the dynamic, or nonequilibrium

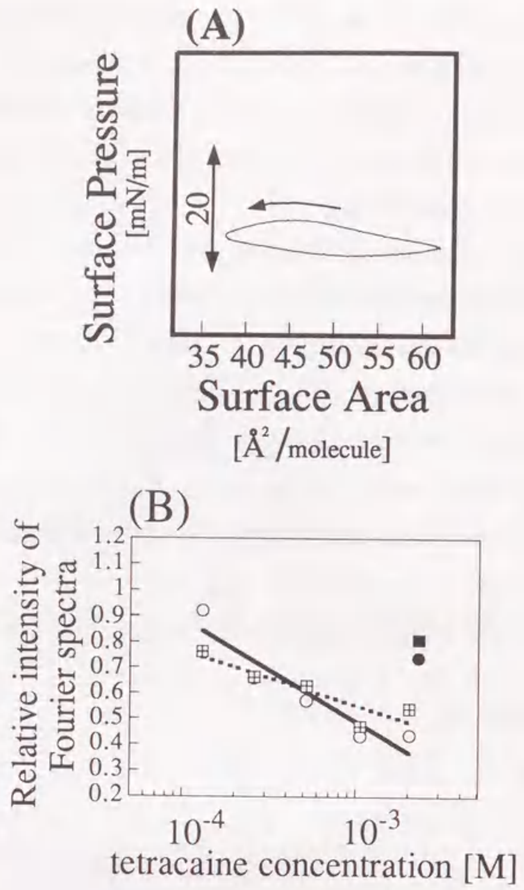

Figure 7-4.

(A) Dynamic π-A curve for the DOPC thin film in the presence of tetracaine(1.06×10^{-3}M) after three cycles of compression and expansion.
(B) Change of relative intensity (○; $|R^t_1/R^0_1|$, ⊞; $|I^t_1/I^0_1|$) in the Fourier-transformation for the measurements shown in Fig. 7-2C (control experiment) and Figure 7-4A, respectively. R^t_1 and I^t_1 represent the first harmonic intensity of Fourier real and imaginary part in the presence of tetracaine. ●; $|R^q_1/R^0_1|$, ■; $|I^q_1/I^0_1|$. R^q_1 and I^q_1 represent the first harmonic intensity of Fourier real and imaginary part in the presence of quinine chloride.

characteristics of the effects of anesthetics, based on a quantitative analysis of the dynamic π-A curve.

Effects of local anesthetics on the linear viscoelasticity of DOPC thin film

Figure 7-4 shows the dynamic π-A curve and the change in the first-harmonic components, including its real and imaginary parts, deduced from the dynamic surface pressure traces in the presence of tetracaine. Note that the real and imaginary parts correspond to the elasticity and viscosity of the DOPC thin film, approximated as a linear, or ideal, viscoelastic-body. Accompanying the decrease in the area of the hysteresis loop in the π-A curve, both components decrease with an increase in the tetracaine concentration in the aqueous subphase from 1.0×10^{-4} to 5.0×10^{-2}M. Thus, the elasticity and viscosity of DOPC thin film decrease with the addition of tetracaine.

Figure 7-5 shows the changes in the relative peak intensities of Fourier real and imaginary fundamental components in the presence of other local anesthetics. Both the real and imaginary intensities decreased with the addition of these local anesthetics, similar to the results with tetracaine. However, no significant change in the peak intensity was observed with mepivacaine. Such an experimental result is attributable to very weak adsorbability of mepivacaine, as that the pKa value, 7.69, of mepivacaine is the smallest among the local anesthetics examined in the present study.(cf. The pKa values of the local anesthetics used in this study are 8.5(tetracaine), 7.89(prilocaine), 8.05(bupivacaine), 7.69(mepivacaine), 7.89(lidocaine), 8.9(procaine), respectively (from MERCK INDEX, eleventh edition).)

In the previous section, we compared the surface density at the air/water interface between local anesthetics and quinine chloride, and found that the intensity of the 0^{th} harmonic component was a useful index. Note that the

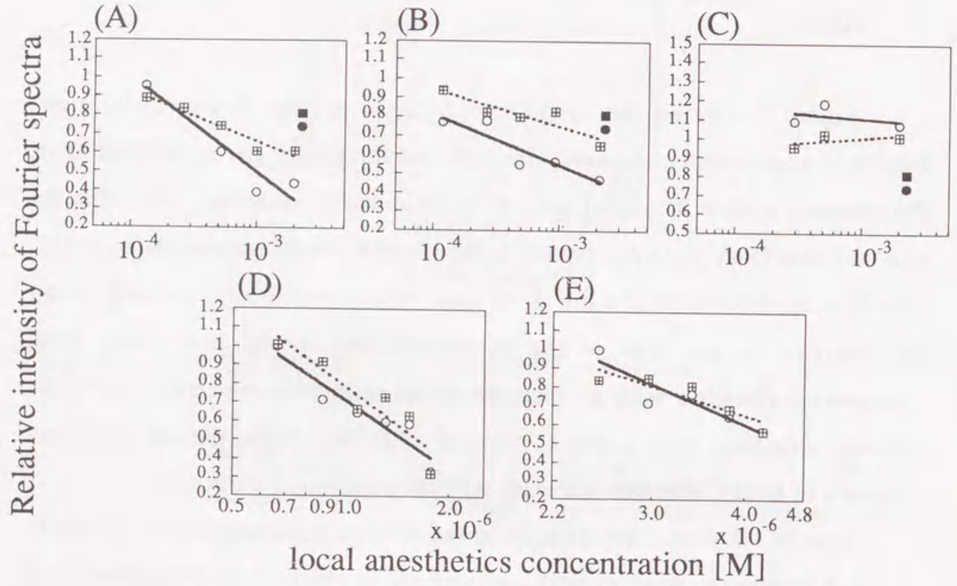

Figure 7-5.

Change of the relative intensity in the Fourier-transformation for the control experiment. ○; $|R_1/R^0_1|$, ⊞; $|I_1/I^0_1|$,
(A) prilocaine, (B) bupivacaine, (C) mepivacaine, (D) lidocaine,
(E) procaine, where ●; $|R^q_1/R^0_1|$, ■; $|I^q_1/I^0_1|$ quinine chloride.

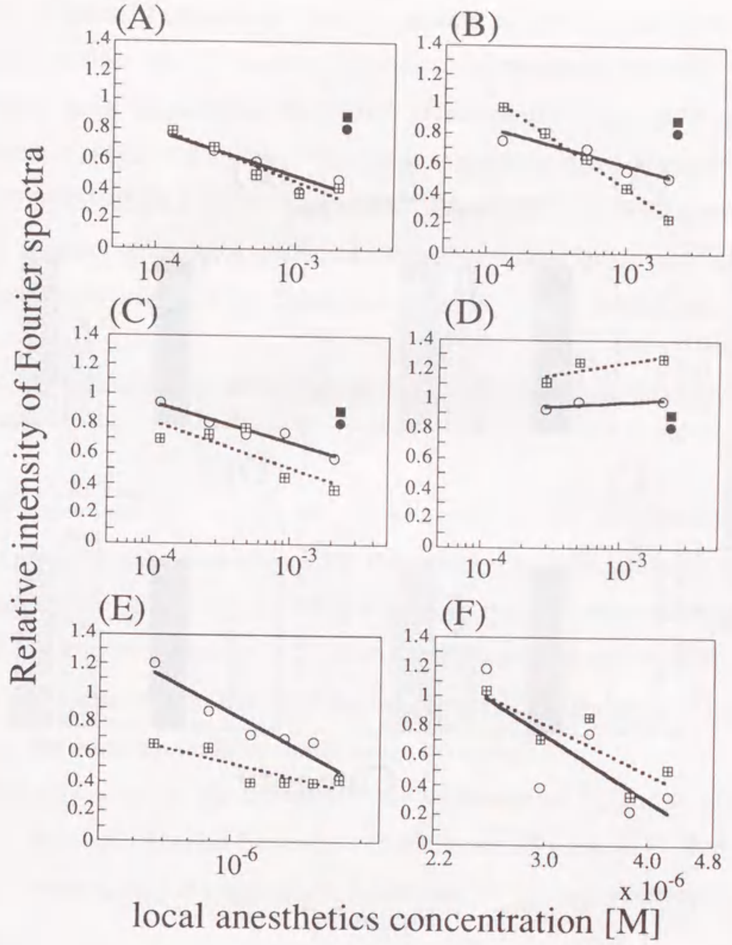

Figure 7-6.

Change of the relative intensity of the Fourier higher-harmonic components. ○; $|R_3/R^0_3|$ is the relative intensity of the third harmonic component in the real part, ⊞; $|I_2/I^0_2|$ is the relative intensity of the second harmonic component in the imaginary part.
(A) tetracaine, (B) prilocaine, (C) bupivacaine, (D) mepivacaine,
(E) lidocaine, (F) procaine,
where ●; $|R^q_3/R^0_3|$, ■; $|I^q_2/I^0_2|$ quinine chloride.

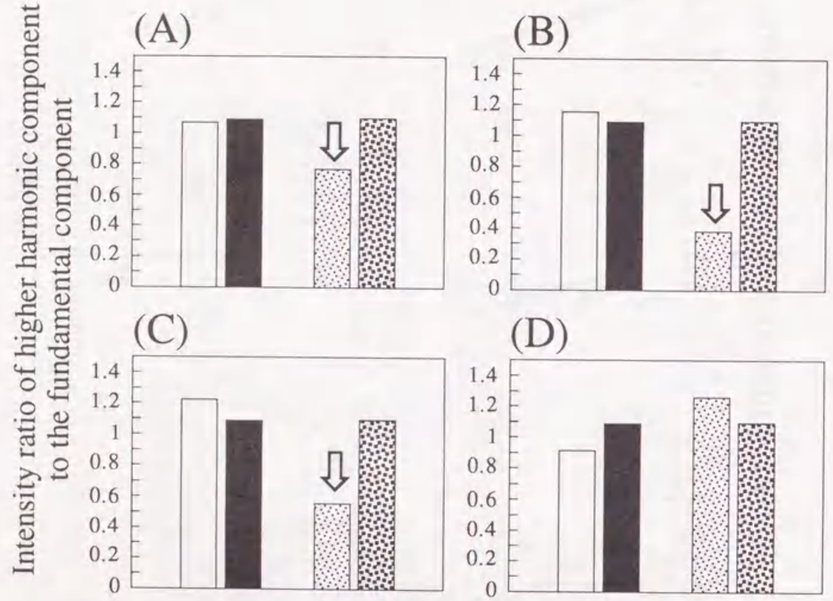

Figure 7-7.

The ratio of the intensity of the Fourier higher-harmonic components (the third harmonic intensity of real part, R_3, and the second harmonic intensity of imaginary part, I_2) to the intensity of the Fourier fundamental harmonic components.

□ ; $(|R_3/R_1|)/(|R^0_3/R^0_1|)$, ⬚ ; $(|I_2/I_1|)/(|I^0_2/I^0_1|)$.

(A) tetracaine, (B) prilocaine, (C) bupivacaine, (D) mepivacaine, quinine chloride, ■ ; $(|R^q_3/R^q_1|)/(|R^0_3/R^0_1|)$, ⬚ ; $(|I^q_2/I^q_1|)/(|I^0_2/I^0_1|)$.

surface densities of prilocaine and bupivacaine at the air/water interface are much lower than that of quinine chloride. In addition, both the real and imaginary peak intensities decreased significantly with prilocaine and bupivacaine (Figs. 7-5A, B). The peak intensities also decreased in the presence of lidocaine and procaine, even though these anesthetics were added using a different procedure. Therefore, these local anesthetics may have quite different effects on the DOPC thin film, compared to quinine chloride.

Effects of local anesthetics on the nonlinear viscoelasticity of DOPC thin film

We now consider the effects of local anesthetics on the higher-harmonic components, which correspond to the nonlinear characteristics of the viscoelasticity of the thin film. By analyzing the experimental results, we noticed that the third real peak (R_3) and the second imaginary peak (I_2) are significantly greater than the other higher-harmonic components. Therefore, we focus our attention on these components hereafter.

Figure 7-6 shows the changes in the intensities of R_3 and I_2 relative to those of the fundamental-harmonic components (R_1 and I_1). Both of the relative intensities ($|R_3/R_1|$, $|I_2/I_1|$) decrease with the addition of local anesthetic.

To compare the changes in the intensities of the higher-harmonic components (R_3 and I_2) with those of the fundamental-harmonic components (R_1 and I_1), we calculated the relative intensities: $(|R_3/R_1|)/(|R^0_3/R^0_1|)$ and $(|I_2/I_1|)/(|I^0_2/I^0_1|)$ (Fig. 7-7). We found that $(|R_3/R_1|)/(|R^0_3/R^0_1|)$ changes very little with local anesthetics. In contrast, $(|I_2/I_1|)/(|I^0_2/I^0_1|)$ decreases markedly, except with mepivacaine. On the other hand, quinine chloride induces only small changes in these components.

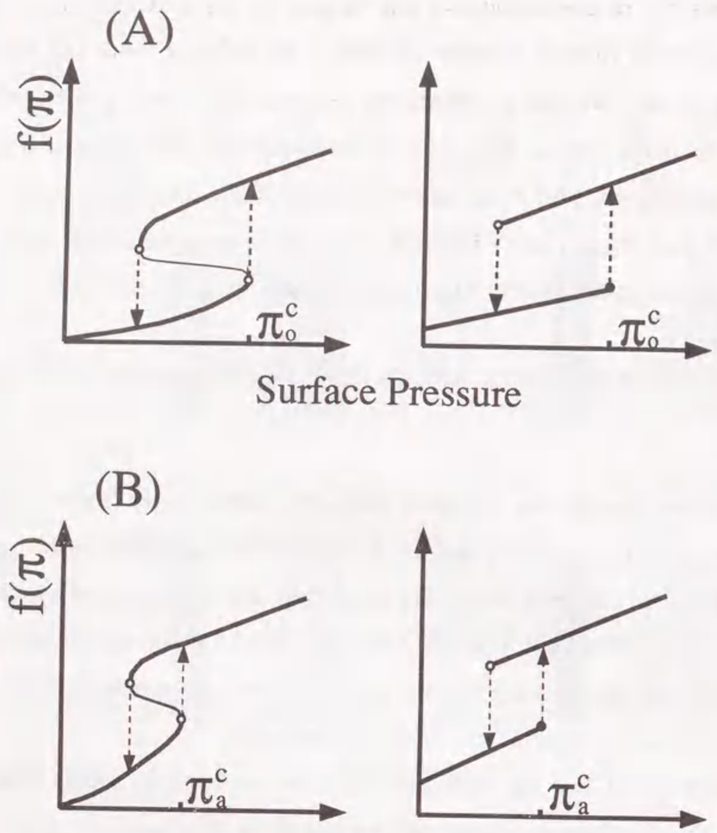

Figure 7-8.

Schematic representation of the function $f(\pi)$ for the DOPC thin film. The arrows indicate the discrete change as in the usual first phase transition. The right-hand side shows the functions adopted for actual numerical calculation.

(A) Without local anesthetics.

$\pi \leq \pi^c{}_o$; $f(\pi) = 0.002\pi + 15$, $\pi > \pi^c{}_0$; $f(\pi) = 2\pi$,

(B) With local anesthetics.

$\pi \leq \pi^c{}_a$; $f(\pi) = 0.02\pi + 25$, $\pi > \pi^c{}_a$; $f(\pi) = 2\pi$.

We have been reported[18,19] in section 5 and 6, the nonlinear behavior of lipid thin film changes in a characteristic manner with the various chemical species, such as metal cations. We suggested that the lipid membrane fluidity and/or the water structure in the vicinity of the membrane were change in terms of the ionic compounds in the aqueous subphase. In this regard, an important new finding here is that local anesthetics decrease the nonlinear viscous properties of DOPC thin film under dynamic experimental conditions.

The main aspects of these experimental results can be summarized as follows. First, the local anesthetics tested here have little effect on the intensity of 0^{th} harmonic components, whereas this was significantly increased by quinine chloride. Second, the area of the hysteresis loop in the dynamic π-A curves shows a marked decrease in the presence of these local anesthetics. Finally, nonlinear viscous components such as $(|I_2/I_1|)/(|I^0{}_2/I^0{}_1|)$ decrease with the addition of local anesthetics, compared to the results with quinine chloride.

Interpretation of the dynamic characteristics using a computer simulation

We assume that, in this section, $f(\pi)$ is also a discontinuous function of surface pressure, π. $f(\pi)$ can be illustrated as an "S"-shaped curve, as shown on the left-hand side of Fig. 7-8A. For the sake of numerical analysis, we approximate the "S"-shaped characteristics with the combination of two straight lines, as shown on the right-hand side of Fig. 7-9A.

We have previously adopted the inhomogeneities of surface pressure in a numerical simulation using a rectangular cell model as described in the section 5.[34] We apply to this model a simple argument that the rate of mass transfer by diffusion is proportional to the difference in concentration among neighboring cells, while the concentration and the surface pressure within each cell are homogeneous.

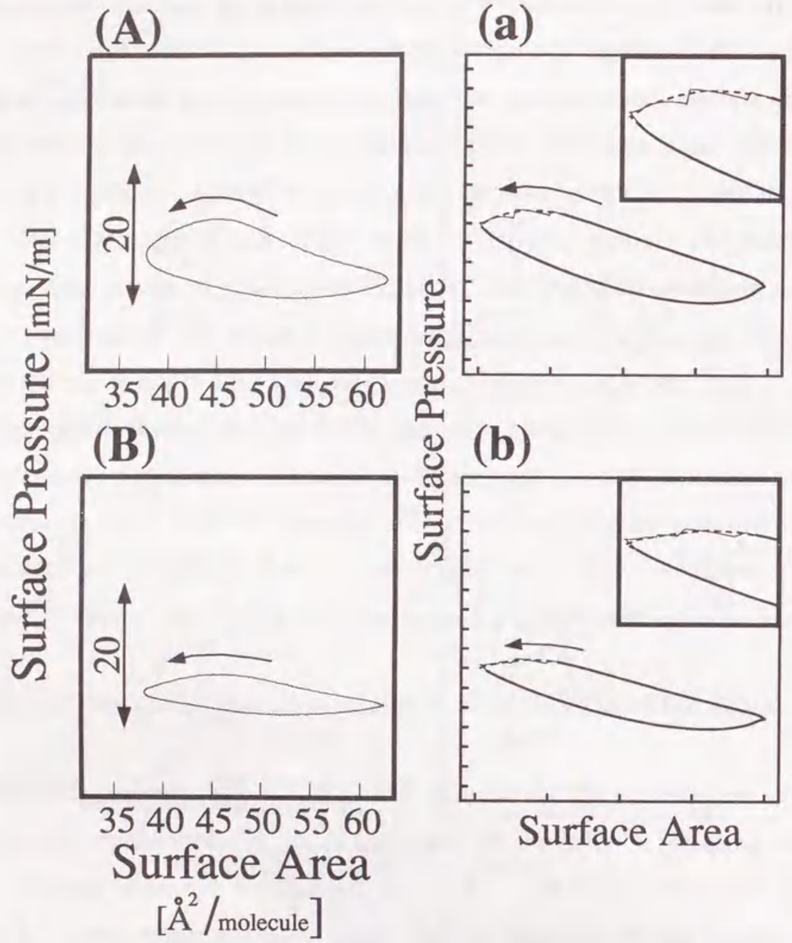

Figure 7-9.

Comparison between the experimental results and the computer simulation for the dynamic π-A curves. (A) and (B) are the same as in Fig. 7-2B and Fig. 7-4A, respectively.
Parameters used for the simulation are;
$k_1 = 17.5$, $k_{-1} = 0.1$, $k'_2 = 0.01$, $k_{-2} = 0.00001$, $\mathbf{a} = 0.5$, $\mathbf{b} = 0.25$,
(a) $\pi^c_o = 21.0$, (b) $\pi^c_a = 17.7$.

Finally, we should explain the effect of local anesthetics on the phospholipid thin film at the air/water interface during periodic compression and expansion. In our experiment, the effects of local anesthetics on the phospholipid thin film can be summarized as follows, (I) the area enclosed by the hysteresis loop in the π-A curve decreases with these anesthetics, and (II) the nonlinearity in viscosity also decreases significantly. Based on these results, it appears as if local anesthetics change the membrane fluidity or the water structure in the vicinity of phospholipid thin film through the hydrophilic head group of the phospholipid molecules. Anesthetics decrease the cooperation among phospholipid aggregates and/or molecules, and this may, in turn, decrease the specific fluidity of phospholipid thin film at the air/water interface.[19,35,36] In other words, a discrete increase in the aggregation rate coefficient (k_2; see (5-ii)) is markedly suppressed in the presence of local anesthetics, in contrast to the effect of quinine chloride. These experimental findings can be explained using a kinetic model in which the critical surface pressure decreases from π^c_0 to π^c_a, as shown in Fig. 7-8B.

We performed a simulation using the model shown in Fig. 7-9. To obtain compression and expansion conditions similar to those in the actual experiment, the surface area was compressed 60% of its maximum value. The results of this numerical simulation correspond to the experimental π-A curve. The simulated results show a small oscillation in the late stage of the compression process. If we include a damping factor, the compression curve should become smooth, as depicted by the dotted line.

7-4. Conclusion

Our simulations essentially reproduce the characteristics observed in the actual experiments. It should be noted that the local anesthetics decreased the nonlinear viscous properties which were represented as the intensity in Fourier Imag. 3^{ed} peak.

To clarify the changes in the film with periodic compression and expansion, spectroscopic measurements may be useful. A BAM, which had been described in section 5, may be particularly useful for obtaining detailed information regarding significant changes in the film with periodical compression and expansion.

References

1) I. Ueda and D. Shieh, J. Masui, **24** (1975) 46.
2) T. Kobayashi, G. Grossmann, B. Robertson, I. Ueda, J. Jpn. Med. Soc. Biol. Interface, **15(2)** (1984) 53.
3) K. Z. Von Neergaard, Gesamte Exp. Med., **66** (1929) 373.
4) R. E. Pattle, Nature, **175** (1955) 1125.
5) J. A. Clements, Proc. Soc. Exp. Biol. Med., **95** (1957) 170.
6) D. O. Shah and J. H. Schulman, J. Lipid Res., **6** (1965) 341.
7) K. J. Miller II, S. R. Goodwin, G. B. Westermann-Clark and D. O. Shah, Langmuir, **9** (1993) 105.
8) R. H. Notter and P. E. Morrow, Ann. Biomed. Eng., **3** (1975) 119.
9) D. Lusted, J. Colloid Interface Sci., **44(1)** (1973) 72.
10) A. F. M. Snik, A. H. M. Joos and A. J. Kruger, J. Colloid Interface Sci., **70(1)** (1979) 147.
11) P. Joos, M. Van Uffelen and G. Serrien, J. Colloid Interface Sci., **152(2)** (1992) 521.
12) E. H. Lucassen-Reynders, Colloids and Surfaces, **25** (1987) 231.
13) T. Ivanova, I. Panaïotov, G. Georgiev, M. A. Launois-Surpas, J. E. Proust and F. Puisieux, Colloids and Surfaces, **60** (1991) 263.
14) R. H. Notter, S. Holcomb and R. D. Mavis, Chem. Phys. Lipids, **27** (1980) 305.
15) J. -P. Fang, K. -D. Wantke and K. Lunkenheimer, J. Phys. Chem, **99** (1995) 4623.
16) R. H. Notter, S. A. Tabak and R. D. Mavis, J. Lipid Res., **21** (1980) 10.
17) M. Morra, E. Occhiello and F. Garbassi, J. Colloid Interface Sci., **149(1)** (1992) 84.
18) K. Yoshikawa, M. Shoji and T. Ishii, Biochem. Biophys. Res. Commun., **160(2)** (1989), 699.
19) M. Makino, K. Yoshikawa and T. Ishii, Nippon Kagaku Kaishi, **10** (1990) 1143.
20) S. W. Hui and H. Yu, Langmuir, **8** (1992) 2724.
21) H. Matsuki, S. Hashimoto and S. Kaneshina, Langmuir, **10** (1994) 1882.
22) H. H. Meyer and R. Gottlieb, Experimental Pharmacology as a Basis for Therapeutics, 2nd ed., transl. by V. E. Henderdson, J. B. Lippincott Co., Philadelphia, 1926, p121.

23) P. Seeman, Pharmacol. Rev., **24(4)** (1972), 583.
24) D. Papahadjopoulos, Biochim. Biophys. Acta, **265** (1972) 169.
25) I. Ueda and H. Kamaya, Anesth. Analg., **63** (1984) 929.
26) J. R. Trudell, Adv. Membr. Fluid, **5** (1991) 1.
27) H. M. McConnell, Molecular motion in biological membranes; In L. J. Berliner, Ed.; "Spin Labeling." New York, p525.
28) N. P. Franks and W. R. Lieb, Br. J. Anaesth., **71** (1993) 65.
29) M. Nakahiro and J. Z. Yeh, E. Brunner and T. Narahashi, FASEB J., **3** (1983) 1850.
30) W. Breisblatt and S. Ohki, J. Membr. Biol., **23** (1975) 385.
31) T. Kato, Y. Hirobe and M. Kato, Langmuir, **7** (1991) 2208.
32) N. L. Gershfeld, Annu. Rev. Phys. Chem., **27** (1976) 349.
33) H. W. Horn and N. L. Gershfeld, Biophys. J., **18** (1977) 301.
34) M. Makino, M. Kamiya, T. Ishii and K. Yoshikawa, Langmuir, **10(4)** (1994) 1287.
35) N. Nakajo,K. Yoshikawa, M. Shoji and I. Ueda, Biochem. Biophys. Res. Commun., **167(2)** (1990) 450.
36) M. Makino, M. Kamiya, N. Nakajo and K. Yoshikawa, Progress in Anesthetics Mechanism, **3** (1995) 247.
37) J. Meunier and L. T. Lee, Langmuir, **7** (1991) 1855.

8. GENERAL CONCLUSIONS

This study showed that a lipid thin film adsorbed on an air/water or a water/oil interface naturally exhibits marked nonlinear characteristics. Although cooperative aggregation among lipid molecules at the critical surface pressure (or the critical surface concentration) is one of the simplest nonlinear phenomena, most of the experimental findings in this study could be explained in terms of this cooperative behavior.

Fourier-transformation of the time trace of the surface pressure is a useful method for analyzing the viscoelastic properties of DOPC thin film quantitatively. From the peak intensity, we can estimate the linear and nonlinear characteristics of a lipid thin film. Thus, new indexes of dynamic viscoelastic properties were found under conditions far from equilibrium. However, it should also be pointed out that the physico-chemical significance of the intensity of the Fourier higher harmonics is not clear. For example, the relationship between anesthetic potency and the Fourier Imaginary 3rd peak-intensity should be clarified. A simple and reasonable definition of each Fourier peak is needed.

Further experimental and theoretical studies on the nonlinear characteristics of lipid films are desirable.

9. ACKNOWLEDGMENTS

This study has been carried out from 1988 to 1997 at the Department of Chemistry, School of Science, Nagoya University and the Graduate School of Environmental Health Science, University of Shizuoka, under the guidance of Professor Kenichi Yoshikawa. The author is sincerely grateful to Professor Kenichi Yoshikawa, who has kindly given valuable suggestions and continuing encouragement throughout this study.

The author is also indebted to Professor Hirofumi Okabayashi, Nagoya Institute Technology, for continuing encouragement, Nobuyoshi Nakajo, Division of Dental Anesthesia, School of Dentistry, University of Tokushima, Dr. Toshio Ishii, School of Dental Medicine, Tsurumi University for helpful discussions, Dr. Yasunori Yoshioka, Kanegafuchi Chemical Industry Co., Ltd., for a gift of phenyl and diacetylene amphiphilic compounds, PhDA2-8; $C_6H_5(CH_2)_2C{\equiv}CC{\equiv}C(CH_2)_8COOH$.

The author expresses his sincere thanks Professor Mamoru Kamiya, University of Shizuoka and Jun-ichi Aihara, Shizuoka University, for continuing encouragement, Professor M. Marek, Prague Institute of Chemical Technology, and Dr. Jerzy Gorecki, Polish Academy of Sciences, for the helpful comments on this study, Professor Tadayoshi Yoshida and Dr. Keijiro Taga, Nagoya Institute Technology, Dr. Noriyuki Kumazawa, Ibaraki University, Dr. Yoshihito Mori, Nagoya Institute of Technology, Dr. Satoshi Nakata, Nara University of Education, Keiji Minagawa, University of Tokushima, Yukiko Matsuzawa, Toyohashi University of Technology, and Shigeki Obata, Aichi College of Technology, for useful advice and encouragement.

Thanks are also due to the students and graduates, who have helped and encouraged the author as good colleagues, in Yoshikawa Laboratory: Messrs.

Masaru Shoji, Minoru Yoshimoto, You Kato, Toshinori Kusumi, Nobuyuki Magome, Masanori Ueda, Sergey M. Mel'nikov, Satoru Kidoaki, Hirosato Matsuura, Misses. Kimiko Kajiya, Masumi Takahashi, and Mina Okamura. Furthermore, the author would like to express his thanks to his close friends who have also encouraged him: Messrs. Kazuo Matsuoka and *the late* Noboru Ooyama.

Finally, the author expresses his deep gratitude to his family for kind consideration and encouragement.

10. PUBLICATION LIST

Book

1. NONLINEAR CHARACTERISTICS OF THIN LIPID FILMS.
   M. Makino and K. Yoshikawa.
   New Developments in Construction and Functions of Organic Thin Film, eds. T. Kajiyama and M. Aizawa(Elsevier Science, Amsterdam) pp211-246(1996).

Original Papers

1. NON-LINEAR CHARACTERISTICS OF LIPID MONOLAYERS IN RELATION TO THE ABILITY TO SELF-ORGANIZE.
   K. Yoshikawa, **M. Makino**, S. Nakata, and T. Ishii.
   Thin Solid Films, **180**(1989), pp117-121.

2. SELF-PULSING AT OIL/WATER INTERFACE IN THE PRESENCE OF PHOSPHOLIPID.
   K. Yoshikawa and **M.Makino**.
   Chemical Physics Letters, **160**(1989), pp623-626.

3. YUUKIHAKUMAKU NO HISENKEITOKUSEI TO MIKAKU(Japanese).
   K. Yoshikawa and **M. Makino**.
   OME, **54**(1989), pp31-35.

4. HISENKEINENDANSEITAI TOSHITENO SHISHITSU TANBUNSHI-MAKU(Japanese).
   M. Makino, K. Yoshikawa, and T. Ishii.
   Nippon Kagaku Kai-shi, **10**(1990), pp1143-1150.

5. AUTOCATALYTIC AGGREGATION OF FATTY ACID WITH PHENYL AND DIACETYLENE MOIETIES AT AN AIR-WATER INTERFACE.
M. Makino, M. Kamiya, T. Ishii, and K. Yoshikawa.
Langmuir, **10**(1994), pp1287-1291.

6. CHARACTERISTIC EFFECTS OF LOCAL ANESTHETICS ON THE DYNAMIC BEHAVIOR OF PHOSPHOLIPID MONOLAYER.
M. Makino, M. Kamiya, N. Nakajo, and K. Yoshikawa.
Progress in Anesthetic Mechanism, **3**(1995), pp247-252.

7. EFFECTS OF LOCAL ANESTHETICS ON THE DYNAMIC BEHAVIOR OF PHOSPHOLIPID THIN FILM.
M. Makino, M. Kamiya, N. Nakajo, and K. Yoshikawa.
Langmuir, **12**(1996), pp4211-4217.

8. EFFECTS OF METAL CATIONS ON THE DYNAMIC CHARACTERISTICS OF A PHOSPHOLIPID THIN FILM AT AN AIR/WATER INTERFACE.
M. Makino, M. Kamiya, T. Ishii, and K. Yoshikawa.
Bulletin of the Chemical Society of Japan, **69**(1996), pp3429-3434.

9. AN OVERSHOOT-HUMP IN A π-A CURVE AND THE COOPERATIVE AGGREGATION AMONG DINITROPHENYL MOIETIES IN PHOSPHOLIPID AT AN AIR/WATER INTERFACE.
M. Makino, K. Nakamura, C. Sasaki, M. Kamiya, and K. Yoshikawa.
Progress in Colloid and Polymer Science, in press.

10. DYNAMIC PROPERTIES OF A PHOSPHOLIPID THIN FILM AT AN AIR/WATER INTERFACE WITH A PERIODIC CHANGE IN SURFACE AREA.
M. Makino, M. Kamiya, and K. Yoshikawa.
Langmuir, in submitting.

RELATED PUBLICATIONS

Original Papers

1. FORMATION OF RADICALS AND CHEMI-LUMINESENCE DURING THE AUTOXIDATION OF TEA CATECHINS.
H. Yoshioka, K. Sugiura, R. Kawahara, T. Fujita, **M. Makino**, M. Kamiya, and S. Tsuyumu.
Agric. Biol. Chem., **55**(1991), pp2717-2723.

2. ANALYSIS OF THE INDUCED ROTATIONAL STRENGTH OF MONO- AND DISUBSTITUTED BENZENES INDUCED IN β-CYCLODEXTRIN.
M. Kamiya, S. Mitsuhashi, **M. Makino**, and H. Yoshioka.
J. Phys. Chem., **96**(1992), pp95-99.

3. PHOTODEGRADATION MECHANISM OF 2,3,7,8-TETRACHLORO-DIBENZO-*p*-DIOXIN AS STUDIED BY THE PM3-MNDO METHOD.
M. Makino, M. Kamiya, and H. Matsushita.
Chemosphere, **24**(1992), pp291-307.

4. CATALYTIC PROPERTIES OF CYCLODEXTRINS ON THE HYDROLYSIS OF PARATHION AND PARAOXON IN AQUATIC MEDIUM CONTAINING HUMIC ACIDS.
M. Kamiya, S. Mitsuhashi, and **M. Makino**.
Chemosphere, **25**(1992), pp1839-1849.

5. COMPUTER-ASSISTED PREDICTION OF GAS CHROMATO-GRAPHIC RETENSION TIMES OF POLYCHLORINATED BIPHENYLS BY USE OF QUANTUM CHEMICAL MOLECULAR PROPERTIES.
M. Makino, M. Kamiya, and H. Matsushita.
Chemosphere, **25**(1992), pp1839-1849.

6. PREDICTION OF GAS CHROMATOGRAPHIC RETENTION INDEXES OF ENVIRONMENTAL POLYCHRORINATED DIBENZO-*p*-DIOXINS AND DIBENZOFURANS BY USE OF COMPUTER-CALCULATED MORECULAR PROPERTIES.
M. Makino, M. Kamiya, and H. Matsushita.
Environ. International, **19**(1993), pp203-211.

7. PHOTOCHEMICAL DECHLORINATION OF 2,3,7,8-, 1,3,6,8-, AND 1,2,3,4-TETRACHLORODIBENZO-*p*-DIOXINS AS STUDIED BY THE FRONTIER-ELECTRON REACTIVITY INDEXES.
M. Makino, S. Kazama, and M. Kamiya.
Chem. Pharm. Bull., **41**(1993), pp1-5.

8. SYNTHESIS OF GALACTOSE DERIVATIVES THAT RENDER LECTINE-INDUCED AGGLUTINATING ABILITY TO LIPOSOMES.
H. Yoshioka, T. Ohmura, M. Hasegawa, S. Hirota, **M. Makino**, and M. Kamiya.
J. Parm. Sci., **82**(1993), pp273-275.